ORNL-3091
UC-34 - Physics

DIFFUSION OF SLOW ELECTRONS IN GASES

D. W. Forester
L. W. Cochran

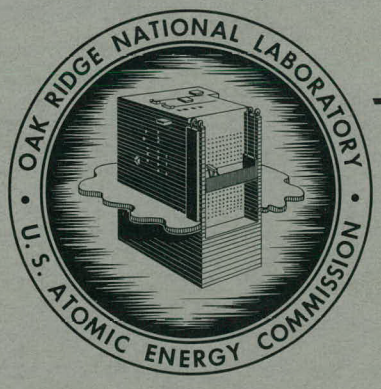

OAK RIDGE NATIONAL LABORATORY
operated by
UNION CARBIDE CORPORATION
for the
U.S. ATOMIC ENERGY COMMISSION

DISCLAIMER

ORNL-3091

Contract No. W-7405-eng-26

DIFFUSION OF SLOW ELECTRONS IN GASES

D. W. Forester[1] and L. W. Cochran[2]

HEALTH PHYSICS DIVISION

Submitted as a thesis to the Graduate Council of the University of Tennessee in partial fulfillment of the requirements for the degree of Master of Science in Physics.

Date Issued

OCT 24 1961

Oak Ridge National Laboratory
Oak Ridge, Tennessee
Operated by
Union Carbide Corporation
for the
U. S. Atomic Energy Commission

[1]University of Tennessee
[2]University of Kentucky (Consultant to ORNL)

ACKNOWLEDGMENTS

The authors express their gratitude to the following members of the Health Physics Division, Oak Ridge National Laboratory, for their support and assistance: Dr. G. S. Hurst, Dr. R. H. Ritchie, Mr. T. E. Bortner, Mr. L. B. O'Kelly, and Mr. H. B. Eldridge. They are also indebted to Dr. E. G. Harris and Dr. William Bugg of the University of Tennessee, Physics Department, for helpful suggestions concerning the final write-up of this report.

TABLE OF CONTENTS

LIST OF TABLES

LIST OF FIGURES

CHAPTER I

INTRODUCTION

A swarm of electrons diffusing through a gas under the action of an external electric field will attain, because of electron acceleration between molecular collisions, an energy of agitation which is somewhat, if not considerably greater than that of the molecules in the gas. Townsend's energy factor $k_T = \frac{\text{mean energy of agitation of an electron}}{\text{mean energy of thermal agitation of a molecule}}$ may be obtained experimentally in terms of the ratio w/K which should be constant for a given field to pressure ratio E/P. K is the diffusion coefficient, and w is the mean drift velocity of the electrons in the direction of the field. It is found that $w/K = \text{constant}/Ak_T$, where A depends on the electron energy distribution in the gas. Although knowledge of the electron energy distribution is necessary to determine k_T accurately, it may first be obtained in the form w/K and then the appropriate distribution may be applied in the form of dimensionless ratios of mean agitational velocities and reciprocals of these quantities. Thus, w/K data may be taken without a precise distribution function, and the value of k_T may be obtained when the correct distribution of energies is determined. From the ratio k_T many physically important properties of electrons in gases may be calculated. Among these properties are the mean agitational velocity $\bar{U}$, the mean free path at unit pressure L, the mean proportion of energy lost per collision η, and the effective cross section of gas molecules for electron collisions σ. The last three

quantities require an independent measurement of the drift velocity w. While the swarm type experiment leads only to average values of the various quantities mentioned and certain assumptions required for the interpretation of data are more naive than is desirable, it still offers the only convenient means of investigation in the range of mean electron energy less than 2 ev.

The primary purpose of this work was to investigate the above mentioned properties with electrons having energies less than 2 ev in several gases which are used in the fields of radiation detection and dosimetry. Another purpose was to put an energy scale on the attachment of electrons by small concentrations of attaching gases in non-attaching gases. It is known that the attachment of electrons depends upon their energy in the gas[1] and this energy is primarily determined by the larger concentration of non-attaching gas. This latter purpose is very limited because the attaching gases produce negative ions whose mass difference from the electrons give a distorted picture of the actual electron energy where experiment is based on diffusion.

Most of the data for w/K and related quantities in the gases which have been investigated were taken in the 1920's and 1930's. The results of these early investigations have been summarized by R. H.

---

[1] G. S. Hurst and T. E. Bortner, "Capture of Electrons in Molecular Oxygen," Oak Ridge National Laboratory Report ORNL-2670 (September, 1959).

Healey and J. W. Reed.[2] More recently, L. H. G. Huxley and his associates[3,4] have done work with hydrogen, nitrogen, and air. Several of these gases were again investigated in this experiment using the purest gases available from modern commercial cylinders and using improved vacuum and low current measuring equipment. Methane, ethylene, cyclopropane, nitrogen, hydrogen, carbon dioxide, and argon were studied. Methane and cyclopropane have not previously been studied in this type of experiment and the only published data on w/K for argon are those of Townsend and Bailey[5] in 1922 with gas which was probably very impure. More recently, data have been taken by Crompton and Sutton[4] on nitrogen and hydrogen using very exacting conditions of measurement and gas purity. These two gases have been used as a comparison to give at least an idea of the reliability of results on the other gases.

The method of approach is essentially that of Huxley and his co-workers and is a modification of the lateral diffusion method and theoretical considerations of Sir John Townsend[5,6] in the early 1900's.

---

[2] R. H. Healey and J. W. Reed, The Behaviour of Slow Electrons in Gases (Amalgamated Wireless Ltd., Australia, 1941).

[3] L. G. H. Huxley and A. A. Zaazou, Proc. Roy. Soc. (Lond.) A196, 402 (1940).

[4] R. W. Crompton and D. J. Sutton, Proc. Roy. Soc. (Lond.) A215, 467 (1952).

[5] J. S. Townsend and V. A. Bailey, Phil. Mag. 44, 1033 (1922).

[6] J. S. Townsend, in Electrons in Gases (Hutchinson's Scientific and Technical Publications, New York, 1948).

In this method electrons are emitted from an appropriate source and travel in an electric field between circular field rings. Their lateral diffusion is symmetric about the direction of the electric field which is along the axis of a cylindrical chamber. The diffusion is isotropic and conditions are such that the electrons are in an equilibrium steady-state motion. In such a state their concentration is expressed by the basic diffusion equation $\Delta^2 n = \frac{w}{K} \frac{\partial n}{\partial z}$ which, when solved with suitable boundary conditions and integrated over the receiving electrodes yields a ratio $R = \frac{i_b}{i_b + i_c}$ of the current striking the center electrode to that striking the inner and outer receiving electrodes. This ratio is a function of the known dimensions of the chamber and w/K. Using a theoretical plot of this ratio versus w/K in conjunction with the experimentally determined R yields the desired data.

CHAPTER II

THEORY

Under the conditions of uniform total pressure, small density variation, and no external field, the diffusion of electrons across a surface in a gas is proportional to the space rate of change of the electron density at right angles to the surface. The constant of proportionality is the diffusion coefficient K. The expression for the electron transport per unit area per unit time may be written as

$$\underline{G} = n\underline{V} = -K \text{ grad } n, \tag{1}$$

where $\underline{V}$ is the transport velocity and n is the partial density of electrons in the gas. In one dimension Eq. (1) may be written

$$G(z) = nV_z = -K \frac{\partial n}{\partial z} . \tag{2}$$

Consider the transport of electrons G(z) entering the region between two planes at z and z + dz and the transport out of the region,

$$G(z + dz) = G(z) + \frac{\partial G}{\partial z} dz.$$

The net inflow of electrons is

$$G(z) - G(z + dz) = - \left(\frac{\partial G}{\partial z}\right) dz = - \frac{\partial}{\partial z}\left(- K \frac{\partial n}{\partial z}\right) dz. \tag{3}$$

Assuming no sources or sinks in the region, the equation of continuity yields

$$\underline{\nabla}\,(G) = -\frac{\partial n}{\partial t}\,. \tag{4}$$

Therefore,

$$\frac{\partial n}{\partial t} = \frac{\partial}{\partial z}\left(K\,\frac{\partial n}{\partial z}\right), \tag{5}$$

and if K is independent of z, Eq. (5) becomes

$$\frac{\partial n}{\partial t} = K\,\frac{\partial^2 n}{\partial z^2}\,. \tag{6}$$

This derivation is extended to Eq. (11) in a discussion by Healey and Reed,[1] using the following steps. If now a uniform electric field is applied in the z direction, the number of electrons crossing unit area per unit time becomes

$$n\underline{V} = -K\ \text{grad}\ n + n\underline{w}\,, \tag{7}$$

where $\underline{w}$ is the mean drift velocity of the electrons in the direction of the field and $\underline{V}$ is the net transport velocity.

Equation (7) may be rewritten using the fact that the electron

---

[1] R. H. Healey and J. W. Reed, The Behaviour of Slow Electrons in Gases (Amalgamated Wireless Ltd., Australia, 1941).

partial pressure is $P_e = 1/3\ nm\overline{U^2}$, and assuming $\overline{U^2}$, the mean square velocity of the electron, is constant in the steady state throughout the gas,

$$\frac{\partial P_e}{\partial z} = \frac{w}{K} P_e - \frac{P_e V}{K} = \text{momentum transferred to a unit volume of gas molecules per second by the electrons.} \tag{8}$$

Since, in the absence of an electric field, $-\frac{P_e V}{K}$ is the momentum transferred to a unit volume in unit time, $\frac{w}{K} P_e$ represents the momentum transferred to a unit volume in unit time due to the field and is also neE. Therefore, $neE = \frac{wP_e}{K}$, or

$$\frac{w}{K} = \frac{neE}{P_e} . \tag{9}$$

Applying the equation of continuity to Eq. (7), it may be seen that

$$\frac{1}{K} \frac{\partial n}{\partial t} = \frac{1}{K} \frac{\partial}{\partial z} (G) = \frac{\partial}{\partial z} \left(- \frac{\partial n}{\partial z} + n \frac{w}{K} \right) ,$$

or

$$\frac{1}{K} \frac{\partial n}{\partial t} = - \frac{\partial^2 n}{\partial z^2} + \frac{w}{K} \frac{\partial n}{\partial z} , \tag{10}$$

assuming $\frac{w}{K}$ is constant through the gas in the steady state. But in the steady state, $\frac{\partial n}{\partial t} = 0$. Equation (10) then becomes

$$\frac{\partial^2 n}{\partial z^2} = \frac{w}{K}\frac{\partial n}{\partial z} = 2\lambda \frac{\partial n}{\partial z} = \frac{neE}{P_e}\frac{\partial n}{\partial z}, \qquad (11)$$

where $\frac{w}{K} = 2\lambda$ = constant. The electron pressure in expression (11) may be put in terms of the gas pressure. The previously defined Townsend energy factor may be written as

$$k_T = \frac{1/2\ m\ \overline{U^2}}{1/2\ M\ \overline{\Omega^2}} = \frac{\text{K.E. of agitation of electrons}}{\text{K.E. of agitation of molecules}}, \qquad (12)$$

where $\overline{\Omega^2}$ is the mean square velocity of the molecules. Since atmospheric pressure is $1/3\ N\ M\ \overline{\Omega^2} = P_o$, where N is the number of molecules per cubic centimeter at atmospheric pressure and at the temperature 25° C of the experiment, Eq. (9) becomes

$$\frac{w}{K} = \frac{neE}{P_e} = \frac{neE}{1/3\ nm\ \overline{U^2}} = \frac{3eE}{k_T\ M\ \overline{\Omega^2}} = \frac{NeE}{k_T\ P_o} = 38.92\ \frac{E}{k_T}, \qquad (13)$$

or

$$\frac{w}{KP} = \frac{38.92}{k_T}\frac{E}{P},$$

where KP is the diffusion coefficient at unit pressure at T = 298° K. k_T depends, however, on the energy distribution of the electrons. It will be shown later that $k_T = k_1/A$ where A is a dimensionless ratio of averages taken from the appropriate distribution, and $k_1 = \frac{P_o}{NeE}\frac{w}{K}$ is the experimental factor measured. It will be found also

that $A = 1$ and $k_l = k_T$ for the case of a Maxwellian distribution.

The basic diffusion equation, (11), may be written,

$$\nabla^2 n = \frac{w}{K} \frac{\partial n}{\partial z} = 2\lambda \frac{\partial n}{\partial z} . \tag{14}$$

In this experiment, electrons leave a point source at the origin and drift under the action of an electric field along the z axis of a cylindrical chamber. The concentration is assumed to be zero at the receiving electrodes while the effects of the plate at $z = 0$ and the sides of the cylinder are assumed negligible.

A solution of Eq. (14) which satisfies boundary conditions similar to those of the experimental arrangement is derived below. The discussion follows that of Huxley,[2,3] and is included primarily to keep in mind the approximations which have been made in interpreting the data.

Writing $n = e^{\lambda z} V$, where $V = V(x,y,z)$, Eq. (14) yields

$$\frac{\partial^2 e^{\lambda z} V}{\partial z^2} + e^{\lambda z} \frac{\partial^2 V}{\partial y^2} + e^{\lambda z} \frac{\partial^2 V}{\partial x^2} = 2\lambda \frac{\partial e^{\lambda z} V}{\partial z} ,$$

$$e^{\lambda z} \nabla^2 V + \lambda^2 e^{\lambda z} V + 2\lambda e^{\lambda z} \frac{\partial V}{\partial z} = 2\lambda \left(\lambda e^{\lambda z} V + e^{\lambda z} \frac{\partial V}{\partial z} \right) .$$

---

[2] L. G. H. Huxley and F. W. Bennett, Phil. Mag. 30, 396 (1940).

[3] L. G. H. Huxley and R. W. Crompton, Proc. Phys. Soc. B68, 381 (1955).

or

$$\nabla^2 V = \lambda^2 V. \tag{15}$$

Writing Eq. (15) in spherical coordinates,

$$r^2 \frac{\partial^2 V}{\partial r^2} + 2r \frac{\partial V}{\partial r} + \frac{1}{\sin\theta} \frac{\partial}{\partial \theta} \left(\sin\theta \frac{\partial V}{\partial \theta} \right) + \frac{1}{\sin^2\theta} \frac{\partial^2 V}{\partial \phi^2} - \lambda^2 r^2 V = 0 . \tag{16}$$

This may be solved by separation of variables. Let $V = R_k S_k$ where $R_k = R_k(r)$ and $S_k = S_k(\theta, \phi)$. Rewriting Eq. (16) and dividing by $R_k S_k$, yields

$$\left[\frac{r^2}{R_k} \frac{\partial^2 R_k}{\partial r^2} + \frac{2r}{R_k} \frac{\partial R_k}{\partial r} - \lambda^2 r^2 \right] = - \left[\frac{1}{S_k \sin\theta} \frac{\partial}{\partial \theta} \left(\sin\theta \frac{\partial S_k}{\partial \theta} \right) + \frac{1}{\sin^2\theta \, S_k} \frac{\partial^2 S_k}{\partial \phi^2} \right] . \tag{17}$$

In order that these two bracketed terms, which are each functions of different independent variables, always be equal they must be equal to a constant. For the second bracketed term take this constant to be $k(k + 1)$ where k is an integer.

$$\frac{1}{\sin\theta} \frac{\partial}{\partial \theta} \left(\sin\theta \frac{\partial S_k}{\partial \theta} \right) + \frac{1}{\sin^2\theta} \frac{\partial^2 S_k}{\partial \phi^2} + \left[k(k + 1) \right] S_k = 0. \tag{18}$$

The solution of this equation is an associated Legendre function $S_k = P_k^m(\cos\theta)\cos m\phi$.

The radial part of Eq. (17) becomes

$$r^2 \frac{\partial^2 R_k}{\partial r^2} + 2r \frac{\partial R_k}{\partial r} - \left[k(k+1) + \lambda^2 r^2 \right] R_k = 0 .$$

Putting $t = \lambda r$,

$$t^2 \frac{\partial^2 R_k}{\partial t^2} + 2t \frac{\partial R_k}{\partial t} - \left[k(k+1) + t^2 \right] R_k = 0. \qquad (19)$$

Equation (19) is a modified Bessel's equation which has as a general solution,

$$R_k = (-1)^k (\pi/2)^{1/2} t^k \left(\frac{1}{t} \frac{d}{dt} \right)^k \left[\frac{Ae^t + Be^{-t}}{t} \right]. \qquad (20)$$

A and B are arbitrary constants. In order for R_k to remain finite as $t \to \infty$, A must equal zero. Giving the arbitrary constant B the value of unity, Eq. (20) becomes

$$R_k = (-1)^k (\pi/2)^{1/2} t^k \left(\frac{1}{t} \frac{d}{dt} \right)^k \left(\frac{e^{-t}}{t} \right) = t^{-1/2} K_{k+\frac{1}{2}}(t). \qquad (21)$$

$K_{k+\frac{1}{2}}(t)$ is a modified Bessel's function of half integral order. Thus the general solution of Eq. (14) is

$$n = \frac{e^{\lambda z}}{(\lambda r)^{\frac{1}{2}}} \sum_{k} A_k \, K_{k+\frac{1}{2}} (\lambda r) \, P_k^m (\cos \theta) \cos m\phi \, . \qquad (22)$$

A simple solution of Eq. (22) is for m = 0 and k = 0 which corresponds to an isolated point source of electrons in a uniform electric field. Thus,

$$n_M = \frac{Ae^{-\lambda(r - z)}}{r} \, . \qquad (23)$$

Now, to satisfy boundary conditions the concentration must be zero over the receiving electrodes in the plane z = h. One way of obtaining this, in analogy to electrostatic image problems, is to take an image "sink" of electrons of strength $(-)Ae^{2\lambda h}$ at (0, 0, 2h), Fig. 1. Thus,

$$r'n' = (-)Ae^{2\lambda h} e^{-[r_1\lambda - \lambda(z - 2h)]} = (-)Ae^{-\lambda(r_1 - z)} , \qquad (24)$$

where r_1 is the radial distance from the image and

$$n = n_M + n' = Ae^{\lambda z} \left[\frac{e^{-\lambda r}}{r} - \frac{e^{-\lambda r_1}}{r_1} \right] , \qquad (25)$$

which does go to zero in the plane z = h where $r = r_1$. Taking ρ as the perpendicular distance of point P from the z axis,

$$r = \sqrt{\rho^2 + z^2} \qquad r_1 = \sqrt{\rho^2 + (z - 2h)^2} \, ,$$

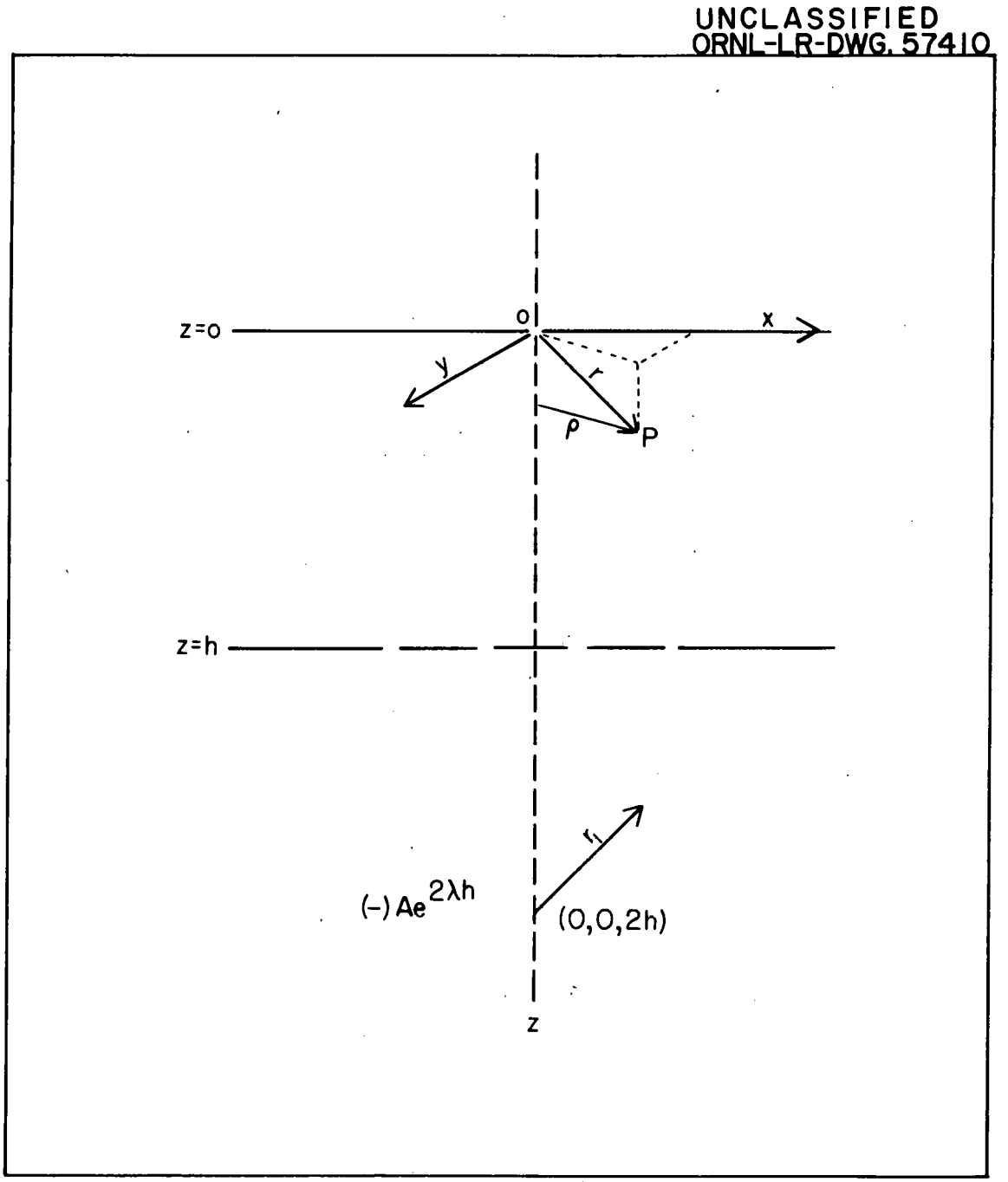

FIG. 1. IMAGE SOURCE TO PRODUCE ZERO CONCENTRATION AT THE PLANE z=h.

and

$$\frac{\partial}{\partial z} = \frac{z}{r}\frac{\partial}{\partial r},$$

or

$$\frac{\partial}{\partial z} = \frac{(z - 2h)}{r_1}\frac{\partial}{\partial r_1}.$$

The current striking an element of area dS on the receiving electrode is

$$I = \frac{\text{No. crossing unit area}}{\text{unit time}} \times \text{area} \times \text{charge},$$

or

$$I = \sim - K\left(\frac{\partial n}{\partial z}\right)_{z=h} dS. \tag{26}$$

Now,

$$\frac{\partial n}{\partial z} = Ae^{\lambda z}\left[\frac{z}{r}\frac{\partial}{\partial r}\left(\frac{e^{-\lambda r}}{r}\right) - \frac{z}{r_1}\frac{\partial}{\partial r_1}\left(\frac{e^{-\lambda r_1}}{r_1}\right) + \frac{2h}{r_1}\frac{\partial}{\partial r_1}\left(\frac{e^{-\lambda r_1}}{r_1}\right)\right]$$

$$+ A\lambda e^{\lambda z}\left(\frac{e^{-\lambda r}}{r} - \frac{e^{-\lambda r_1}}{r_1}\right), \tag{27}$$

and evaluating Eq. (27) at z = h,

$$\left(\frac{\partial n}{\partial z}\right)_{z=h} = \frac{A'e^{\lambda h}}{r}\frac{\partial}{\partial r}\left(\frac{e^{-\lambda r}}{r}\right) = \frac{A'e^{\lambda h}}{r}\frac{d}{dr}\left(\frac{e^{-\lambda r}}{r}\right) \tag{28}$$

which is the second term (m = 0, k = 1) in the series of Eq. (22) corresponding to a dipole source of electrons at the origin evaluated at z = h.

Experimentally, the ratio of current striking the inner electrode of radius b to that striking both inner and outer electrodes with total radius c is measured. This ratio is obtained theoretically by first finding the ratio R_b of current at the inner electrode to an infinite plane electrode and then dividing this by the similar ratio R_c for the inner plus outer electrodes:

$$R_b = \frac{\int_0^b \frac{\partial n}{\partial z}_{z=h} \rho d\rho}{\int_0^\infty \frac{\partial n}{\partial z}_{z=h} \rho d\rho} = \frac{\int_h^{\sqrt{h^2+b^2}=d} \frac{\partial n}{\partial z}_{z=h} r dr}{\int_h^\infty \frac{\partial n}{\partial z}_{z=h} r dr} = \frac{\int_h^d \frac{d}{dr}\left(\frac{e^{-\lambda r}}{r}\right) dr}{\int_h^\infty \frac{d}{dr}\left(\frac{e^{-\lambda r}}{r}\right) dr}, \qquad (29)$$

where $d = \sqrt{h^2 + b^2}$, ρ, r, and h are previously defined.

Integration of Eq. (29) gives

$$R_b = \frac{\frac{e^{-\lambda d}}{d} - \frac{e^{-\lambda h}}{h}}{-\frac{e^{-\lambda h}}{h}} = 1 - \frac{h}{d} e^{-\lambda(d - h)} . \qquad (30)$$

Correspondingly,

$$R_c = 1 - \frac{h}{g} e^{-\lambda(g - h)}, \tag{31}$$

where $g = \sqrt{h^2 + c^2}$.

Now taking the ratio,

$$R = \frac{R_b}{R_c} = \frac{\frac{i_b}{i_\infty}}{\frac{i_c + i_b}{i_\infty}} = \frac{1 - \frac{h}{\sqrt{h^2 + b^2}} e^{-\lambda (\sqrt{h^2 + b^2} - h)}}{1 - \frac{h}{\sqrt{h^2 + c^2}} e^{-\lambda (\sqrt{h^2 + c^2} - h)}} . \tag{32}$$

Since $\lambda = \frac{w}{2K} = 19.46 \frac{E}{k_1}$, Eq. (32) may be written,

$$R = \frac{1 - \frac{1}{\sqrt{1 + (b/h)^2}} \exp\left\{19.46 \frac{Eh}{k_1} \left(\sqrt{[1 + (b/h)^2]} - 1\right)\right\}}{1 - \frac{1}{\sqrt{1 + (c/h)^2}} \exp\left\{19.46 \frac{Eh}{k_1} \left(\sqrt{[1 + (c/h)^2]} - 1\right)\right\}} . \tag{33}$$

Noting that Eh is the voltage applied across the height h of the chamber, it is now a relatively simple calculation to obtain k_1 from the experimental ratios at a known value of b/h and c/h.

Theoretical plots of R vs $\frac{Eh}{k_1}$ for different values of b/h and a constant value of c/h appear in Fig. 2. Using $R = \frac{R_b}{R_c}$ rather than $R = \frac{i_b}{i_\infty}$ makes a considerable difference in the curves plotted at a lower field to pressure ratios where diffusion is more pronounced and some of the electrons are not collected on either electrode.[4] This causes a higher ratio at lower fields than would be had if all the electrons were collected on an infinite plane.

As has already been mentioned $\frac{w}{K} = \frac{NeE}{k_1 P_o}$ where $k_1 = Ak_T$. This constant A which depends on the energy distribution may be found by taking the ratio of the mean value of w and K. From kinetic theory, $K = \frac{1}{3}\bar{\ell}\bar{U}$ where $\bar{\ell}$ is the mean free path and $\bar{U}$ is the mean velocity. The assumption made in this equation is that the density of electrons is low so that their mutual repulsion does not affect their diffusion. At 10^{-12} amperes, the order of magnitude of current measured, the density is small.

The drift velocity w of an electron in the direction of the electric field may be derived in the following manner.[5] Consider an electron making a collision at O and moving with free path length ℓ to P when there is no field applied. If the electron has agitational velocity U, the time for the free path is $\frac{\ell}{U}$. If now an electric field E is applied as shown in Fig. 3, the electron path will be curved and

---

[4] R. W. Crompton and D. J. Sutton, Proc. Roy. Soc. (Lond.) A215, 467 (1952).

[5] Healey and Reed, op. cit.

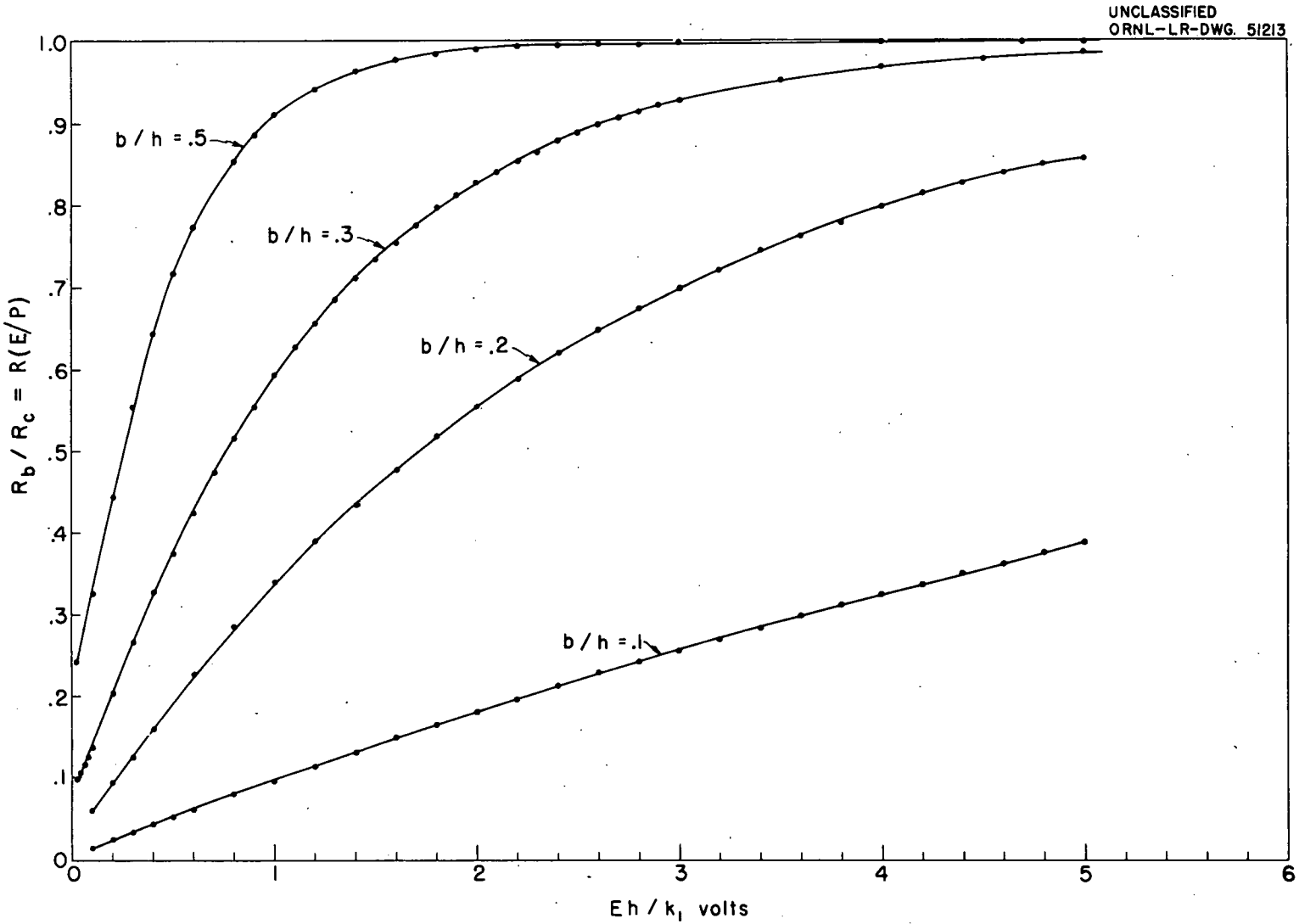

FIG. 2. CURVES SHOWING THE ELECTRON CURRENT RATIO R_b/R_c AS A FUNCTION OF Eh/k_1 FOR SEVERAL VALUES OF b/h.

UNCLASSIFIED
ORNL-LR-DWG. 56763

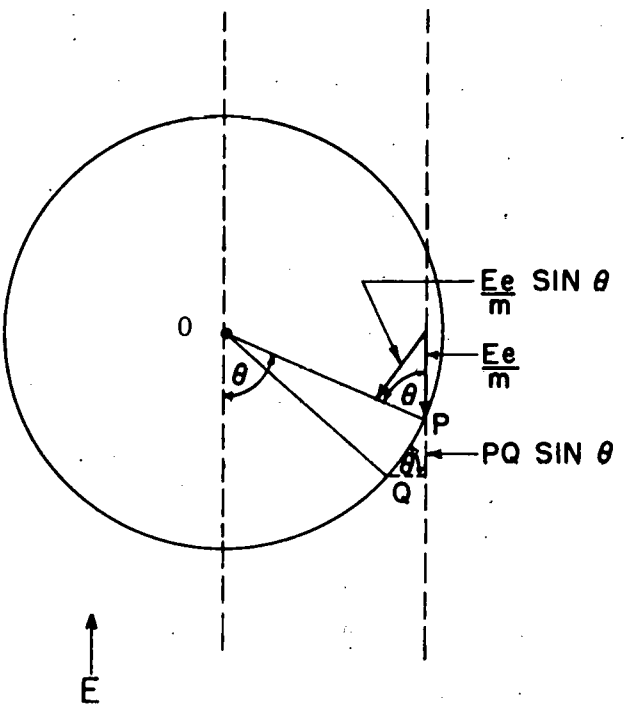

FIG. 3 DIAGRAM FOR OBTAINING DRIFT VELOCITY EXPRESSION.

it will traverse the path OQ. Since the drift velocity w, from experiment, is approximately 1/100 the agitational velocity, the curvature will be very slight and OP will approximately equal OQ, and the time of flight is still $\frac{\ell}{U}$. The displacement PQ is $\frac{1}{2}\left(\frac{Ee}{m}\right)\sin\theta\left(\frac{\ell}{U}\right)^2$. The displacement parallel to z is then $\frac{1}{2}\left(\frac{Ee}{m}\right)\sin^2\theta\left(\frac{\ell}{U}\right)^2$. Since the velocity of the electrons is much higher than that of the molecules, the latter are assumed to be fixed scatterers. If the further assumption is made that the electron energy does not exceed the lowest energy level of the molecules, the molecules may be considered as fixed elastic scatterers and all directions of motion after impact are equally probable. In such a case the probability of an electron being scattered into an angle between θ and $\theta + d\theta$ is

$$P(\theta)d\theta = \frac{(2\Pi v \sin\theta)vd\theta}{4\Pi v^2} = \frac{\sin\theta d\theta}{2} \qquad (34)$$

which is the ratio of an element of area of a sphere with radius v in velocity space to the total area of the sphere. The mean displacement in the direction of the field is then

$$\Delta z = \frac{\int_0^{\Pi} P(\theta)d\theta\left[\frac{1}{2}\left(\frac{Ee}{m}\right)\left(\frac{\ell}{U}\right)^2\sin^2\theta\right]}{\int_0^{\Pi} P(\theta)d\theta} = \frac{1}{3}\left(\frac{Ee}{m}\right)\left(\frac{\ell}{U}\right)^2. \qquad (35)$$

The average over the distribution in free paths is now taken. If F_o is

the number of electrons which start at the plane x = 0, and F is the number that arrive at a distance x without having made a collision, then $F = F_o e^{-\alpha x}$ is the distribution of free paths. Then, $F_o e^{-\alpha x} \alpha dx$ is the number of paths whose lengths lie between x and x + dx and the mean free path.

$$\bar{\ell} = \frac{1}{F_o} \int_0^\infty F_o e^{-\alpha x} \alpha x dx = \frac{1}{\alpha} . \tag{36}$$

The mean square of the free paths is

$$\overline{\ell^2} = \frac{1}{F_o} \int_0^\infty F_o e^{-x/\bar{\ell}} \frac{x^2}{\bar{\ell}} dx = 2\bar{\ell}^2 . \tag{37}$$

Therefore, Eq. (35) becomes

$$\overline{\Delta z} = \frac{2}{3} \left(\frac{Ee}{m} \right) \left(\frac{\bar{\ell}}{U} \right)^2 . \tag{38}$$

Dividing by the average time between collisions, $\frac{\bar{\ell}}{U}$, where the velocity U of all the electrons is still assumed to be the same,

$$w = \frac{\overline{\Delta z}}{\overline{\Delta t}} = \frac{2}{3} \frac{Ee}{m} \left(\frac{\bar{\ell}}{U} \right),$$

or, in the general case

$$w = \frac{2}{3}\frac{Ee}{m}\left(\overline{\frac{\ell}{U}}\right). \tag{39}$$

The assumption is now made that ℓ does not vary sharply with U which is a valid assumption for most of the gases studied but not for gases such as argon and methane whose Ramsauer effect gives a marked variation of cross section with energy. With this assumption, Eq. (39) becomes

$$w = \frac{2}{3}\frac{Ee}{m}\,\bar{\ell}\,\overline{[U^{-1}]}. \tag{40}$$

Taking the ratio of w to K,[6]

$$\frac{w}{K} = \frac{\frac{2}{3}\frac{Ee}{m}\,\bar{\ell}\,\overline{[U^{-1}]}}{\frac{1}{3}\,\bar{\ell}\,\bar{U}} = \frac{2Ee}{m}\,\frac{\overline{[U^{-1}]}}{\bar{U}} = \frac{Ee}{\frac{1}{2}\,m\overline{U^2}}\left[\frac{\overline{[U^{-1}]}\;\overline{[U^2]}}{\bar{U}}\right], \tag{41}$$

and since

$$k_T = \frac{\frac{1}{2}\,m\,\overline{U^2}}{\frac{1}{2}\,m\,\overline{\Omega^2}} = \frac{\frac{1}{2}\,m\,\overline{U^2}}{\frac{3}{2}\,kT},$$

where k is the gas constant per molecule then,

---

[6] L. G. H. Huxley and A. A. Zaazou, Proc. Roy. Soc. (Lond.) A196, 402 (1949).

$$\frac{w}{K} = \frac{2}{3}\frac{NeE}{k_T\, NkT}\left[\frac{\overline{[U^{-1}]}\ \overline{[U^2]}}{\bar{U}}\right] = \frac{NeE}{k_1\, P_o}\,, \tag{42}$$

or

$$\frac{w}{(KP)} = \frac{Ne}{k_1\, P_o}\left(\frac{E}{P}\right), \tag{43}$$

where P = experimental gas pressure, and $P_o = NkT$ = atmospheric pressure. This is the expression we derived earlier with $k_1 = Ak_T$ and

$$A = \frac{3}{2}\left[\frac{\bar{U}}{\overline{U^2}\ \overline{[U^{-1}]}}\right], \tag{44}$$

where now the electron distribution is not assumed to be the Maxwellian for which A = 1 and k_1 does equal k_T. Thus, with a given distribution function the dimensionless constant A may be found and from this the correct Townsend energy factor k_T when k_1 is given from experiment.

Using Eq. (40), the mean free path at unit pressure L is obtained. Since $\bar{\ell}$ is inversely proportional to the pressure,

$$L = P\bar{\ell} = \frac{3}{2}\frac{m}{e}\frac{w}{(E/P)}\frac{1}{\overline{[U^{-1}]}} = \frac{3}{2}\frac{m}{e}\frac{w}{(E/P)}\,\frac{\overline{[U^2]}^{\frac{1}{2}}}{\left[\overline{[U^2]}^{\frac{1}{2}}\ \overline{[U^{-1}]}\right]}\,. \tag{45}$$

Let us look at $\overline{[U^2]}^{\frac{1}{2}}$,

$$k_T = \frac{\frac{1}{2} m \overline{U^2}}{\frac{1}{2} m \overline{\Omega^2}} = \frac{m \overline{U^2}}{3 kT} ,$$

where k is the Boltzman constant, or

$$\overline{[U^2]}^{\frac{1}{2}} = (k_T)^{\frac{1}{2}} \left(\frac{3kT}{m}\right)^{\frac{1}{2}} = (k_1)^{\frac{1}{2}} \, 1.16 \times 10^7 \text{ cm/sec for a Maxwellian distribution, and}$$

$$\overline{[U^2]}^{\frac{1}{2}} = (k_1)^{\frac{1}{2}} \, 1.09 \times 10^7 \text{ cm/sec for a Druyvesteyn distribution.} \quad (46)$$

It should be noted here that several energy distributions have been derived for the motion of slow electrons in gases. The actual distribution should be quite complicated and should vary for each E/P ratio even when collisions can be assumed to be elastic. Two simpler distributions will be used in this paper to present data. The Maxwellian, which would require the electrons to be in thermal equilibrium with the molecules, is physically unrealistic because of the external electric force and is used merely as a comparison. The Druyvesteyn distribution will be discussed later. In spite of the simplifying assumptions which are made in its derivation, this distribution appears to be very close to the actual one. Even though the Maxwellian distribution is physically unrealistic, it will be noted that the average quantities calculated from both distributions differ only slightly. This is because A in Eq. (44) is 1 in the Maxwellian

case and 1.14 in the Druyvesteyn. Thus, although the energy distributions derived may be very different, they are narrow enough that their ratios in A are very close to the same and the interpretation of this experiment is not altered very much. Putting Eq. (46) into Eq. (45), the mean free path at unit pressure becomes

$$L = 7.20 \times 10^{-9} \frac{w\sqrt{k_1}}{E/P} \text{ cm Maxwellian,}$$

$$\text{at } T = 298^\circ \text{ K} \qquad (47)$$

$$L = 7.47 \times 10^{-9} \frac{w\sqrt{k_1}}{E/P} \text{ cm Druyvesteyn,}$$

where $\overline{[U^{-1}]}\ \overline{[U^2]}^{\frac{1}{2}} = 1.38$ and 1.24, respectively, for the Maxwellian and Druyvesteyn distributions.

Now,

$$U = \left[\frac{\bar{U}}{\overline{[U^2]}^{\frac{1}{2}}}\right] \overline{[U^2]}^{\frac{1}{2}}$$

$$\bar{U} = \sqrt{k_1}\ 1.07 \times 10^7 \text{ cm/sec Maxwellian} \qquad (48)$$

$$\bar{U} = \sqrt{k_1}\ 1.04 \times 10^7 \text{ cm/sec Druyvesteyn.}$$

The mean proportion of energy lost per collision η may be derived by equating the power $P = Eew$, which an electron gains from the electric field as it drifts through the gas, to the power dissipated in

molecular collisions where there is a steady state motion of the electrons. If $Q = \frac{1}{2} m \overline{U^2}$ equal the mean agitational energy of the electron, then ηQ is the overall energy lost per collision. $\eta Q \, \overline{U}/\overline{\ell}$ is the power dissipated per collision, or

$$\eta = \frac{Ee \, w \, \overline{\ell}}{Q \, \overline{U}} = \frac{2Ee \, w \, \overline{\ell}}{m \, \overline{U^2} \, \overline{U}} , \tag{49}$$

but

$$\overline{\ell} = \frac{3}{2}\left(\frac{m}{e}\right)\frac{w}{E}\overline{[U^2]}^{\frac{1}{2}}\left[\frac{1}{\overline{U^{-1}}\;\overline{[U^2]}^{\frac{1}{2}}}\right] .$$

Therefore,

$$\eta = \frac{Ee \, w}{\frac{1}{2} m \, \overline{U^2} \, \overline{U}}\left\{\frac{3}{2}\left(\frac{m}{e}\right)\frac{w}{E}\overline{[U^2]}^{\frac{1}{2}}\left[\frac{1}{\overline{U^{-1}}\;\overline{[U^2]}^{\frac{1}{2}}}\right]\right\} , \tag{50}$$

and

$$\eta = \frac{3w^2}{\overline{U^2}\left[\overline{U}\;\overline{U^{-1}}\right]} . \tag{51}$$

Using relations (46),

$$\begin{aligned} \eta &= 1.74 \times 10^{-14} \, (w^2/k_1) \quad \text{Maxwellian,} \\ \eta &= 2.14 \times 10^{-14} \, (w^2/k_1) \quad \text{Druyvesteyn,} \end{aligned} \tag{52}$$

where

$$\frac{1}{\bar{U}\,\overline{U^{-1}}} = 0.7874 \text{ Maxwellian}, \quad 0.8475 \text{ Druyvesteyn}.$$

Since the mass and diameter of the electron are much smaller than those of the molecule and the molecules are assumed to be fixed scatterers, the effective cross section for collision of electrons with molecules is

$$\sigma = \pi d^2 = \frac{1}{nL} \tag{53}$$

where n is the number of molecules per cc at 1 mm pressure, T = 298° K, and d is the effective radius for collision. Therefore,

$$\sigma = \frac{1}{3.24 \times 10^{-16}} \frac{1}{L} .$$

$$\sigma = 4.26 \times 10^{-9} \frac{E/P}{w\, k_1^{\frac{1}{2}}} \quad \text{Maxwellian,}$$

$$\sigma = 4.14 \times 10^{-9} \frac{E/P}{w\, k_1^{\frac{1}{2}}} \quad \text{Druyvesteyn.} \tag{54}$$

It has already been mentioned that two energy distributions have been used in discussion of data for this paper. The Maxwellian distribution would require the electrons to be in thermal equilibrium with the gas molecules and under the action of no external field. This distribution in speeds may be written,

$$f(v)dv = \left(\frac{m}{2\Pi kT} \right)^{3/2} e^{-\frac{mv^2}{2kT}} 4\Pi v^2 dv. \qquad (55)$$

Using $E_A = 3/2\ kT$, this becomes

$$f(v)dv = \frac{4}{(\Pi)^{\frac{1}{2}}} \left(\frac{3m}{4E_A} \right)^{3/2} e^{-\frac{3mv^2}{4E_A}} v^2 dv = \frac{4}{(\Pi)^{\frac{1}{2}}} \frac{1}{\alpha^3} e^{-\frac{v^2}{\alpha^2}} v^2 dv, \qquad (56)$$

where

$$\alpha = \left(\frac{4E_A}{3m} \right)^{\frac{1}{2}}.$$

The Druyvesteyn distribution has been derived by Druyvesteyn,[7] using a modification of Hertz's method and by Morse, Allis, and Lamar[8] and others, using treatments of the Boltzmann transport theory. Using the Boltzmann transport equation, Morse, Allis, and Lamar have obtained the Druyvesteyn law in the following form:

$$N(E)dE = \frac{2N\Gamma\ (5/4)^{3/2}}{\Gamma\ (3/4)^{5/2}} \frac{E^{1/2}}{E_A^{3/2}} \exp - \frac{E^2}{E_A^2} \left[\frac{\Gamma\ (5/4)}{\Gamma\ (3/4)} \right]^2 dE \qquad (57)$$

assuming only elastic collisions and constant cross section.

---

[7] M. J. Druyvesteyn, Physica 10, 61 (1930).

[8] P. M. Morse, W. P. Allis, and E. S. Lamar, Phys. Rev. 48, 412 (1935).

Using $E^2 = mv^2/2$, this becomes

$$f(v)\,dv = \left[\frac{m}{2}\,\frac{\Gamma\,(5/4)}{\Gamma\,(3/4)\;E_A}\right]^{3/2} \frac{4v^2}{\Gamma\,(3/4)}\, e^{-v^4\left[\frac{m\quad\Gamma\,(5/4)}{2\;E_A\;\Gamma\,(3/4)}\right]^2} dv\ , \quad (58)$$

where Γ is the gamma function, or

$$f(v)\,dv = \frac{4}{\Gamma\,(3/4)\;\beta^3}\, v^2\, e^{-v^4/\beta^4}\, dv\ , \quad (59)$$

where

$$\beta = \left[\frac{2\Gamma\,(3/4)\;E_A}{m\Gamma\,(5/4)}\right]^{\frac{1}{2}}\ .$$

To plot these two distributions on a convenient scale, let $\alpha = 1$, then $E_A/m = 3/4$, and $\beta = [2.028]^{\frac{1}{2}}$, assuming E_A to be the same for both distributions where $\Gamma\,(5/4) = 0.9064$ and $\Gamma\,(3/4) = 1.2254$. Using this α and β, Eqs. (56) and (59) become

$$\begin{aligned} f(v)\,dv &= \frac{4v^2}{(\Pi)^{\frac{1}{2}}}\, e^{-v^2}\, dv \quad \text{Maxwellian,} \\ f(v)\,dv &= \frac{4}{\Gamma\,(3/4)\;(1.424)^3}\, v^2\, e^{-v^4/(1.424)^4}\, dv \quad \text{Druyvesteyn.} \end{aligned} \quad (60)$$

Using Eq. (60), the two speed distributions are drawn in Fig. 4.at the same average energy E_A. Note that although their average energies

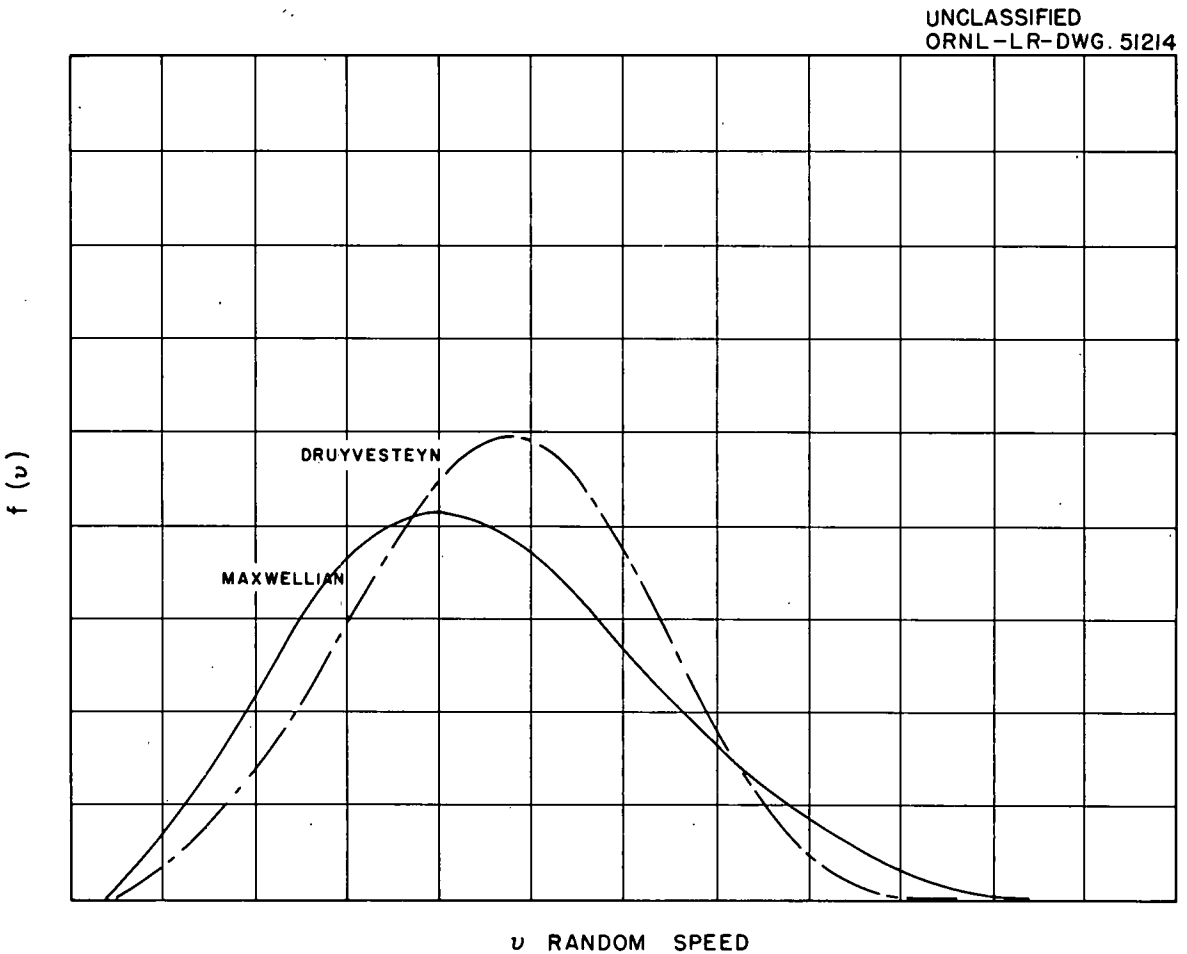

FIG. 4 THE MAXWELLIAN AND DRUYVESTEYN SPEED DISTRIBUTIONS PLOTTED AT THE SAME AVERAGE ENERGY.

are the same, the Druyvesteyn distribution has a sharper cut-off at the higher energy. The Maxwellian high energy tail would allow for ionization processes which are not actually observed in experiments. These distributions are only two of many which have been derived to describe the energy of slow electrons in gases. A historical summary of the various distribution laws is found in Loeb.[9]

---

[9] L. B. Loeb, Basic Processes of Gaseous Electrons (University of California Press, Berkeley and Los Angles, 1955).

CHAPTER III

APPARATUS AND METHOD

The apparatus for this experiment consisted essentially of a cylindrical plane electrode chamber, an electron source, a system of gas purification, and a vacuum tube electrometer for the measurement of very small currents.

Figure 5 is a diagram of the chamber used. It was a brass cylinder closed at the top end and sealed to its base with a teflon gasket and apiezon N grease. Six bolts held the cylinder tightly to the gasket. The field rings and plates were brass and were equally spaced at 1.5 cm on fluorathene insulators. A shield S was placed around the portion of the chamber lying above the small hole at 0 to prevent electrons from entering the chamber except through 0. All interior surfaces including field rings and electrodes were gold plated.

The upper field plate was held at its potential by a well-regulated 0 to (-) 500-volt D.C. Hewlett Packard model 711A power supply. The bottom three sections were held at their potential by a 0 to (-) 600-volt D.C. Fluke model 407 supply with a .05% long term stability. The E/P voltage across the height h of the last two sections was read with a Fluke differential voltmeter model 800 with accuracy better than $\pm$ 0.1%. Each field ring as shown in Fig. 5 was separated by a 0.5 megohm resistor. All electrical leads were connected into the chamber through vacuum type fittings and special

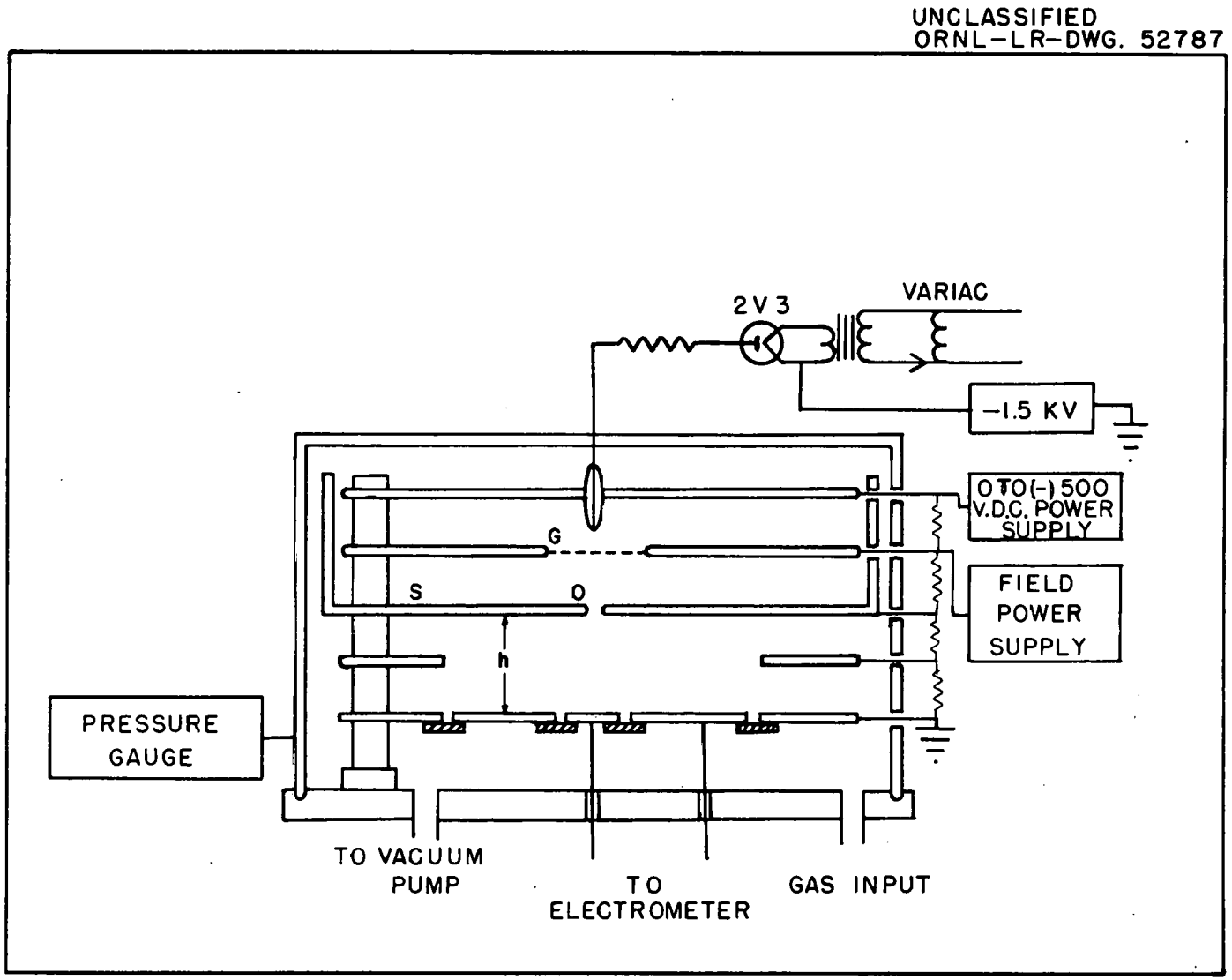

FIG. 5. SCHEMATIC DIAGRAM OF THE ELECTRON DIFFUSION CHAMBER

care was taken to see that there were no leaks about these connections. Wiring inside the chamber was teflon insulated to decrease outgassing.

The electron source (Fig. 6) was fastened at the top center of the chamber and extended through a hole in the first field plate to approximately 1 cm above the grid G (Fig. 7) located in the second plate. Two different types of sources were used. The negative corona discharge A in Fig. 6 was primarily used but it was found that hydrocarbon gases eventually caused a crust to be formed on the tungsten wire. For this reason the hot filament type source B was used at times to check results in the hydrocarbons and as an independent check at lower E/P values in CO_2. The negative corona source had a 5-mil tungsten wire tightly strung and completely enclosed in a purex glass sheath except for three small holes at the bottom to allow the electrons to escape. The glass sheath served to absorb ultraviolet radiation which would cause production of electrons elsewhere in the chamber. To prevent high voltage arc to the chamber or the first field plate, a teflon guard was placed around the lead-in wire and the top part of the source as seen in Fig. 6. To help eliminate corona discharge at the junction of the two wires in A, ceresin wax was used in the small cap at the top of the source. Crusting on the electron source did not occur or did not affect electron emission from a hot wire source such as the filament of a flashlight bulb. With this advantage it had the disadvantage of burning out after a short length of time in CO_2. The corona source was supplied by a New Jersey Electronics Corporation 0.5 to 2.5 K.V., D.C. negative voltage supply which was connected to

UNCLASSIFIED
ORNL-LR-DWG. 51215

A.

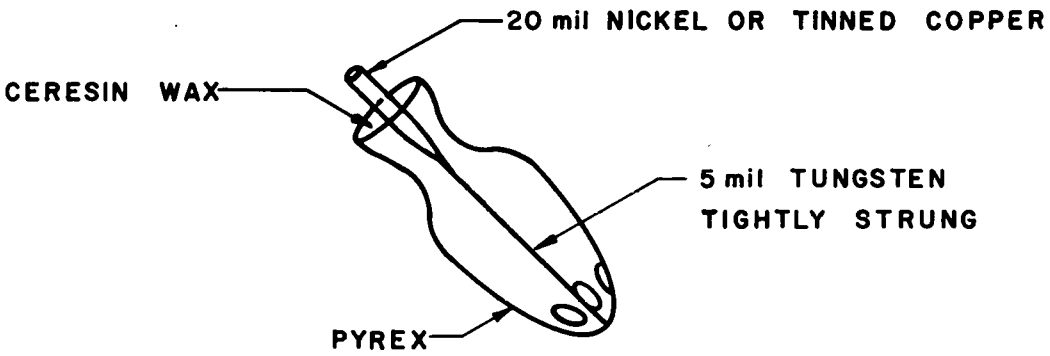

NEGATIVE CORONA DISCHARGE SOURCE

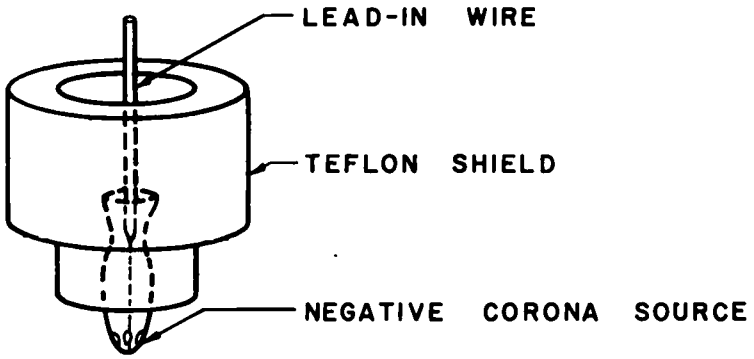

SHIELD FOR NEGATIVE CORONA SOURCE

B.

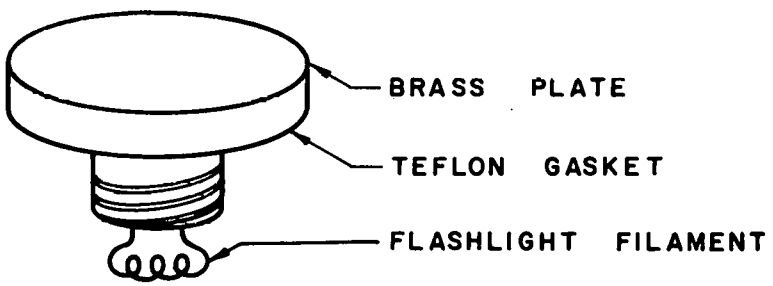

HOT FILAMENT SOURCE

FIG. 6 ELECTRON SOURCES USED IN DIFFUSION CHAMBER.

UNCLASSIFIED
ORNL-LR-DWG. 51216

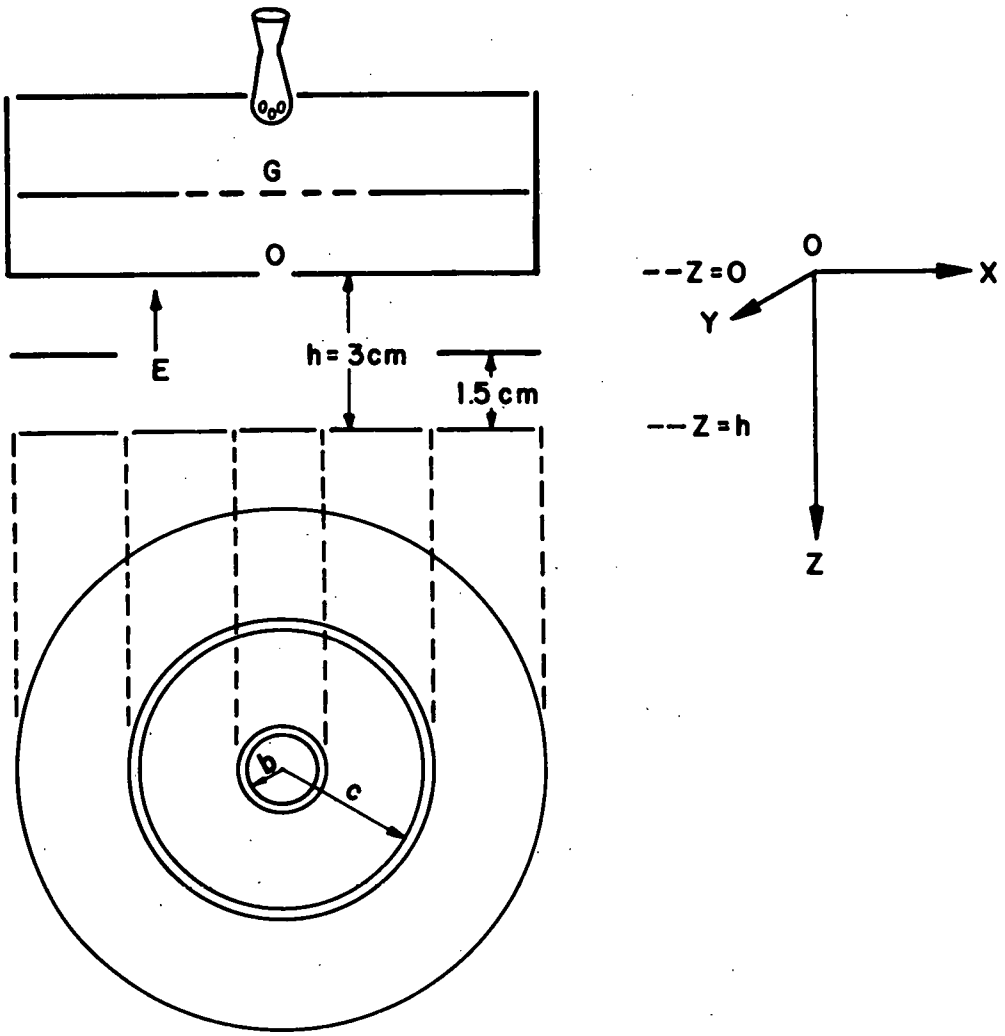

FIG. 7 DIAGRAM OF DIFFUSION CHAMBER AND ELECTRODE ARRANGEMENT

the cathode of a 2V3 current valve as seen in Fig. 5. This current valve limited the current from the source to the order of microamps. Since the majority of the electrons strike the guard rings or the chamber wall, only approximately 10^{-12} amps was read at the receiving electrodes in the bottom of the chamber. For currents of this magnitude, calculations show that the interaction of electrons with each other is negligible.

The two circular concentric receiving electrodes (Fig. 7) were located 3 cm beneath the source hole 0. The inner electrode of radius b was separated from the outer of radius c with a teflon strip and a 5-mil gap. Surrounding the outer electrode was a guard ring with a separation of 10 mils. The surfaces were flat to less than 0.005 in. and separations were better than 1 mil. The radius b of the inner electrode was varied with radii 0.3, 0.6, 0.9, and 1.5 cm to give different b/h ratios while the radius c was held constant at 4.5 cm. All radii were measured to the center of the separating gaps. Different b/h ratios were used according to the requirements of the gas and to give experimental check to the theoretical curves shown in Fig. 2. The radius b was always kept large enough to collect at least 30% or 40% of the total current striking both electrodes. Spurious results were often obtained when this was not done. Variations in b and h were found to be much more critical than variations in hole size at 0. In fact, data showed no measurable difference in k_1 with holes from 0.0145 in. to 0.052 in. at a constant b/h.

The electron current reaching the receiving electrodes was

measured by two methods, Fig. 8. For most of the measurements the currents were read directly using an E-H Research Laboratories feedback electrometer amplifier, model 201C, having a grid current of about 3×10^{-15} amps. This electrometer had a range of current reading from 10^{-6} to 3×10^{-14} amperes and the ranges used were 3×10^{-12} and 10^{-12} amperes. The readings were taken from a Brown recorder. The other method was the rate-of-drift method using a conventional vacuum tube electrometer and potentiometer. In this method the current was not read directly but as $i = C\,(dV/dt)$ where C is the capacitance in Fig. 8 and (dV/dt) is the change of voltage in a definite time, as taken from the potentiometer, to keep the potential on the capacitor C at zero. Since the ratios of currents were used, the value of C, as long as it is constant, does not matter.

The chamber was evacuated with a Cenco-Megovac pump in conjunction with an M.C.F. oil diffusion pump. An auxillary Welch Duo-Seal pump was used for "roughing" purposes in order to protect the diffusion pump and to keep water vapor out of the chamber. A Hastings thermocouple gauge was used to check for leaks and outgassing and to get an idea of the degree of vacuum. To measure gas pressures in the chamber a Wallace-Tiernan mechanical gauge calibrated against an oil manometer was employed. Merian No. D-3166 indicating oil with very low vapor pressure was used in the manometer. Different calibrations over a period of two months gave exact agreement.

The gas purification system is shown in Fig. 9. Although the purest commercial gases available were used, the marked error produced

UNCLASSIFIED
ORNL-LR-DWG. 51217

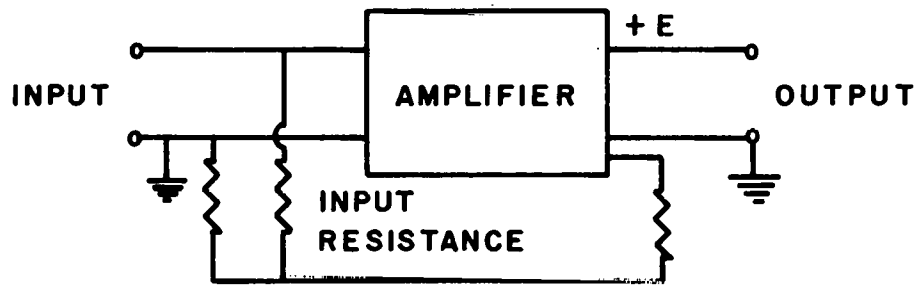

E-H ELECTROMETER AMPLIFIER WITH FEEDBACK. NEGATIVE FEEDBACK STABILIZES GAIN AND REDUCES INPUT IMPEDANCE.

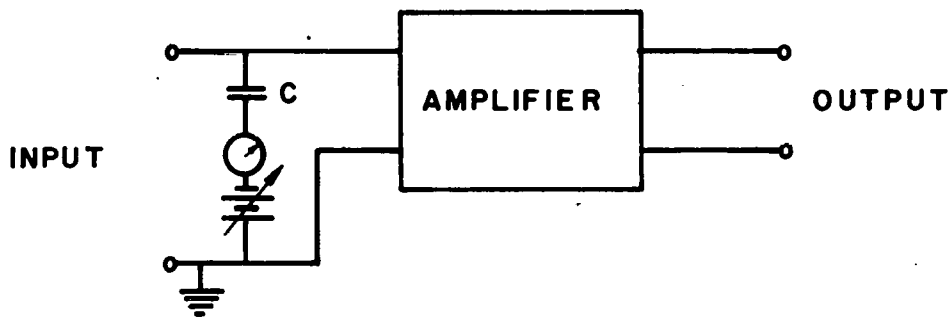

RATE-OF-DRIFT APPARATUS.
C REPLACES INPUT RESISTANCE

FIG.8 DIAGRAM OF METHODS USED FOR SMALL CURRENT MEASUREMENTS

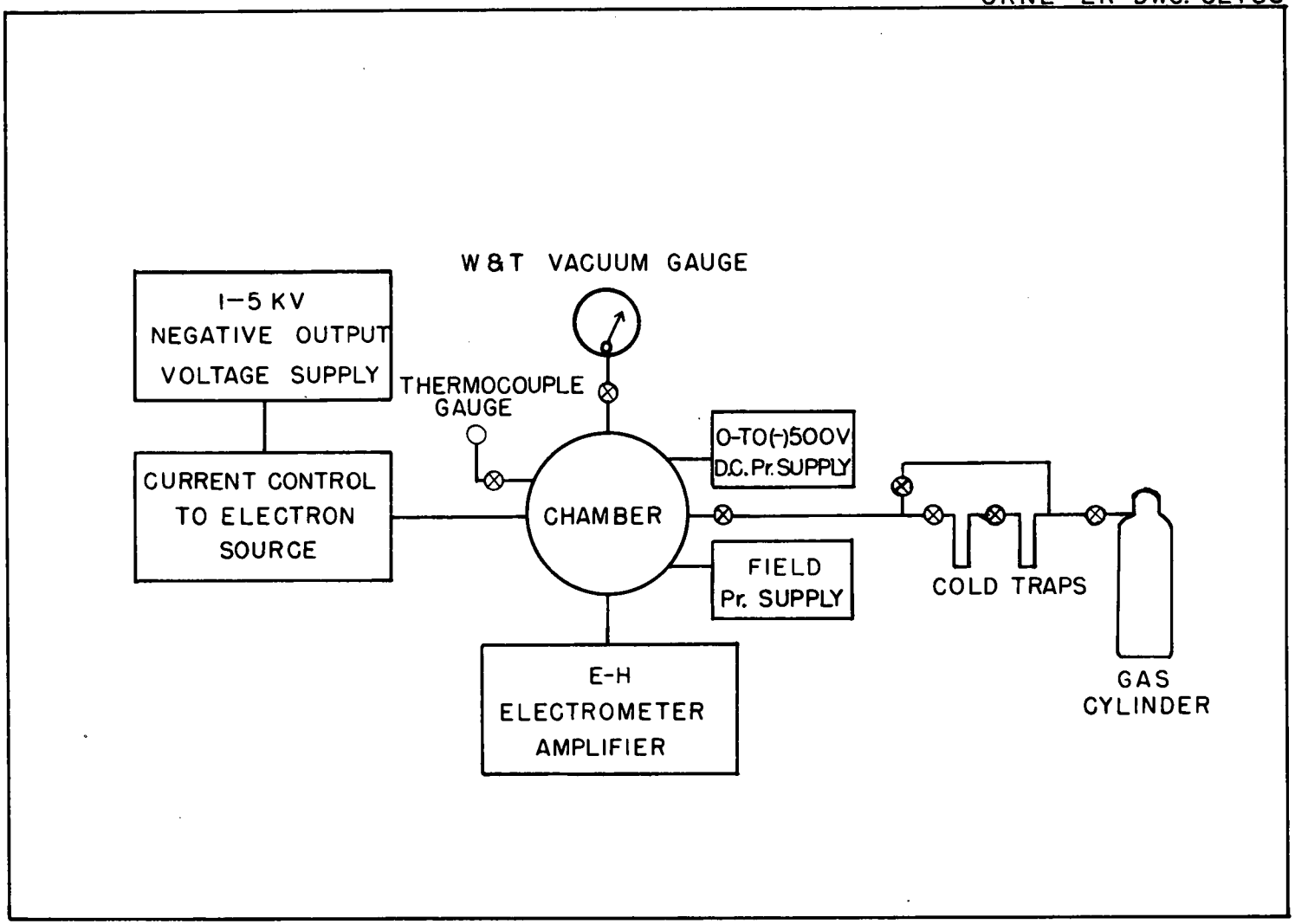

FIG. 9 SCHEMATIC DIAGRAM OF THE ELECTRON DIFFUSION EXPERIMENT

by small amounts of certain impurities (primarily due to attachment with electronegative impurites) made further purification necessary. Each gas was treated individually and appropriate methods of purification were used for the known impurities in the gas. The stated purities of the gases used were as follows: H_2 - 99.8%, CO_2 - 99.956%, CH_4 - 99.0%, C_2H_4 - 99.5%, C_3H_6 - 99.5%, and Ar - 99.994%. Most of these gases had previously been used in this laboratory for electron attachment and drift velocity studies. In the electron attachment studies electronegative impurities of one part per million could be detected. Purification could be monitored in this manner and certain purification techniques proved to be better than others. These methods were employed in the present experiment with a few modifications.

Initially the gas purity depends on the vacuum obtained for the entire apparatus including the valves on the gas cylinders. This was found to be a problem since most valves tested had a leak rate of 50 to 100 μ per hour. Valves were found, however, with leak rates less than 1 μ per hour. At the beginning of each day a check was made for a possible leak rate. After the chamber had been opened to the air it was sealed, outgassed with heat for two or three days, and checked with a helium leak detector. When clean and tight, the chamber showed an out-gas rate of only 0.3 μ per hour.

N_2, CO_2, CH_4, C_2H_4, C_3H_6, and Ar were further purified in cold traps cooled to liquid nitrogen temperature. These cold traps, Fig. 9, were 2-in. brass tubing 8 in. long. The gas being used was first forced under pressure into the cold trap nearest the cylinder. The top

part, including gases of higher vapor pressure, was pumped off slowly for about five minutes with the roughing pump. The gas was then transferred by convection to the second trap where the "roughing" process was repeated. Part of the gas was left in the first trap to be discarded. Hydrogen was purified by passage through a Barker and Company Deoxo Purifier which catalytically combined any oxygen present with the hydrogen to form water. It was then passed through a $Mg(ClO_4)_2$-filled drying tube and cooled in the liquid nitrogen trap. CO_2 was also run through this drying trap before cooling.

The following procedure was followed in taking data for all the gases except argon. The gas was first purified and the chamber and gauge were flushed several times with this gas. The current and accelerating voltages were adjusted until the correct magnitude of current was striking the electrodes. Four sets of the current ratios $i_b/(i_b + i_c)$ were taken for each E/P and various readings were repeated at intervals to help monitor purity in the gas. After a complete run the background current for each electrode was read with only the electron source turned off. This background was subtracted before determining the final ratio. Although there was frequently slow variation in both currents with time, the ratios were reproducible to within 1%. This drift in current caused no serious difficulty in computing the ratios from chart paper since both currents were extrapolated to the same time. The ratios were then applied to the theoretical curves of Eh/k_1 vs R at the given b/h to obtain k_1. These values, if theoretical assumptions are correct, should be only about

3% in error. Data were taken at different pressures and, when possible, at different b/h ratios. Diffusion and electrical breakdown in the gases put a limit on pressure and b/h variation. It was noticed also that erratic currents were obtained at higher purity. The following ranges of pressure were used: CH_4 - 3 to 7 mm, N_2 - 5 to 10 mm, C_2H_4 - 2 to 5 mm, H_2 - 4 to 10 mm, CO_2 - 4 to 8 mm, C_3H_6 - 5 to 20 mm, and Ar - 10 to 100 mm. In all the gases except argon the higher pressure could only be used in the lower E/P range.

The procedure for taking data in argon was somewhat different. The serious problem here was keeping the gas pure while going to and in the chamber since it was found that the order of 0.025% impurity caused as much as 25% change in the k_1 values. Because of the out-gas rate, data could only be taken for about eight to ten minutes before the k_1 ratios had dropped too much to even be compared with overlapping runs. Thus, only one ratio at a time was taken over eight-minute intervals with several overlappings to obtain the complete range of E/P. The apparatus used does not seem to be tight enough to give data in argon within 3% error. The data do, however, seem to be good enough and consistent enough to show certain definite phenomena which will be discussed later.

CHAPTER IV

RESULTS

The results are summarized in Tables I through VIII and in Figs. 10 through 57. w/K is the experimentally determined quantity, and k_T, the Townsend energy factor, is calculated for both the Maxwellian and Druyvesteyn distributions. w/K values are tabulated and plotted using the diffusion coefficient at unit pressure. The mean velocity $\bar{U}$, mean free path at unit pressure L, mean proportion of energy lost per collision η, and effective cross section σ are calculated only for the Druyvesteyn distribution using the relations in Table IX. Drift velocity data used in the calculation of L, η, and σ for N_2, CO_2, CH_4, C_2H_4, and C_3H_6 are those determined by Bortner, Hurst, and Stone;[1] the data of Nielsen and Bradbury[2] were used in the calculation of these quantities for H_2. Only the values of w/K and k_1 have been presented for argon.

The data for H_2 and N_2 are in good agreement with those of Crompton and Sutton.[3] The parameters using drift velocity differ somewhat in H_2 because of the different sources of w. Values of k_T

---

[1] T. E. Bortner, G. S. Hurst, and W. G. Stone, Rev. Sci. Instr. 28, 103 (1957).

[2] R. A. Nielsen and N. E. Bradbury, Phys. Rev. 49, 388 (1936).

[3] R. W. Crompton and D. J. Sutton, Proc. Roy. Soc. (Lond.) A215, 467 (1952).

TABLE I

SUMMARY OF RESULTS FOR HYDROGEN

$\frac{E/P}{\frac{\text{Volts}}{\text{cm/mm Hg}}}$	$\frac{w/K}{\text{cm}^{-1} \times \text{mm}^{-1}}$	Maxwellian $k_T = k_1$	Druyvesteyn $k_T = 0.875\ k_1$	Druyvesteyn $\bar{u} \times 10^{-7}$ cm/sec	$w \times 10^{-5}$ cm/sec	Druyvesteyn $L \times 10^{2}$ cm	Druyvesteyn $\eta \times 10$	Druyvesteyn $\sigma \times 10^{16}$ cm^2
0.2	2.31	3.37	2.95	1.91	4.8	3.29	1.46	9.39
0.4	3.09	5.04	4.41	2.33	6.6	2.77	1.85	11.2
0.6	3.46	6.75	5.91	2.70	8.0	2.59	2.03	11.9
0.8	3.74	8.34	7.30	3.00	9.0	2.43	2.08	12.7
1.0	3.97	9.82	8.59	3.26	9.9	2.32	2.14	13.3
1.2	4.20	11.1	9.74	3.47	10.7	2.22	2.20	13.9
1.4	4.40	12.4	10.8	3.66	11.7	2.20	2.37	14.0
1.6	4.63	13.5	11.8	3.82	12.6	2.16	2.52	14.3
1.8	4.85	14.5	12.6	3.95	13.6	2.15	2.74	14.4
2.0	5.05	15.4	13.5	4.08	14.3	2.10	2.84	14.7
2.5	5.48	17.8	15.5	4.38	16.1	2.03	3.12	15.2
3.0	5.92	19.7	17.3	4.62	18.0	1.99	3.51	15.5
3.5	6.23	21.9	19.1	4.86	19.6	1.96	3.76	15.8
4.0	6.65	23.4	20.5	5.03	21.3	1.93	4.15	16.0
4.5	7.00	25.0	22.0	5.20	23.0	1.91	4.52	16.2
5.0	7.24	26.9	23.6	5.40	24.5	1.90	4.77	16.3

TABLE II

SUMMARY OF RESULTS FOR NITROGEN

E/P Volts / cm/mm Hg	w/K cm^{-1} x mm^{-1}	Maxwellian $k_T = k_1$	Druyvesteyn $k_T=0.875\ k_1$	Druyvesteyn $\bar{U} \times 10^{-7}$ cm/sec	$w \times 10^{-5}$ cm/sec	Druyvesteyn $L \times 10^{2}$ cm	Druyvesteyn $\eta \times 10^{3}$	Druyvesteyn $\sigma \times 10^{16}$ cm^2
0.2	1.01	7.70	6.74	2.88	3.75	3.88	3.91	7.96
0.4	1.16	13.4	11.7	3.81	4.61	3.15	3.39	9.81
0.6	1.28	18.3	16.0	4.45	5.45	2.90	3.47	10.7
0.8	1.42	22.0	19.3	4.89	6.38	2.80	3.96	11.0
1.0	1.60	24.3	21.3	5.13	7.31	2.69	4.71	11.5
1.2	1.78	26.3	23.0	5.33	8.21	2.62	5.49	11.8
1.4	1.95	27.9	24.4	5.49	9.09	2.56	6.34	12.1
1.6	2.13	29.2	25.6	5.62	10.0	2.52	7.33	12.3
1.8	2.31	30.4	26.6	5.73	10.9	2.50	8.36	12.4
2.0	2.48	31.4	27.5	5.83	11.8	2.47	9.50	12.5
2.5	2.85	34.2	29.9	6.08				
3.0	3.30	35.4	31.0	6.19				
3.5	3.61	37.8	33.1	6.39				
4.0	4.04	38.6	33.8	6.46				
4.5	4.38	40.0	35.0	6.58				
5.0	4.76	40.9	35.8	6.65				

TABLE III

SUMMARY OF RESULTS FOR CARBON DIOXIDE

$\frac{E/P}{\text{Volts}/\text{cm mm Hg}}$	w/K $\text{cm}^{-1} \times \text{mm}^{-1}$	Maxwellian $k_T = k_1$	Druyvesteyn $k_T = 0.875\ k_1$	Druyvesteyn $\bar{U} \times 10^{-7}$ cm/sec	$w \times 10^{-5}$ cm/sec	Druyvesteyn $L \times 10^{2}$ cm	Druyvesteyn $\eta \times 10^{2}$	Druyvesteyn $\sigma \times 10^{16}$ cm^2
0.8	13.6	2.29	2.00	1.57	4.00	5.65	1.50	5.47
1.0	16.6	2.34	2.05	1.59	5.00	5.71	2.29	5.41
1.2	19.3	2.42	2.12	1.62	5.90	5.72	3.09	5.40
1.4	22.4	2.43	2.13	1.62	7.00	5.82	4.32	5.31
1.6	24.7	2.52	2.21	1.65	8.00	5.83	5.43	5.21
1.8	26.6	2.64	2.31	1.69	9.00	6.07	6.57	5.09
2.0	28.5	2.73	2.39	1.72				
2.5	31.3	3.11	2.72	1.83				
3.0	32.8	3.56	3.12	1.96				
3.5	31.6	4.31	3.77	2.16				
4.0	29.2	5.34	4.67	2.40				
4.5	25.3	6.94	6.07	2.74				
5.0	21.7	8.97	7.85	3.11				

TABLE IV

SUMMARY OF RESULTS FOR METHANE

$\frac{E/P}{\text{Volts}/\text{cm mm Hg}}$	w/K $\text{cm}^{-1} \times \text{mm}^{-1}$	Maxwellian $k_T = k_1$	Druyvesteyn $k_T = 0.875\ k_1$	Druyvesteyn $\bar{U} \times 10^{-7}$ cm/sec	$w \times 10^{-5}$ cm/sec	Druyvesteyn $L \times 10^{2}$ cm	Druyvesteyn $\eta \times 10^{2}$	Druyvesteyn $\sigma \times 10^{16}$ cm^2
0.2	3.17	2.46	2.15	1.63	25.5	14.9	5.65	2.07
0.4	4.13	3.77	3.30	2.02	60.0	21.8	20.4	1.42
0.6	4.65	5.02	4.39	2.33	81.3	22.7	28.2	1.36
0.8	4.66	6.69	5.85	2.69	95.2	23.0	29.0	1.34
1.0	4.53	8.59	7.52	3.05	99.8	21.9	24.8	1.41
1.2	4.49	10.4	9.10	3.36	100.	20.1	20.6	1.54
1.4	4.34	12.6	11.0	3.69	100.	18.9	17.0	1.63
1.6	4.18	14.9	13.1	4.02	100.	18.0	14.4	1.71
1.8	4.02	17.4	15.2	4.34				
2.0	3.92	19.9	17.4	4.64				
2.5	3.71	26.2	22.9	5.33				
3.0	3.46	33.8	29.6	6.04				
3.5	3.40	40.1	35.1	6.58				
4.0	3.24	48.1	42.0	7.21				
4.5	3.27	53.6	46.9	7.61				
5.0	3.19	61.0	53.4	8.12				

TABLE V

SUMMARY OF RESULTS FOR ETHYLENE

$\frac{E/P}{\text{Volts}/\text{cm/mm Hg}}$	w/K $\text{cm}^{-1} \times \text{mm}^{-1}$	Maxwellian $k_T = k_1$	Druyvesteyn $k_T = 0.875\ k_1$	Druyvesteyn $\bar{U} \times 10^{-7}$ cm/sec	$w \times 10^{-5}$ cm/sec	Druyvesteyn $L \times 10^2$ cm	Druyvesteyn $\eta \times 10^2$	Druyvesteyn $\sigma \times 10^{16}$ cm^2
0.4	5.77	2.70	2.36	1.71	26.6	8.16	5.61	3.79
0.6	8.08	2.89	2.53	1.77	33.1	7.01	8.11	4.41
0.8	9.67	3.22	2.82	1.87	38.2	6.40	9.70	4.83
1.0	11.0	3.55	3.11	1.96	40.2	5.66	9.74	5.46
1.2	11.7	4.00	3.50	2.08	41.6	5.18	9.26	5.97
1.4	12.5	4.37	3.82	2.17	42.4	4.73	8.80	6.53
1.6	12.7	4.90	4.29	2.30				
1.8	13.0	5.41	4.73	2.42				
2.0	13.5	5.75	5.03	2.49				
2.5	13.4	7.25	6.34	2.80				
3.0	12.8	9.13	7.99	3.14				
3.5	12.6	10.8	9.48	3.42				
4.0	12.1	12.9	11.3	3.74				
4.5	11.7	15.0	13.1	4.02				
5.0	11.5	16.9	14.8	4.27				

TABLE VI

SUMMARY OF RESULTS FOR CYCLOPROPANE

$\frac{E/P}{\text{Volts}/\text{cm/mm Hg}}$	w/K $\text{cm}^{-1} \times \text{mm}^{-1}$	Maxwellian $k_T = k_1$	Druyvesteyn $k_T = 0.875\ k_1$	Druyvesteyn $\bar{U} \times 10^{-7}$ cm/sec	$w \times 10^{-5}$ cm/sec	Druyvesteyn $L \times 10^2$ cm	Druyvesteyn $\eta \times 10^2$	Druyvesteyn $\sigma \times 10^{16}$ cm^2
0.2	2.75	2.83	2.48	1.75	13.9	8.73	1.46	3.54
0.4	5.37	2.90	2.54	1.77	22.9	7.29	3.87	4.24
0.6	7.28	3.21	2.81	1.86	28.0	6.25	5.23	4.94
0.8	8.82	3.53	3.09	1.95	31.3	5.49	5.94	5.63
1.0	9.74	4.00	3.50	2.08	33.6	5.02	6.04	6.16
1.2	10.7	4.38	3.83	2.18	34.3	4.47	5.75	6.91
1.4	11.5	4.73	4.14	2.26	35.0	4.06	5.54	7.61
1.6	12.2	5.09	4.45	2.35				
1.8	12.7	5.52	4.83	2.44				
2.0	13.1	5.97	5.22	2.54				
2.5	14.1	6.95	6.08	2.74				
3.0	14.5	8.07	7.06	2.95				
3.5	14.9	9.15	8.01	3.15				
4.0	15.3	10.2	8.93	3.32				
4.5	15.4	11.4	9.95	3.50				
5.0	15.4	12.7	11.1	3.70				

TABLE VII

SUMMARY OF RESULTS FOR ARGON (b/h = C.3)

E/P	10 mm		20 mm		40 mm		60 mm	
Volts/cm mm Hg	k_1	w/K cm^{-1} x mm^{-1}	k_1	w/K cm^{-1} x mm^{-1}	k_1	w/K cm^{-1} x mm^{-1}	k_1	w/K cm^{-1} x mm^{-1}
0.2					96	0.081	117	0.067
0.4					159	0.098	190	0.082
0.6			167	0.140	214	0.109	247	0.095
0.8			203	0.153	263	0.118	304	0.102
1.0			230	0.169	304	0.128	359	0.108
1.21	212	0.222	265	0.178	328	0.144	411	0.115
1.44	248	0.226	292	0.192	371	0.151	446	0.126
1.69	256	0.257	316	0.208	392	0.168	475	0.138
1.96	257	0.297	315	0.242	402	0.190	516	0.148
2.25	276	0.317	325	0.269	411	0.213	552	0.159
2.56	273	0.365	318	0.313	437	0.228		
2.89	273	0.412	316	0.356	461	0.244		
3.24	267	0.472	326	0.387	524	0.241		
4.0	277	0.562	328	0.475	662	0.235		
4.5	275	0.637	338	0.518				
5.0	280	0.695	353	0.551				

TABLE VIII

SUMMARY OF RESULTS FOR ARGON (b/h = 0.5)

E/P	10 mm		20 mm		40 mm		60 mm		100 mm	
Volts/cm mm Hg	k_1	w/K cm^{-1} x mm^{-1}	k_1	w/K cm^{-1} x mm^{-1}	k_1	w/K cm^{-1} x mm^{-1}	k_1	w/K cm^{-1} x mm^{-1}	k_1	w/K cm^{-1} x mm^{-1}
0.05									82	0.024
0.10							111	0.035	113	0.034
0.15					132	0.044	131	0.045	147	0.040
0.20					139	0.056	154	0.051	173	0.045
0.4			171	0.091	212	0.073	241	0.065	268	0.058
0.6			217	0.108	276	0.085	315	0.074	362	0.065
0.8			257	0.121	336	0.093	390	0.080	460	0.068
1.0	294	0.132	292	0.133	382	0.102	451	0.086	535	0.073
1.21	325	0.145	337	0.140	426	0.111	538	0.088	605	0.078
1.44	349	0.161	365	0.154	472	0.119	601	0.093	714	0.079
1.69	336	0.196	373	0.176	520	0.126	677	0.097		
1.96	330	0.231	354	0.215	560	0.136	743	0.103		
2.25	326	0.269	360	0.243	595	0.147	802	0.109		
2.56	316	0.315	369	0.270	643	0.155	854	0.117		
2.89	303	0.371	367	0.306	692	0.163				
3.24	306	0.412	377	0.334	776	0.163				
3.61	302	0.465	392	0.358	890	0.158				
4.0	308	0.505	401	0.388	1010	0.154				
4.5	311	0.563	442	0.396						
5.0	317	0.614	501	0.388						

TABLE IX

QUANTITIES DEPENDENT ON THE DISTRIBUTION OF VELOCITIES IN THE ELECTRON SWARM*

	Velocity Distribution	
	Maxwell	Druyvesteyn
Townsend energy factor, k_T	$k_T = k_1$	$k_T = 0.875\ k_1$
Root-mean-square velocity, $(\overline{U^2})^{\frac{1}{2}}$	$(\overline{U^2})^{\frac{1}{2}} = 1.16 \times 10^7\ k_1^{\frac{1}{2}}$	$(\overline{U^2})^{\frac{1}{2}} = 1.09 \times 10^7\ k_1^{\frac{1}{2}}$
Mean electron velocity, $\overline{U}$	$\overline{U} = 1.07 \times 10^7\ k_1^{\frac{1}{2}}$	$\overline{U} = 1.04 \times 10^7\ k_1^{\frac{1}{2}}$
Mean free path at unit pressure, L	$L = 7.20 \times 10^{-9} \frac{w\ k_1^{\frac{1}{2}}}{E/P}$	$L = 7.47 \times 10^{-9} \frac{w\ k_1^{\frac{1}{2}}}{E/P}$
Average energy loss per collision, η	$\eta = 1.74 \times 10^{-14}\ w^2/k_1$	$\eta = 2.14 \times 10^{-14}\ w^2/k_1$
Gas kinetic cross section, σ	$\sigma = 4.26 \times 10^{-9} \frac{E/P}{w\ k_1^{\frac{1}{2}}}$	$\sigma = 4.14 \times 10^{-9} \frac{E/P}{w\ k_1^{\frac{1}{2}}}$

*The numerical factors are computed for w in cm/sec, E/P in volts/cm/mm Hg, and T = 298° K.

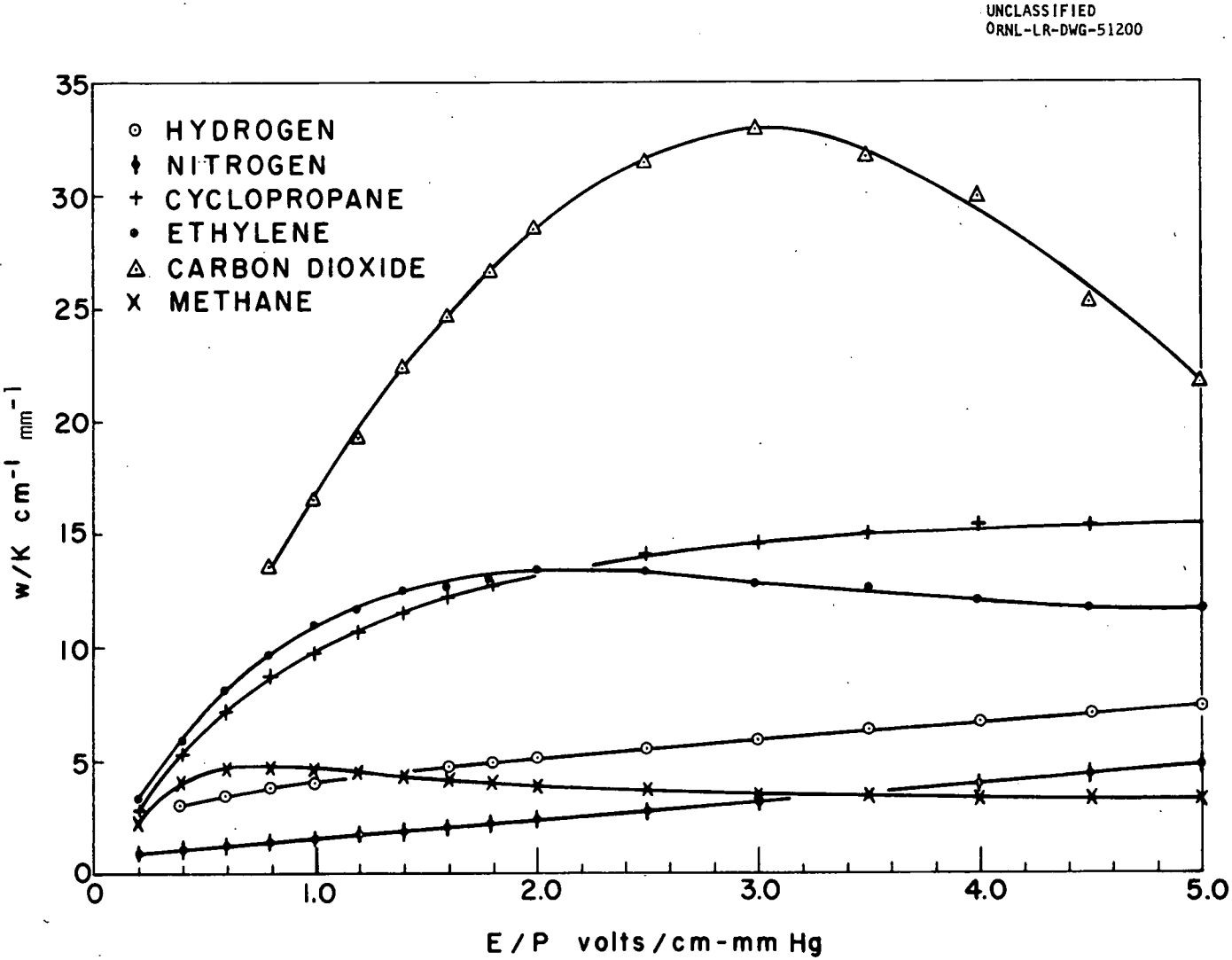

FIG. 10. W/K Vs. E/P FOR HYDROGEN, NITROGEN, CYCLOPROPANE, ETHYLENE, CARBON DIOXIDE AND METHANE.

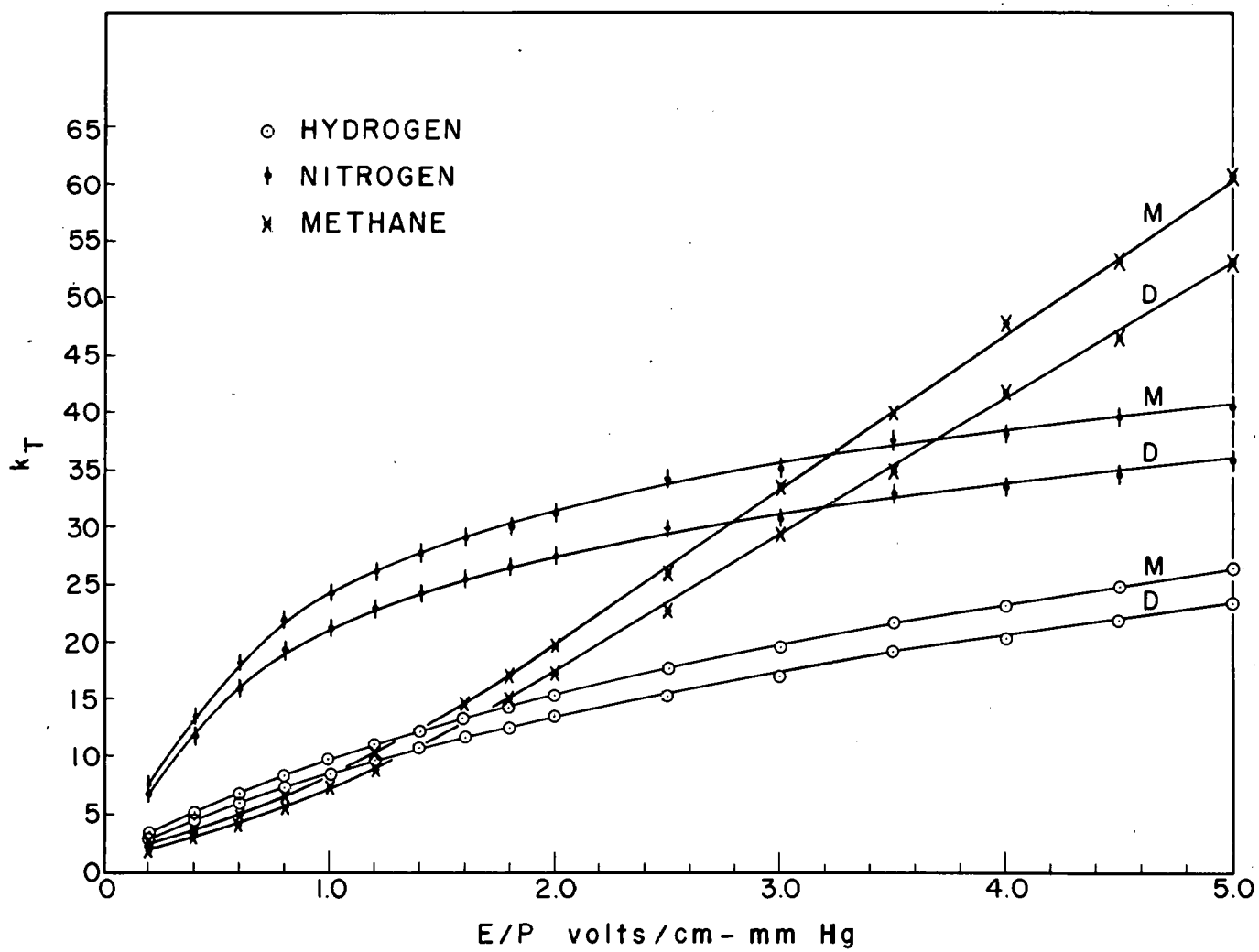

FIG. 11. TOWNSEND ENERGY FACTOR k_T Vs. E/P FOR HYDROGEN, NITROGEN AND METHANE USING THE MAXWELLIAN AND THE DRUYVESTEYN DISTRIBUTIONS.

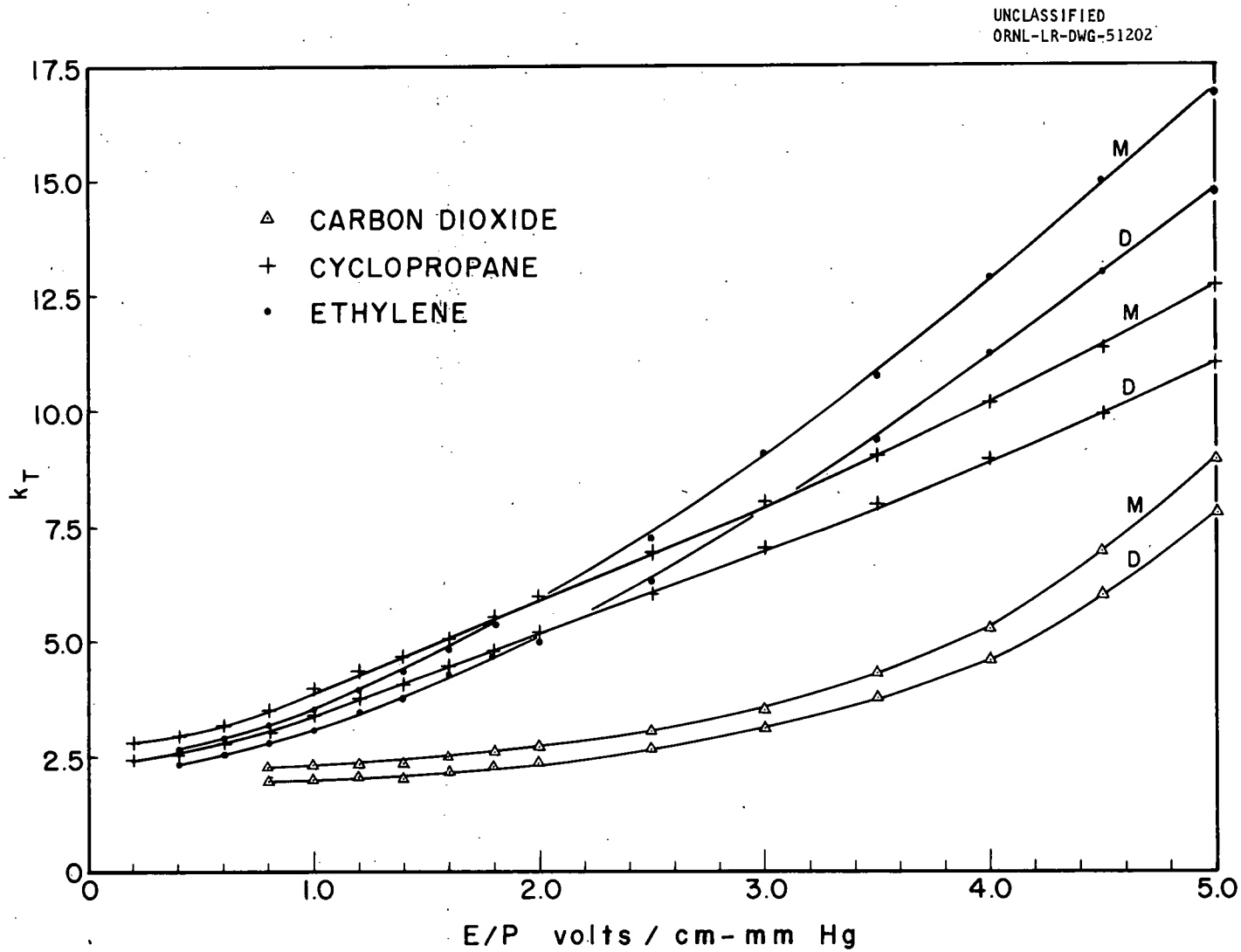

FIG. 12. TOWNSEND ENERGY FACTOR k_T Vs. E/P FOR CARBON DIOXIDE, CYCLOPROPANE AND ETHYLENE USING THE MAXWELLIAN AND THE DRUYVESTEYN DISTRIBUTIONS.

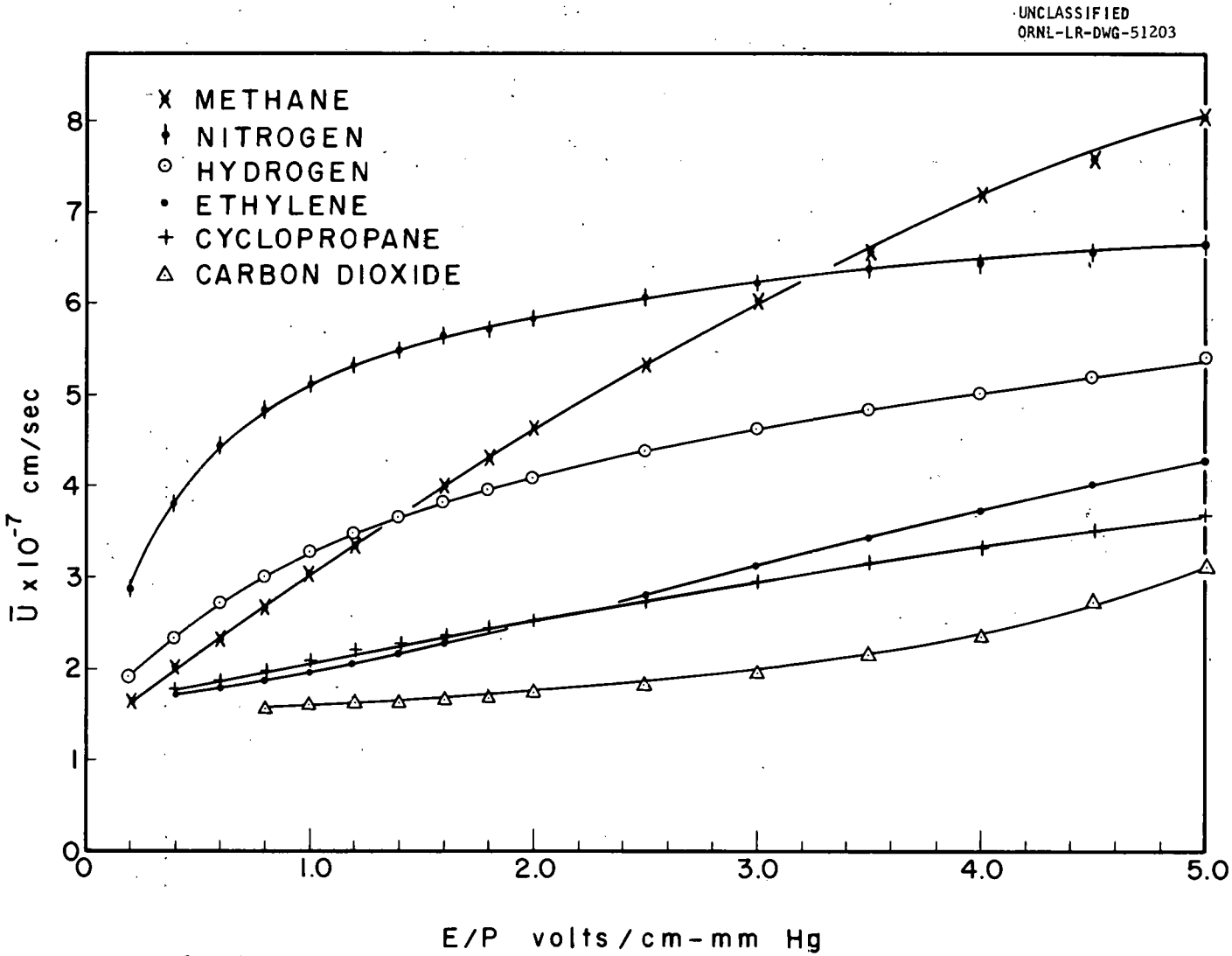

FIG. 13. $\bar{U}$ Vs. E/P FOR METHANE, NITROGEN, HYDROGEN, ETHYLENE, CYCLOPROPANE AND CARBON DIOXIDE USING THE DRUYVESTEYN DISTRIBUTION.

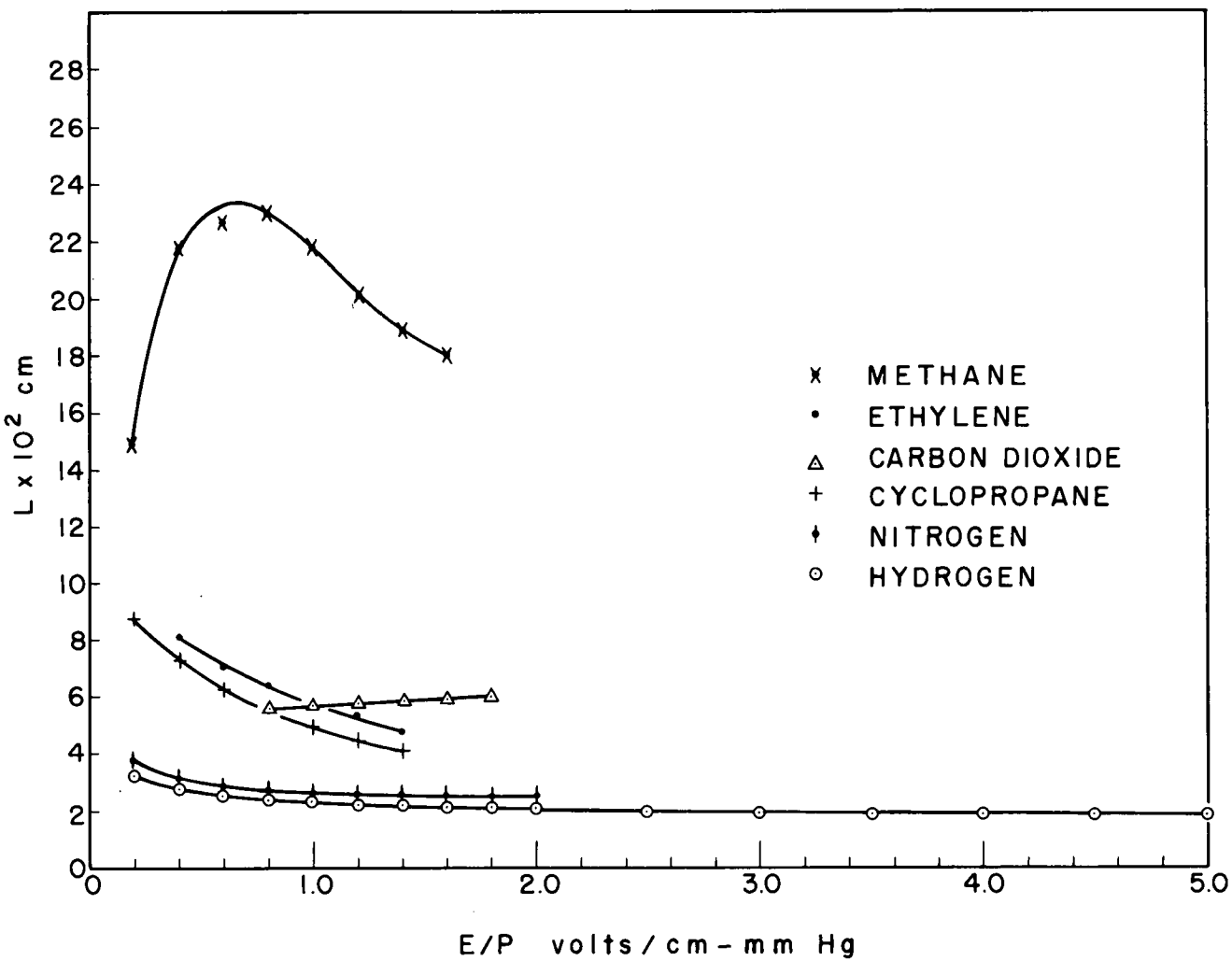

FIG. 14. L Vs. E/P FOR METHANE, ETHYLENE, CARBON DIOXIDE, CYCLOPROPANE, NITROGEN AND HYDROGEN USING THE DRUYVESTEYN DISTRIBUTION.

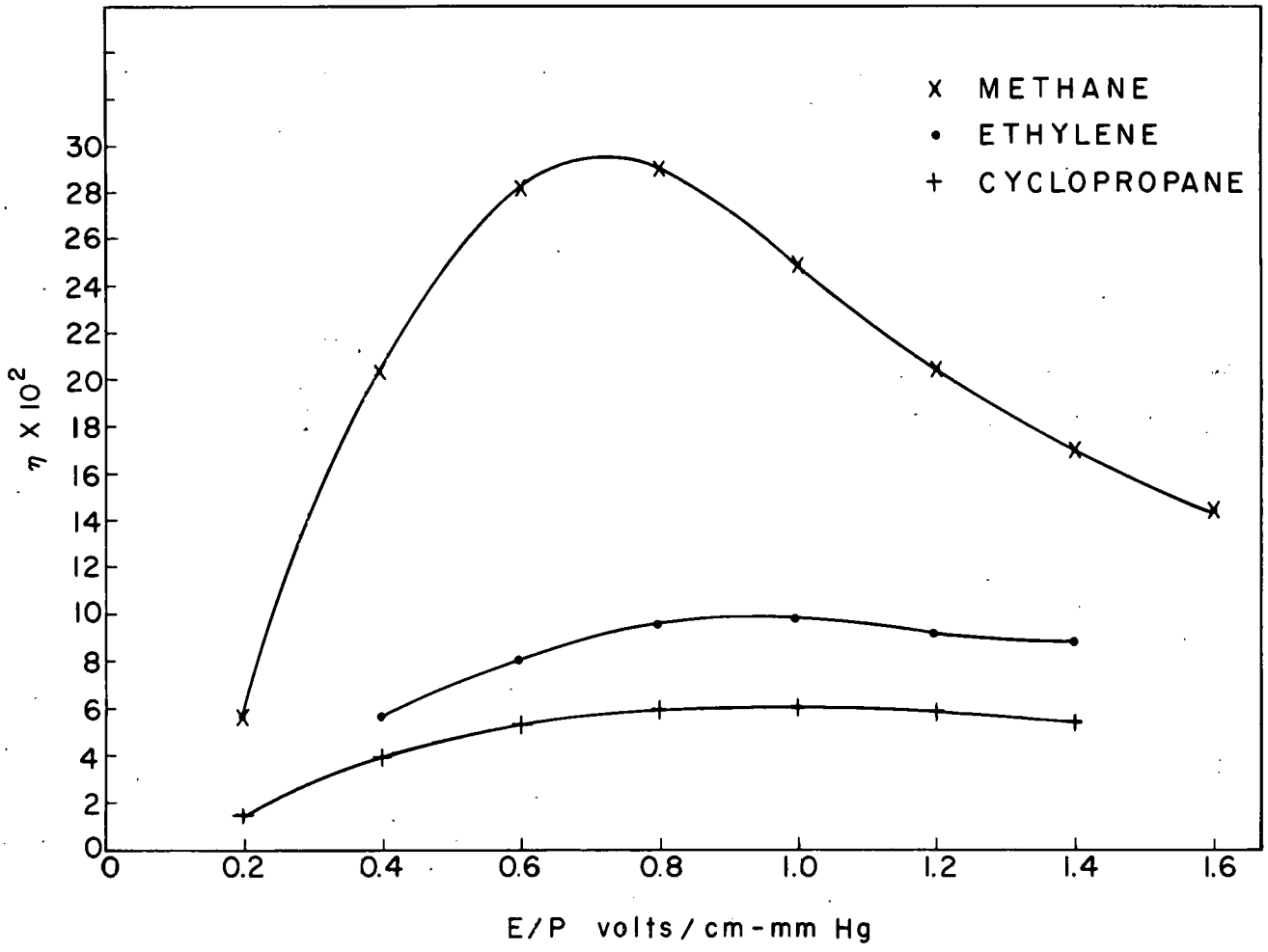

FIG. 15. η Vs. E/P FOR METHANE, ETHYLENE AND CYCLOPROPANE USING THE DRUYVESTEYN DISTRIBUTION.

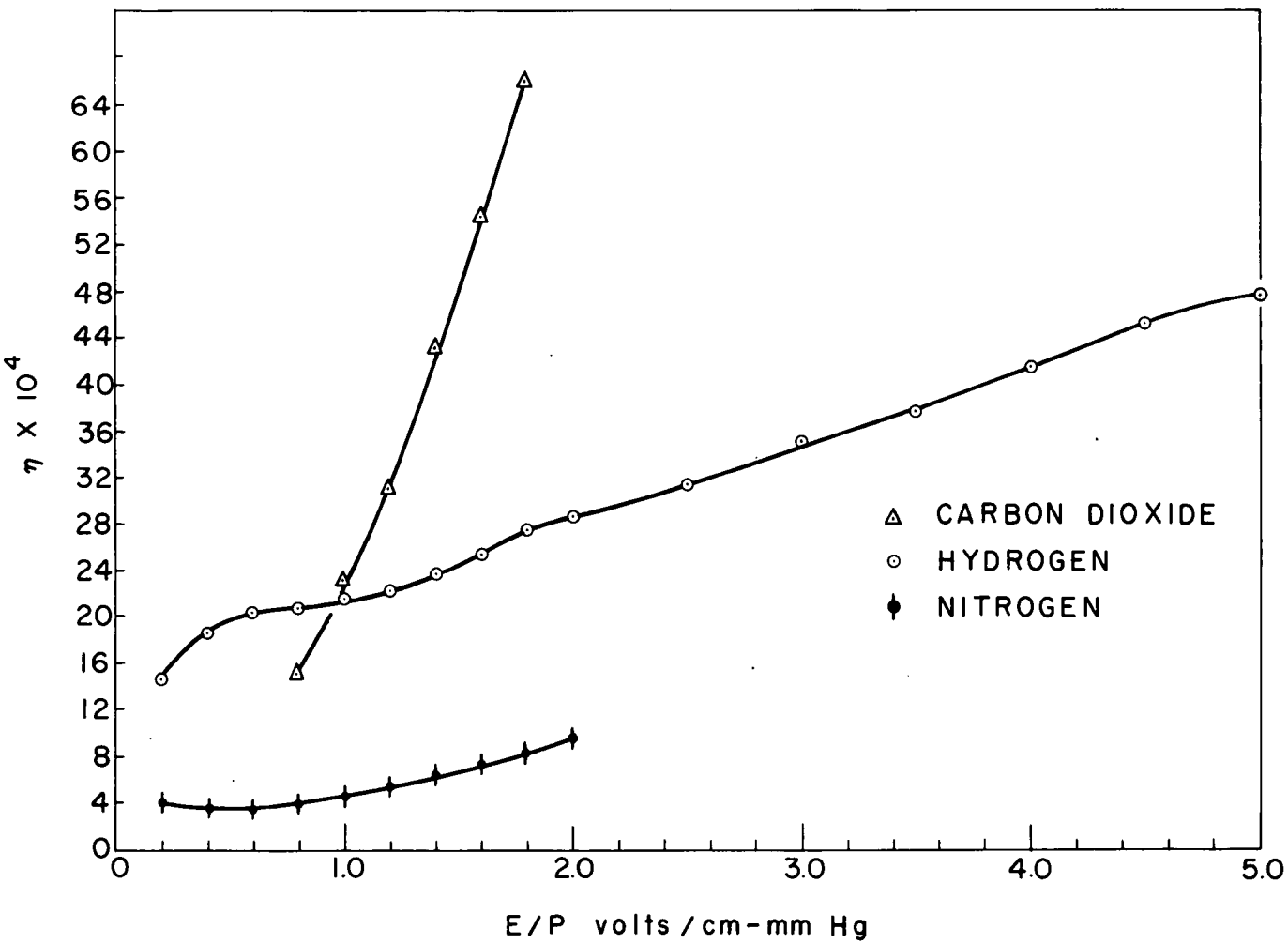

FIG. 16. η Vs. E/P FOR CARBON DIOXIDE, HYDROGEN AND NITROGEN USING THE DRUYVESTEYN DISTRIBUTION.

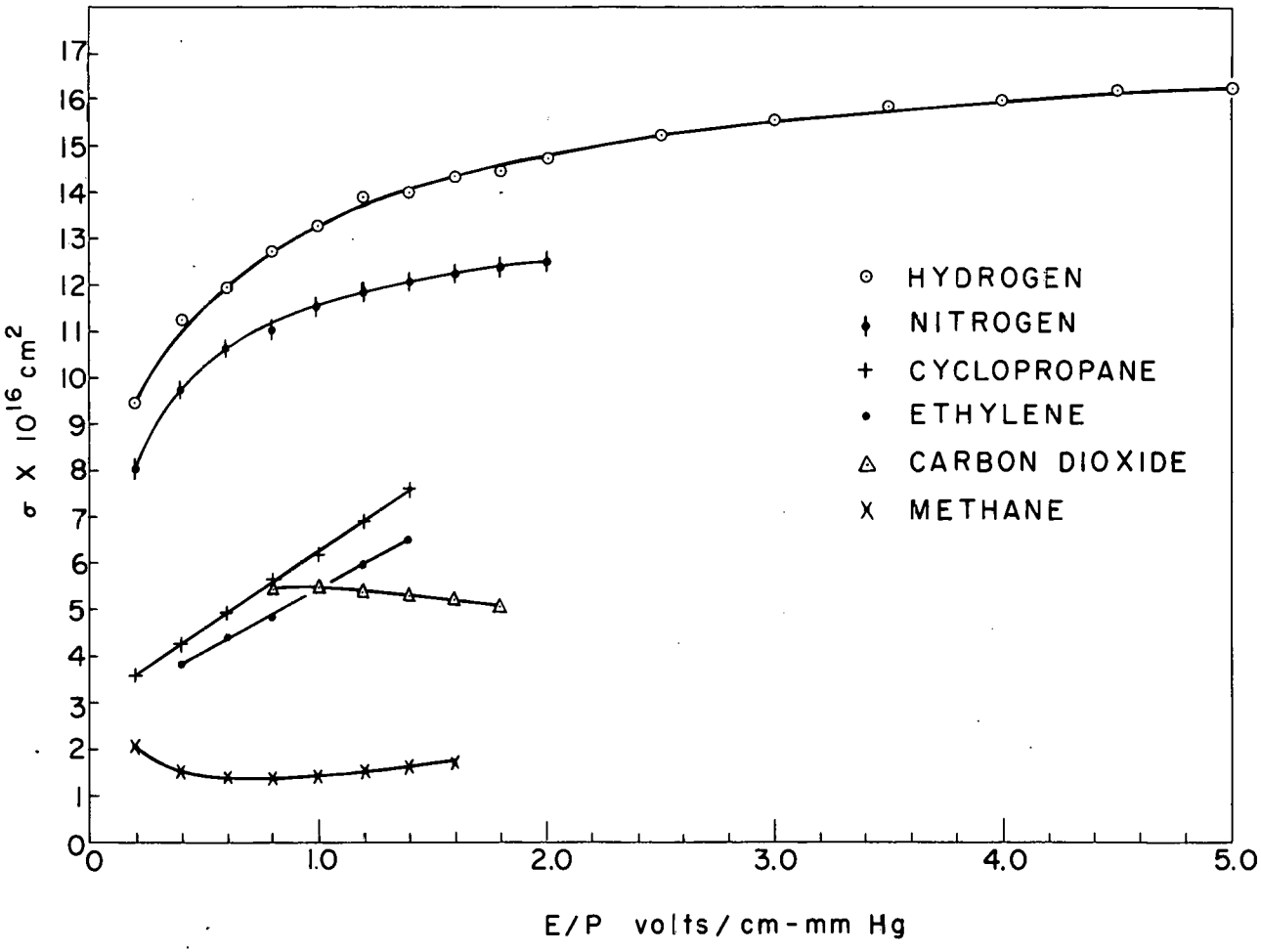

FIG. 17. COLLISION CROSS SECTION σ Vs. E/P FOR HYDROGEN, NITROGEN, CYCLOPROPANE, ETHYLENE, CARBON DIOXIDE, AND METHANE USING THE DRUYVESTEYN DISTRIBUTION.

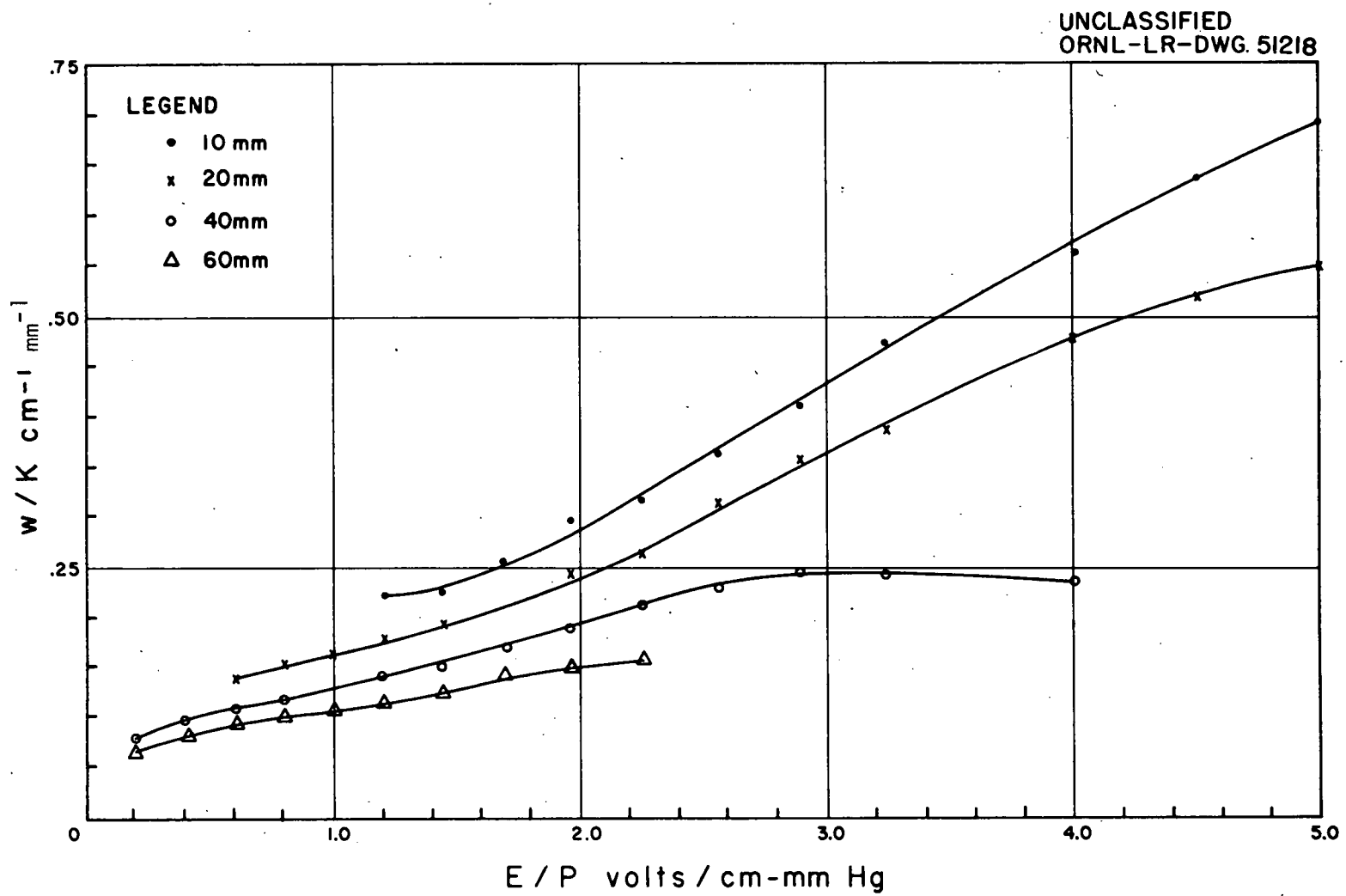

FIG. 18. w/K Vs. E/P FOR ARGON AT VARIOUS PRESSURES AND b/h = 0.3.

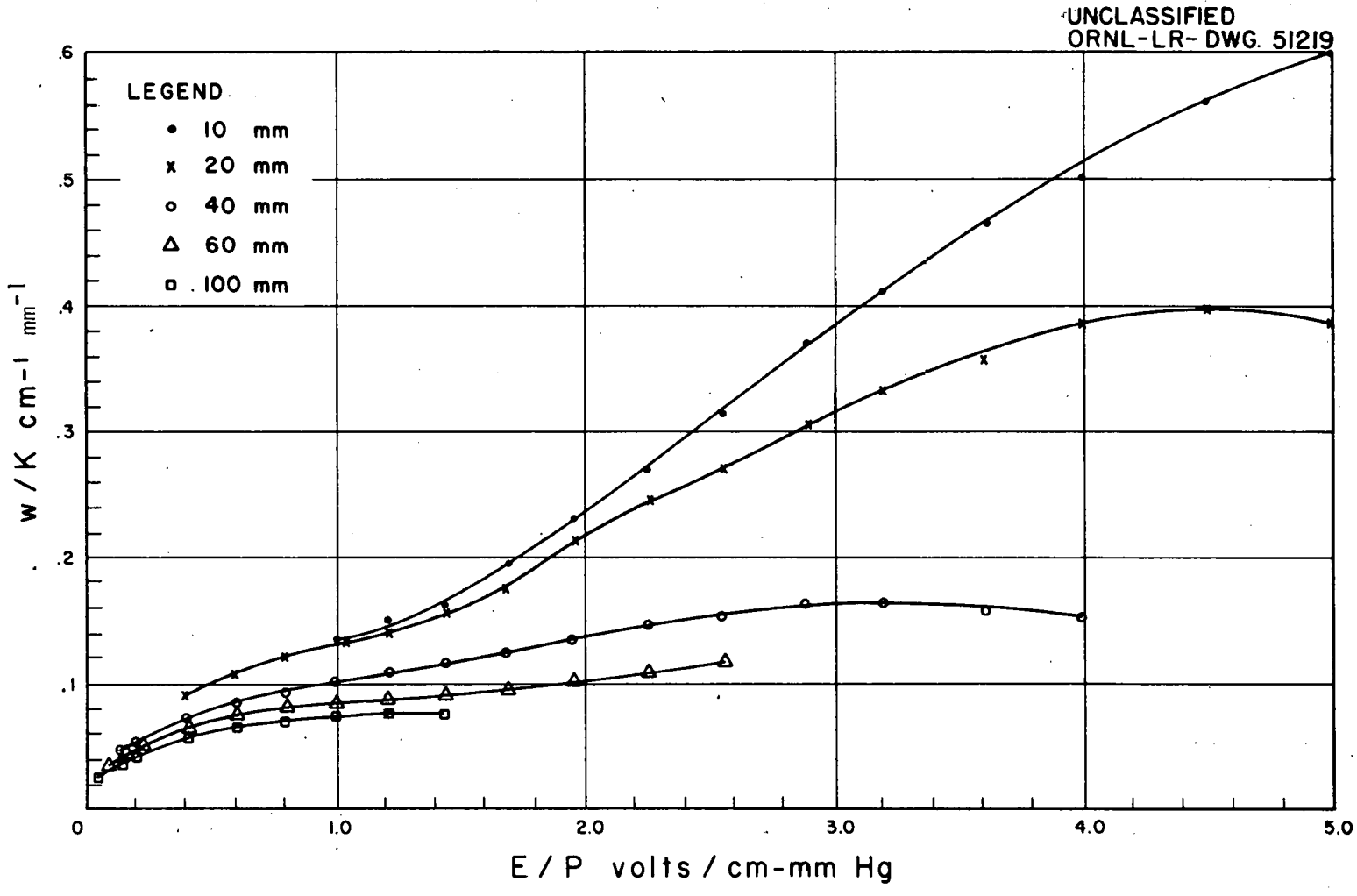

FIG. 19. w/K Vs. E/P FOR ARGON AT VARIOUS PRESSURES AND b/h = 0.5.

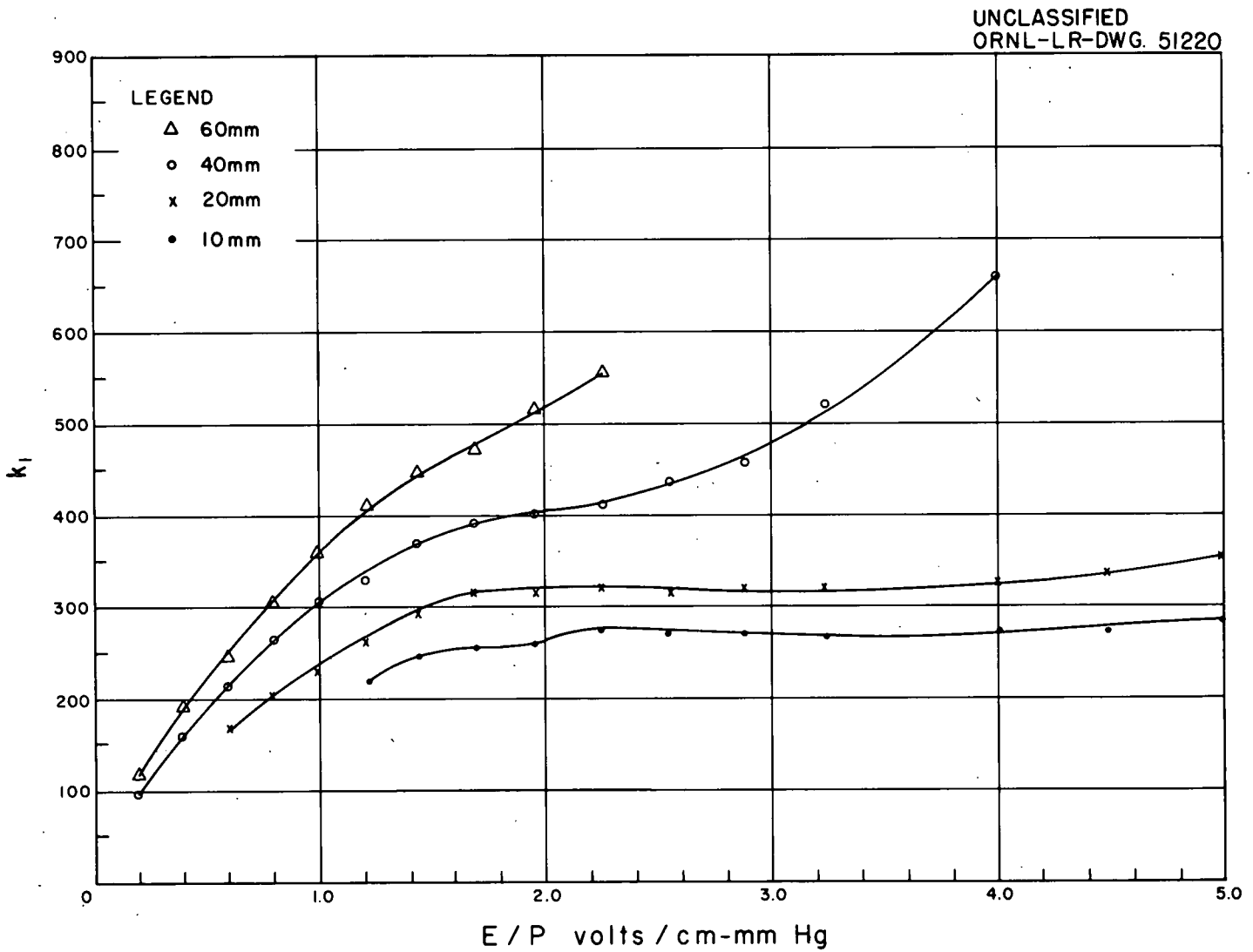

FIG. 20. EXPERIMENTAL k_1 FACTOR Vs. E/P FOR ARGON AT VARIOUS PRESSURES AND b/h = 0.3.

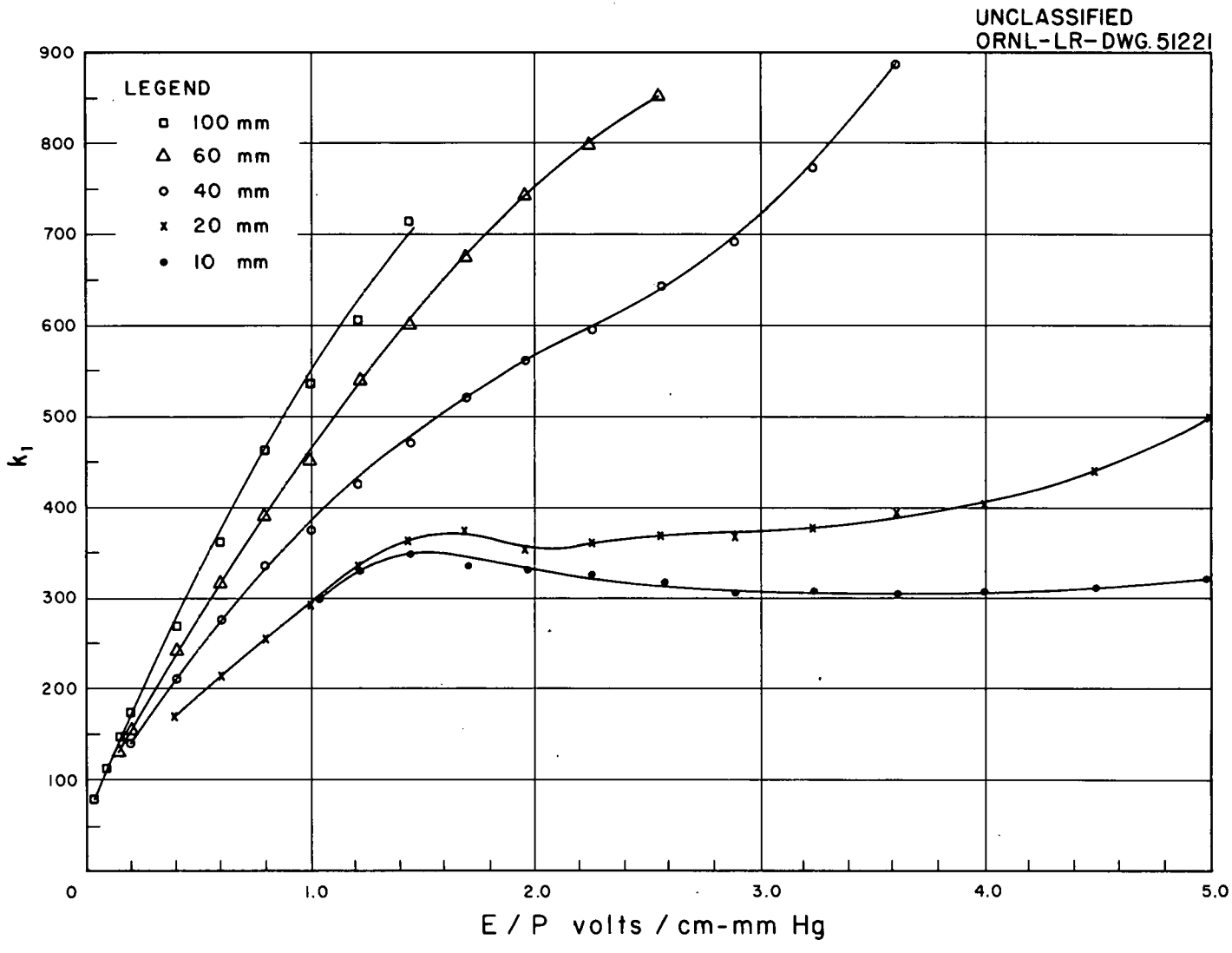

FIG. 21. EXPERIMENTAL k_1 FACTOR Vs. E/P FOR ARGON AT VARIOUS PRESSURES AND b/h = 0.5.

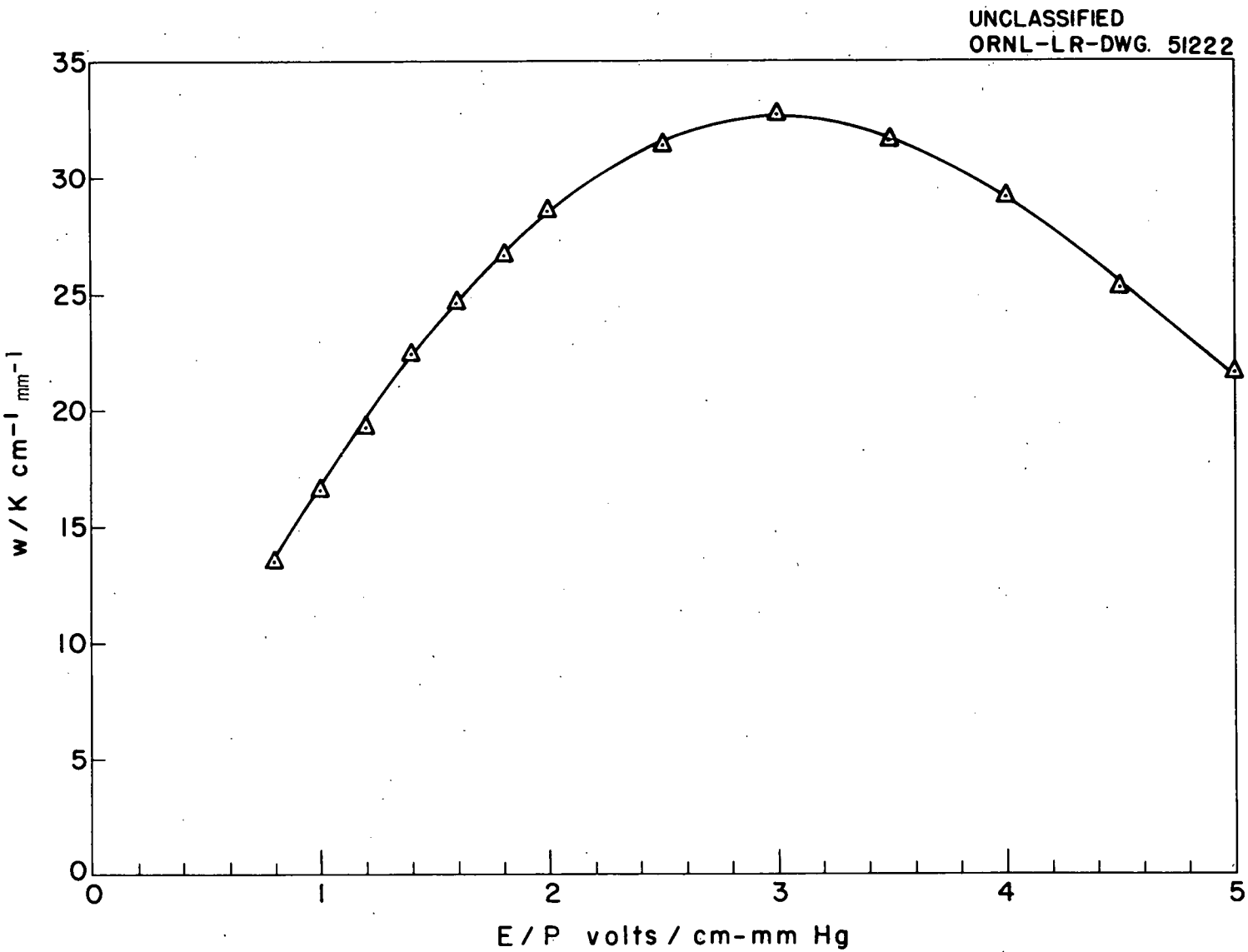

FIG. 22. w/K Vs. E/P FOR CARBON DIOXIDE.

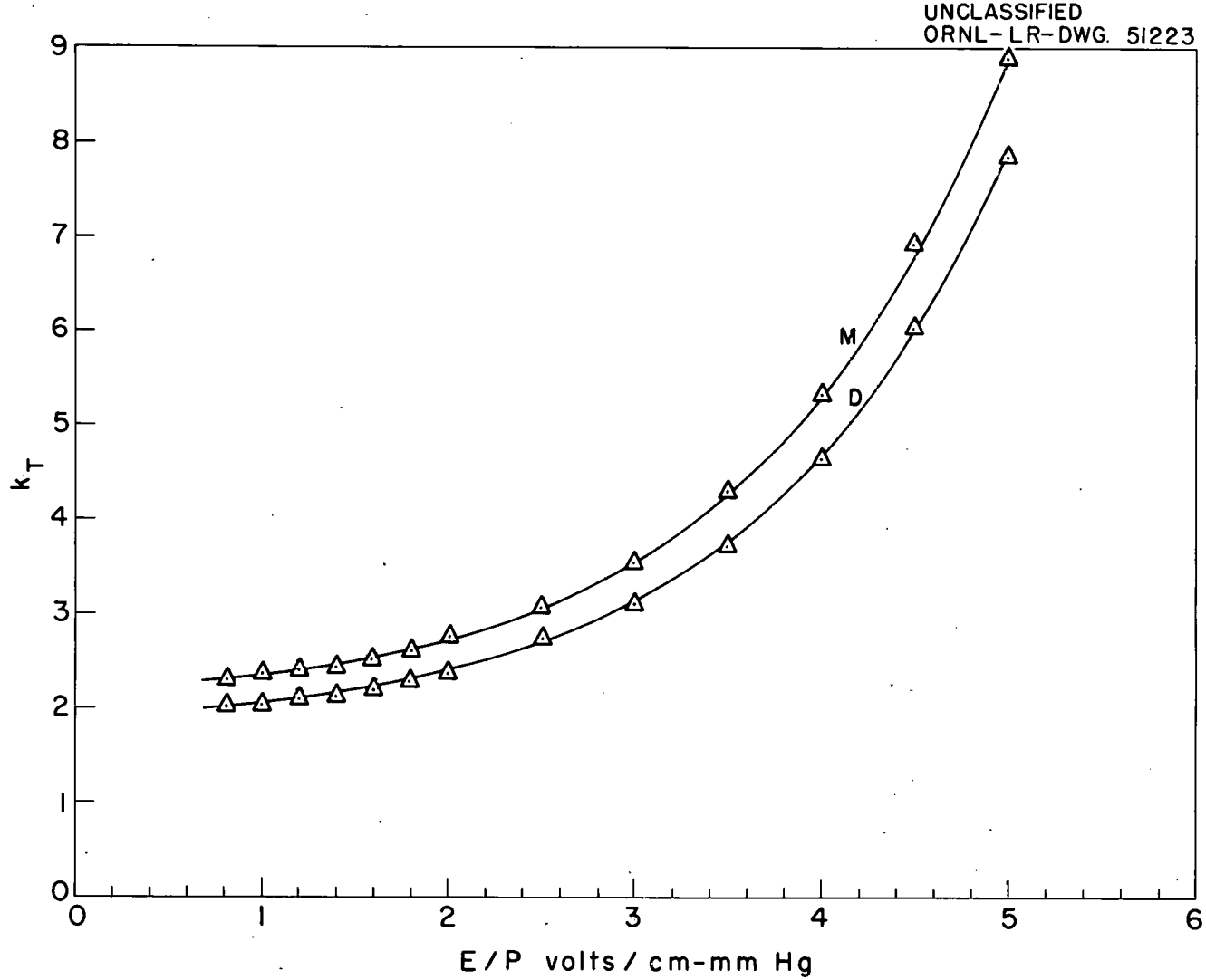

FIG. 23. TOWNSEND ENERGY FACTOR k_T Vs. E/P FOR CARBON DIOXIDE USING THE MAXWELLIAN AND THE DRUYVESTEYN DISTRIBUTIONS.

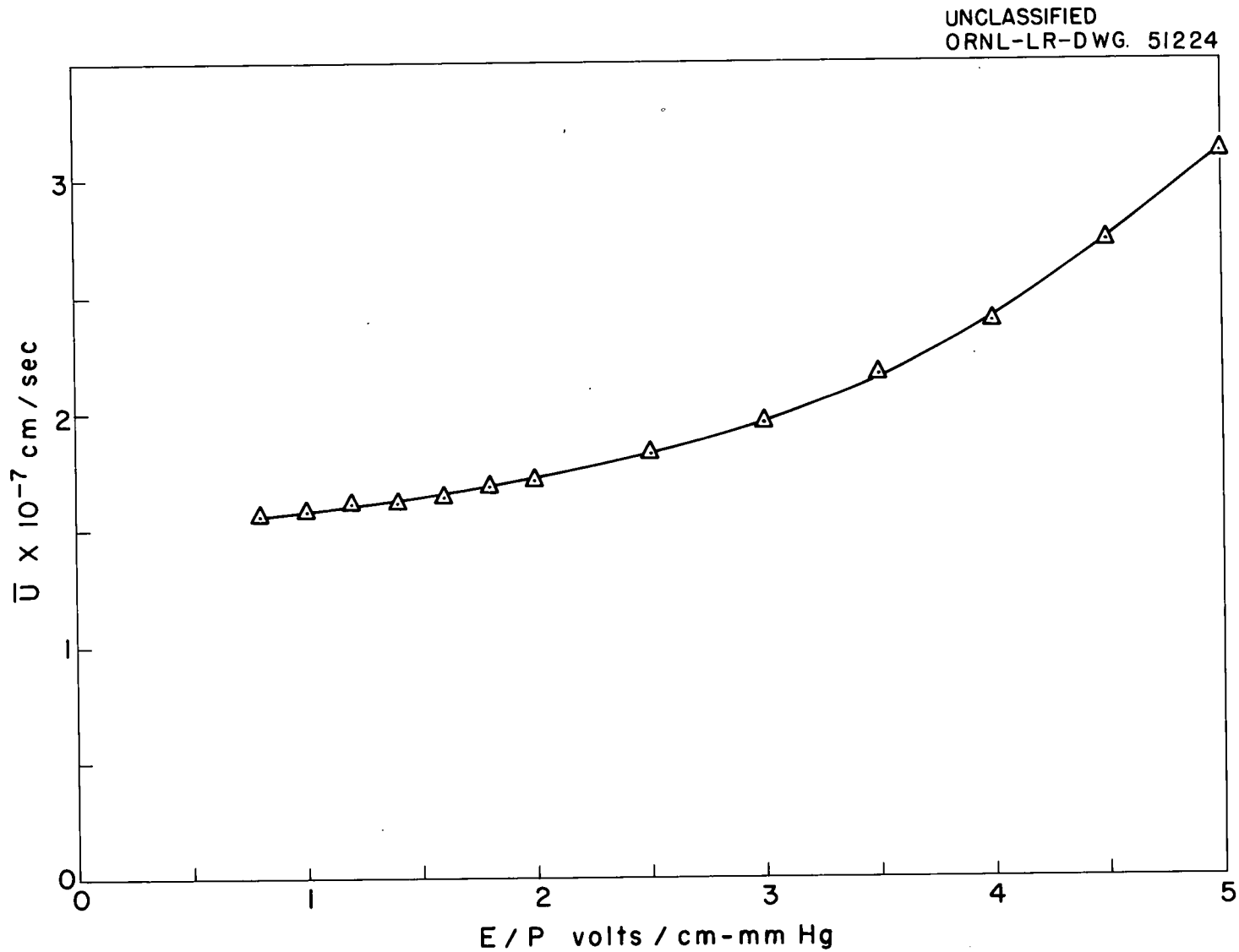

FIG. 24. $\bar{U}$ Vs. E/P FOR CARBON DIOXIDE USING THE DRUYVESTEYN DISTRIBUTION.

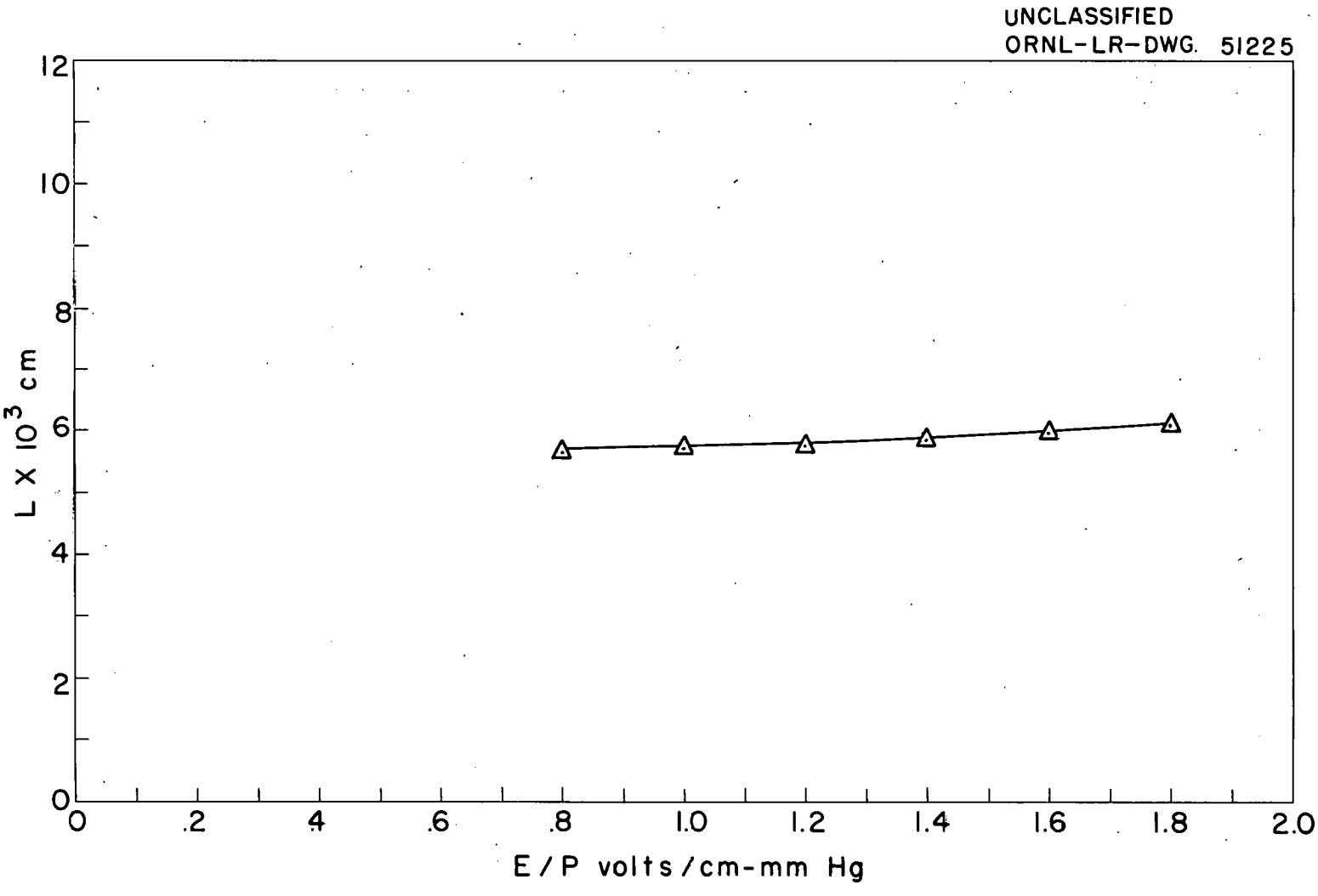

FIG. 25. L Vs. E/P FOR CARBON DIOXIDE USING THE DRUYVESTEYN DISTRIBUTION.

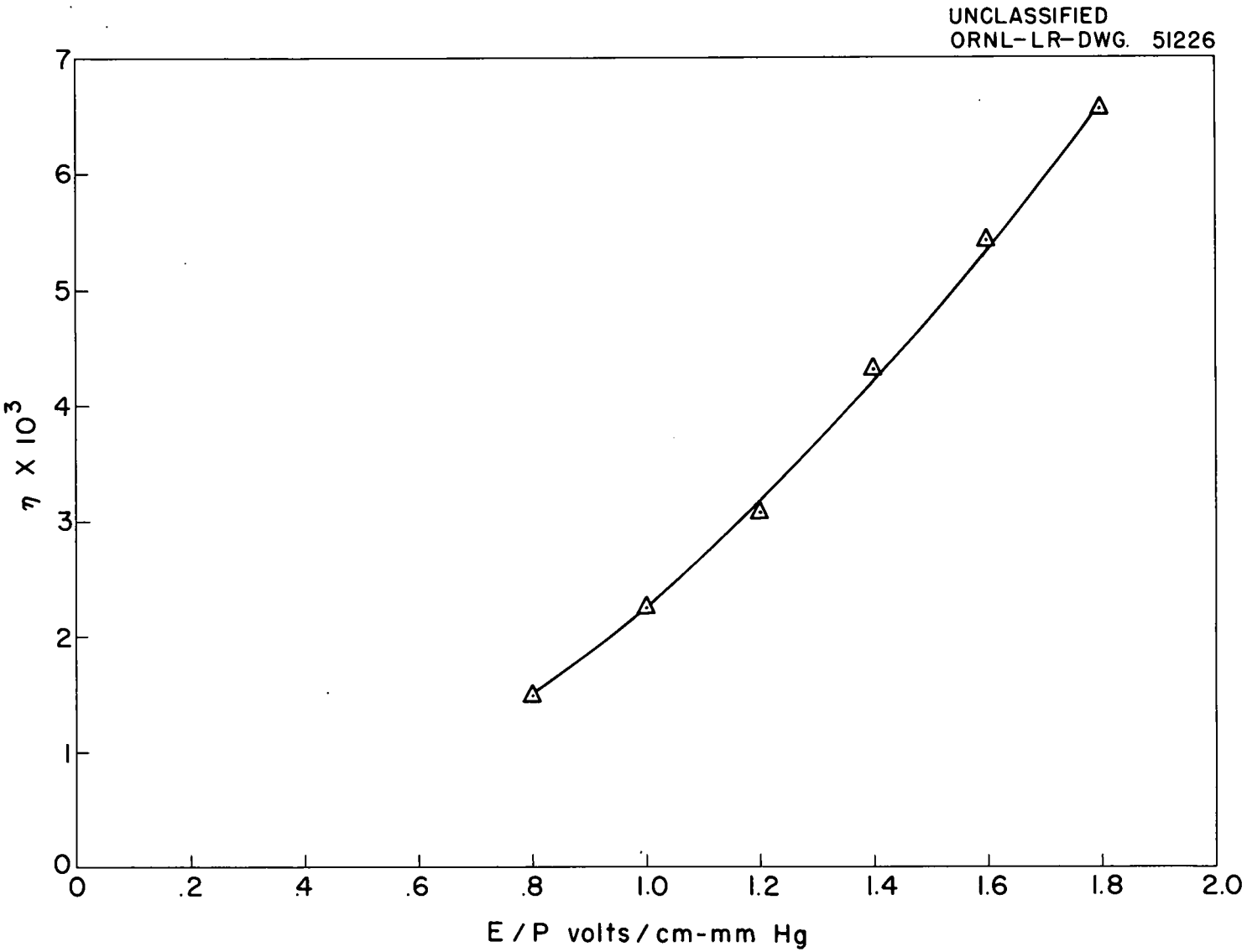

FIG. 26. η Vs. E/P FOR CARBON DIOXIDE USING THE DRUYVESTEYN DISTRIBUTION.

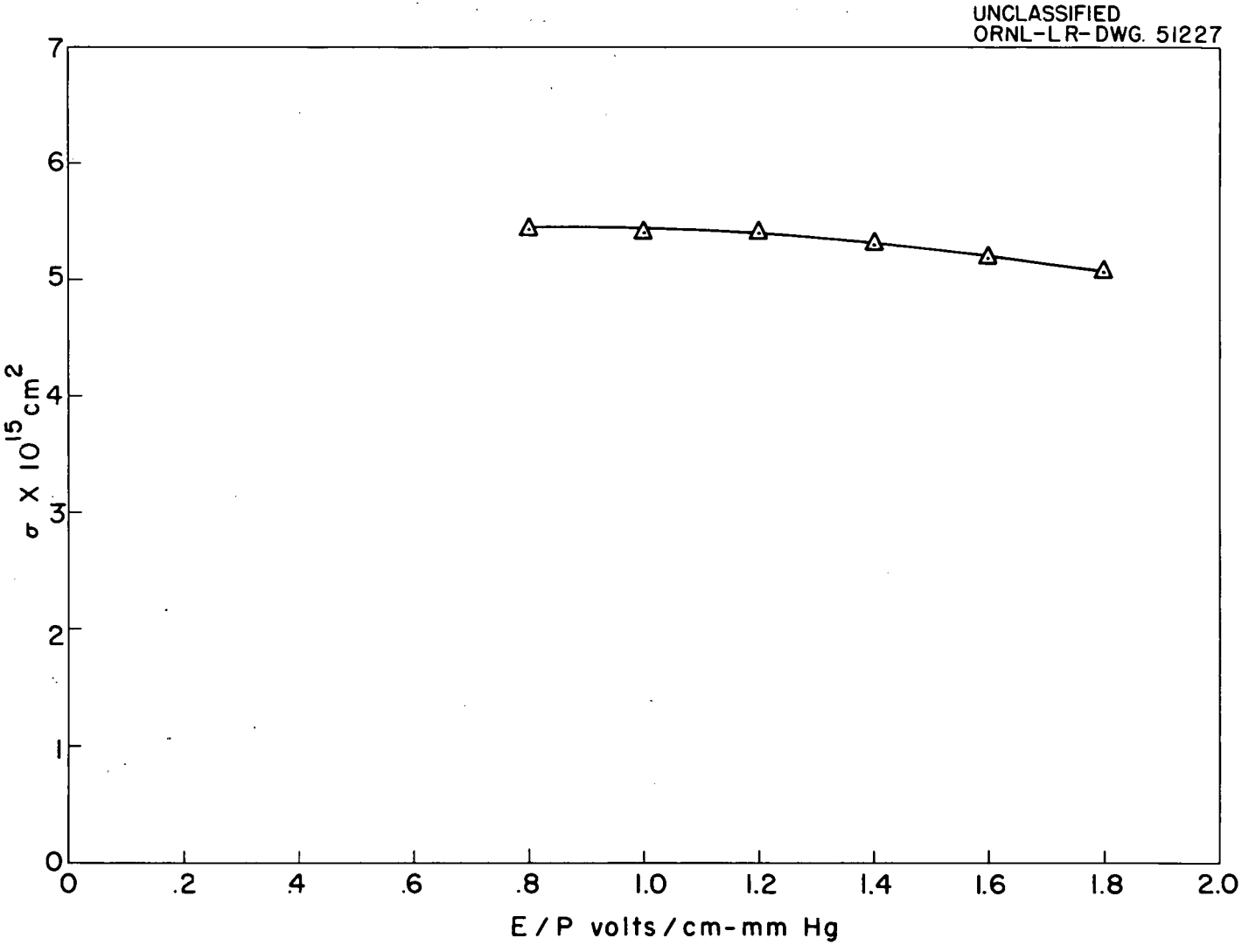

FIG. 27. COLLISION CROSS SECTION σ Vs. E/P FOR CARBON DIOXIDE USING THE DRUYVESTEYN DISTRIBUTION.

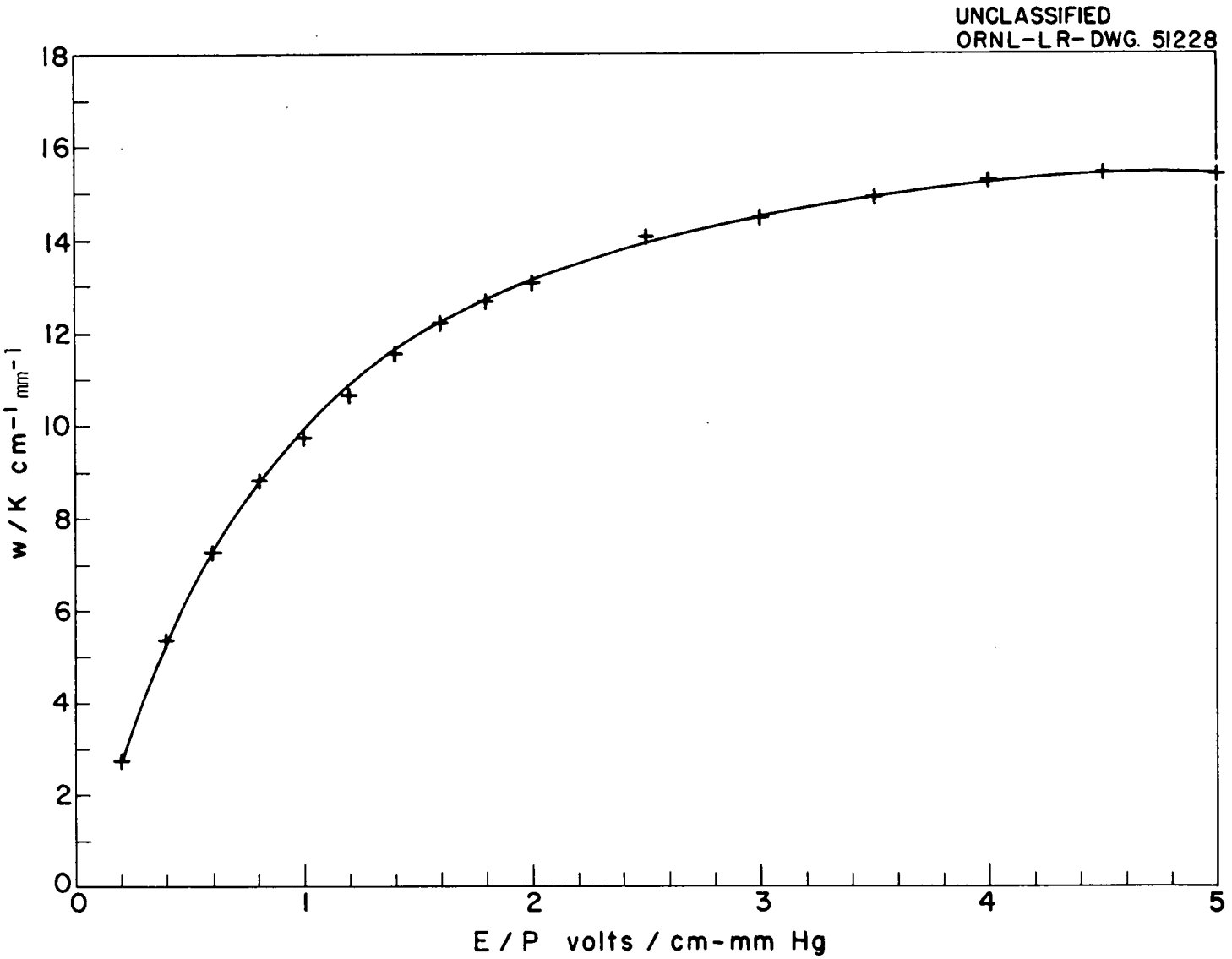

FIG. 28. w/K Vs. E/P FOR CYCLOPROPANE.

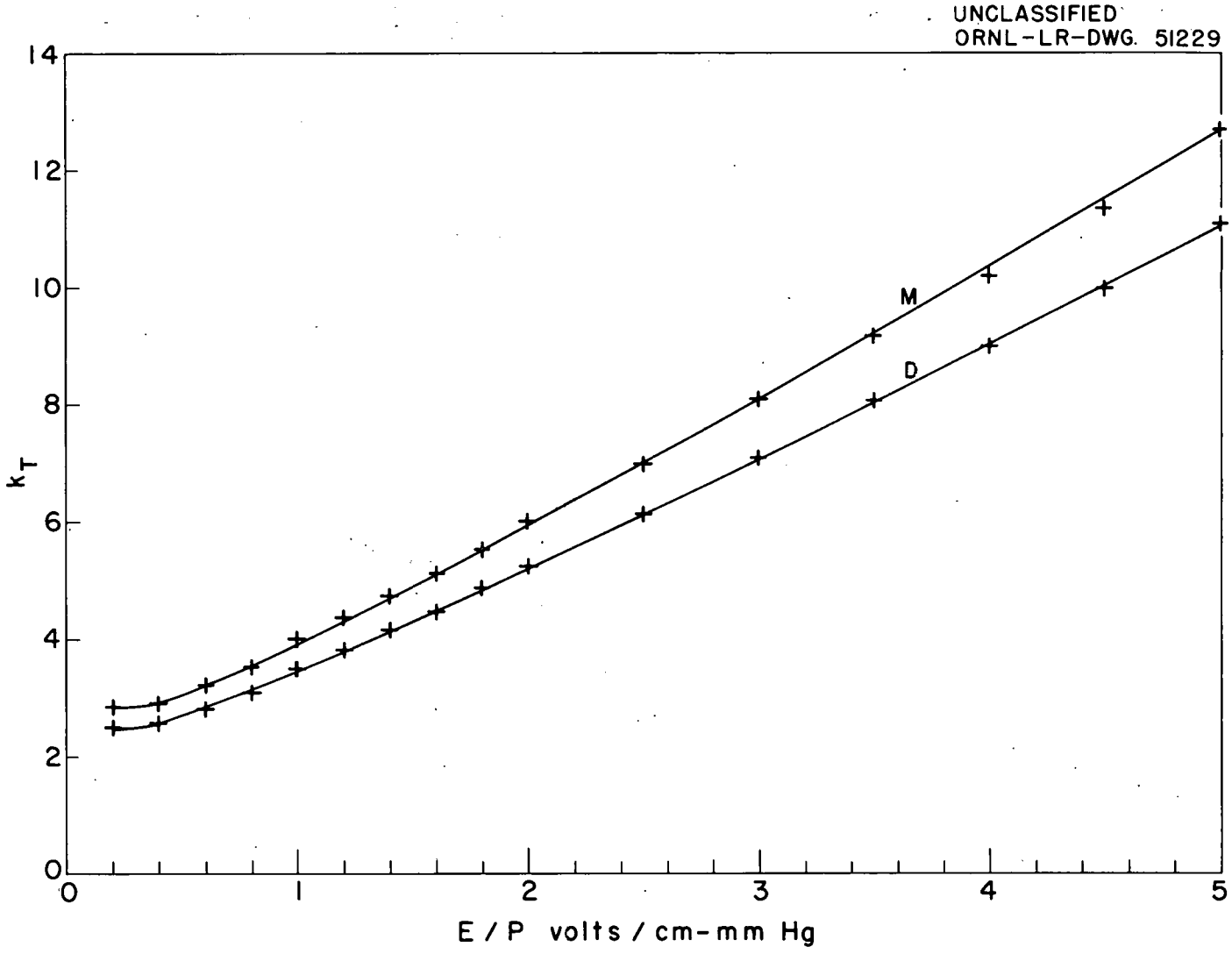

FIG. 29. TOWNSEND ENERGY FACTOR k_T Vs. E/P FOR CYCLOPROPANE USING THE MAXWELLIAN AND THE DRUYVESTEYN DISTRIBUTIONS.

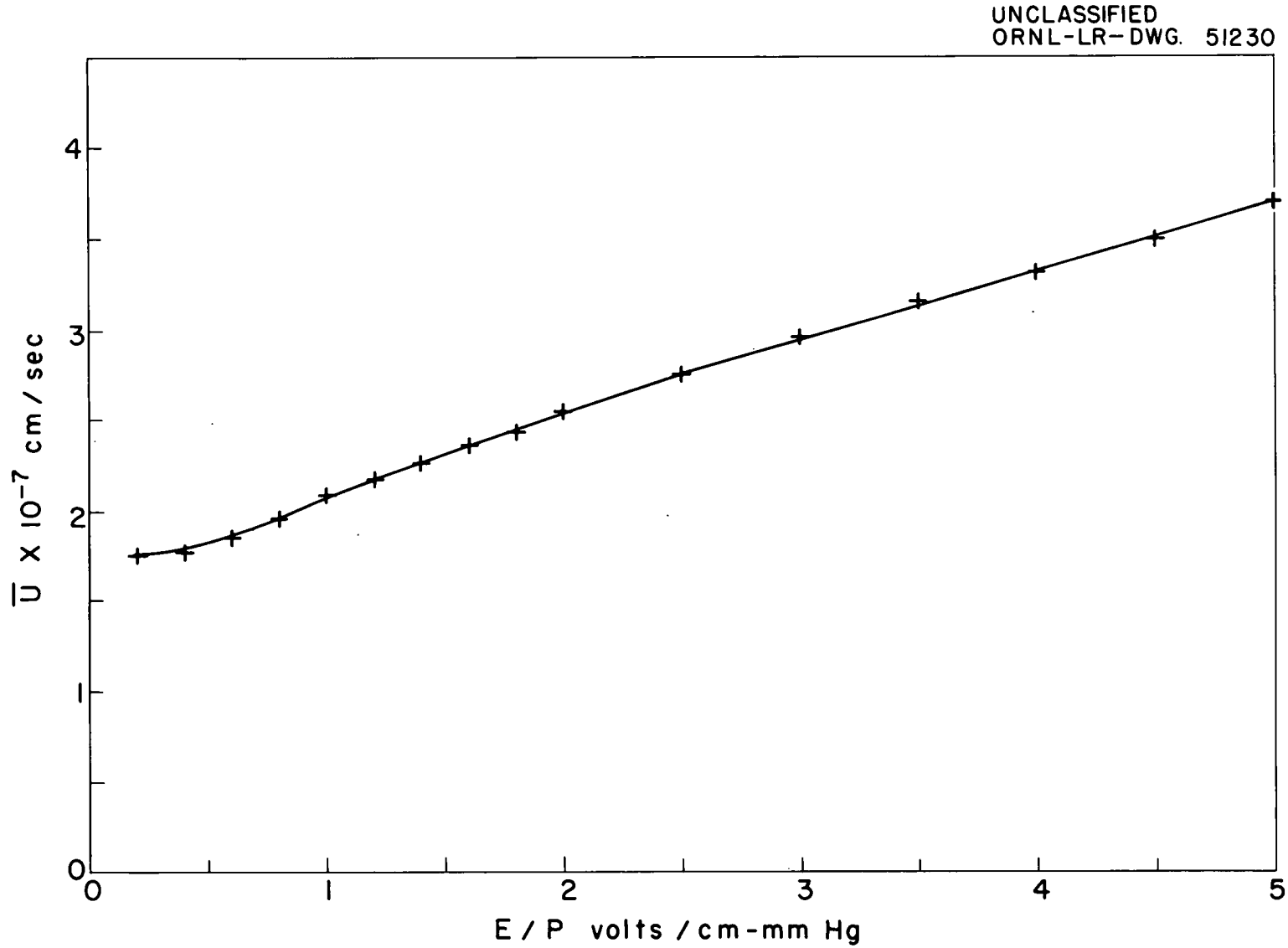

FIG. 30. $\bar{U}$ Vs. E/P FOR CYCLOPROPANE USING THE DRUYVESTEYN DISTRIBUTION.

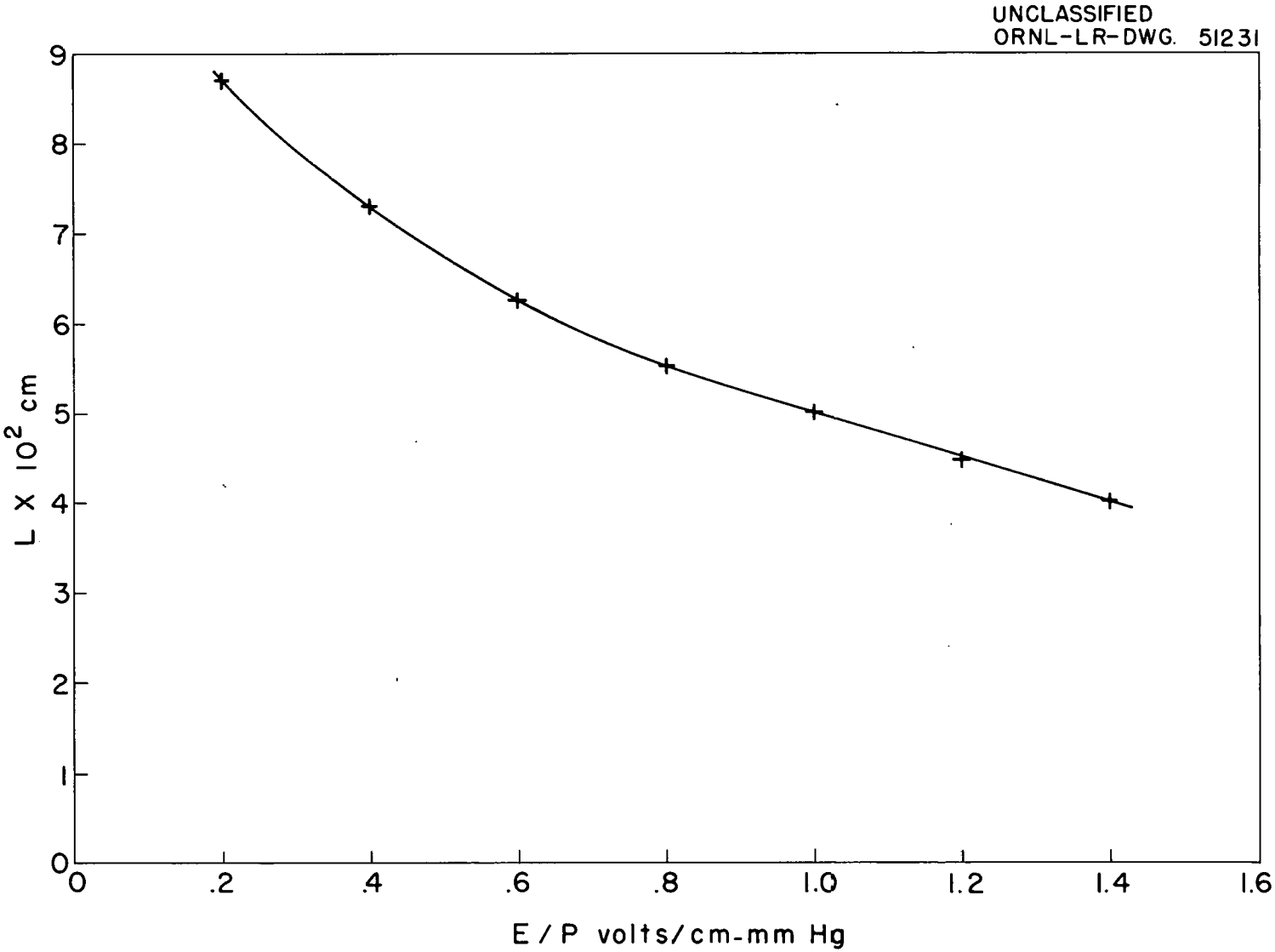

FIG. 31. L Vs. E/P FOR CYCLOPROPANE USING THE DRUYVESTEYN DISTRIBUTION.

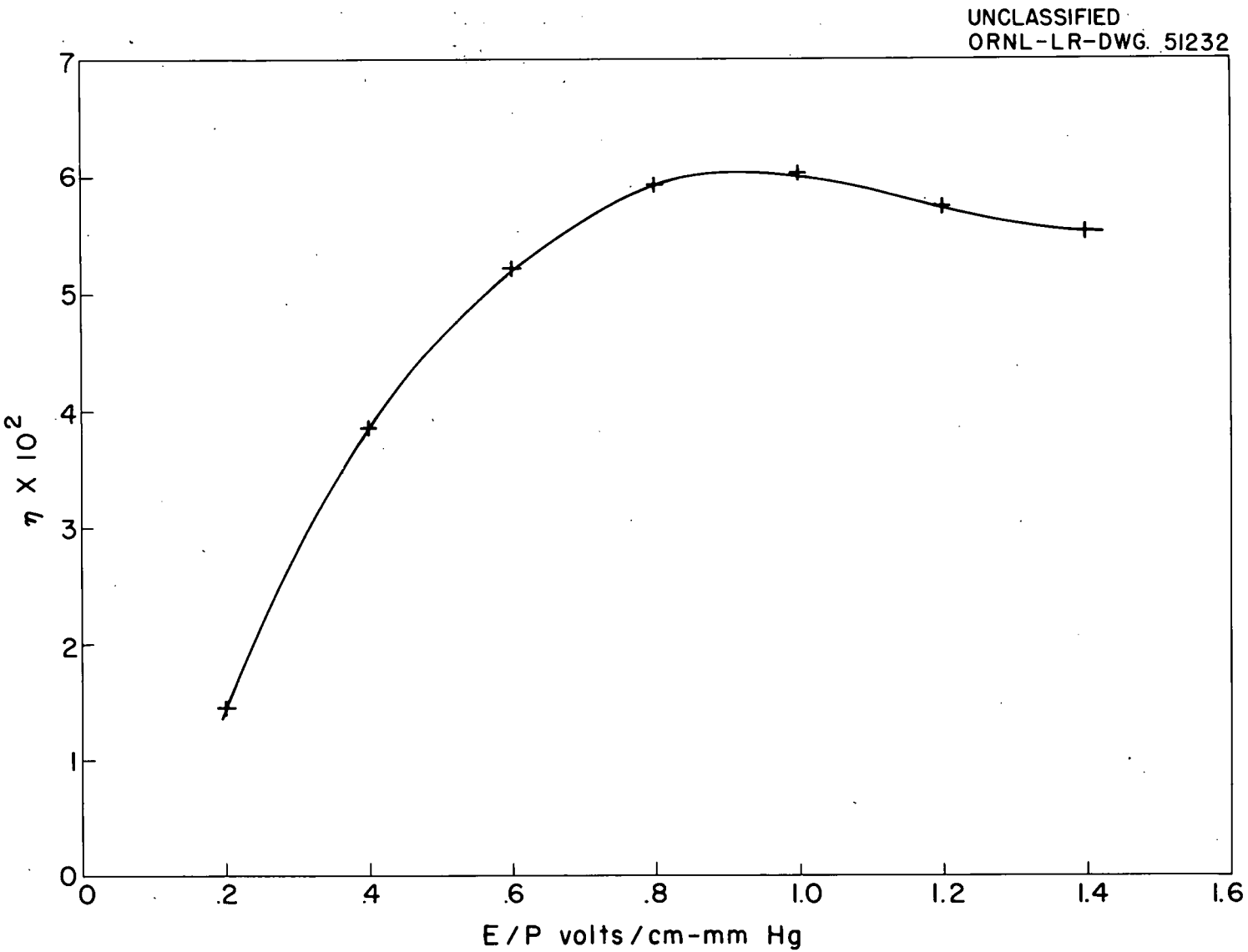

FIG. 32. η Vs. E/P FOR CYCLOPROPANE USING THE DRUYVESTEYN DISTRIBUTION.

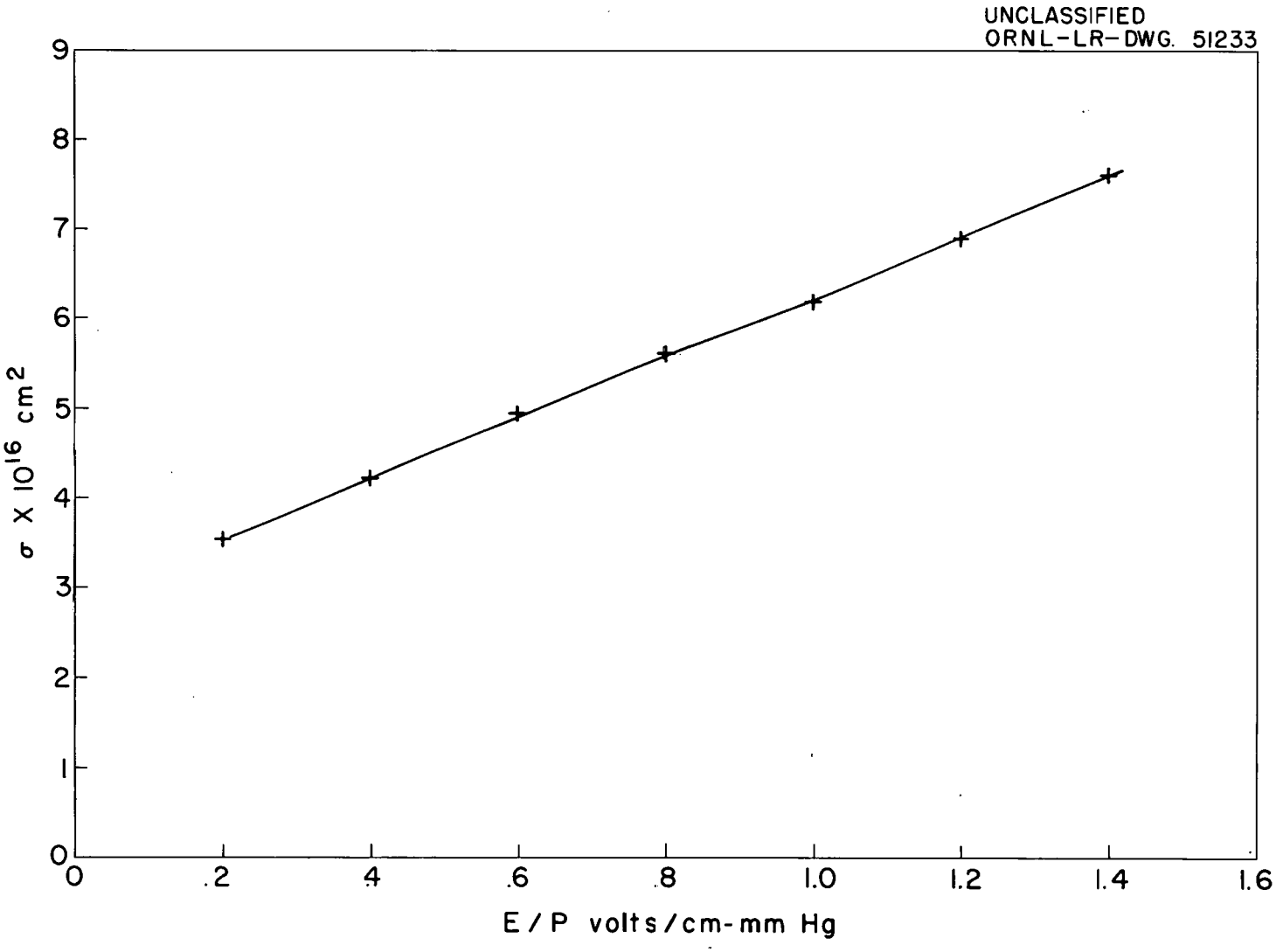

FIG. 33. COLLISION CROSS SECTION σ Vs. E/P FOR CYCLOPROPANE USING THE DRUYVESTEYN DISTRIBUTION.

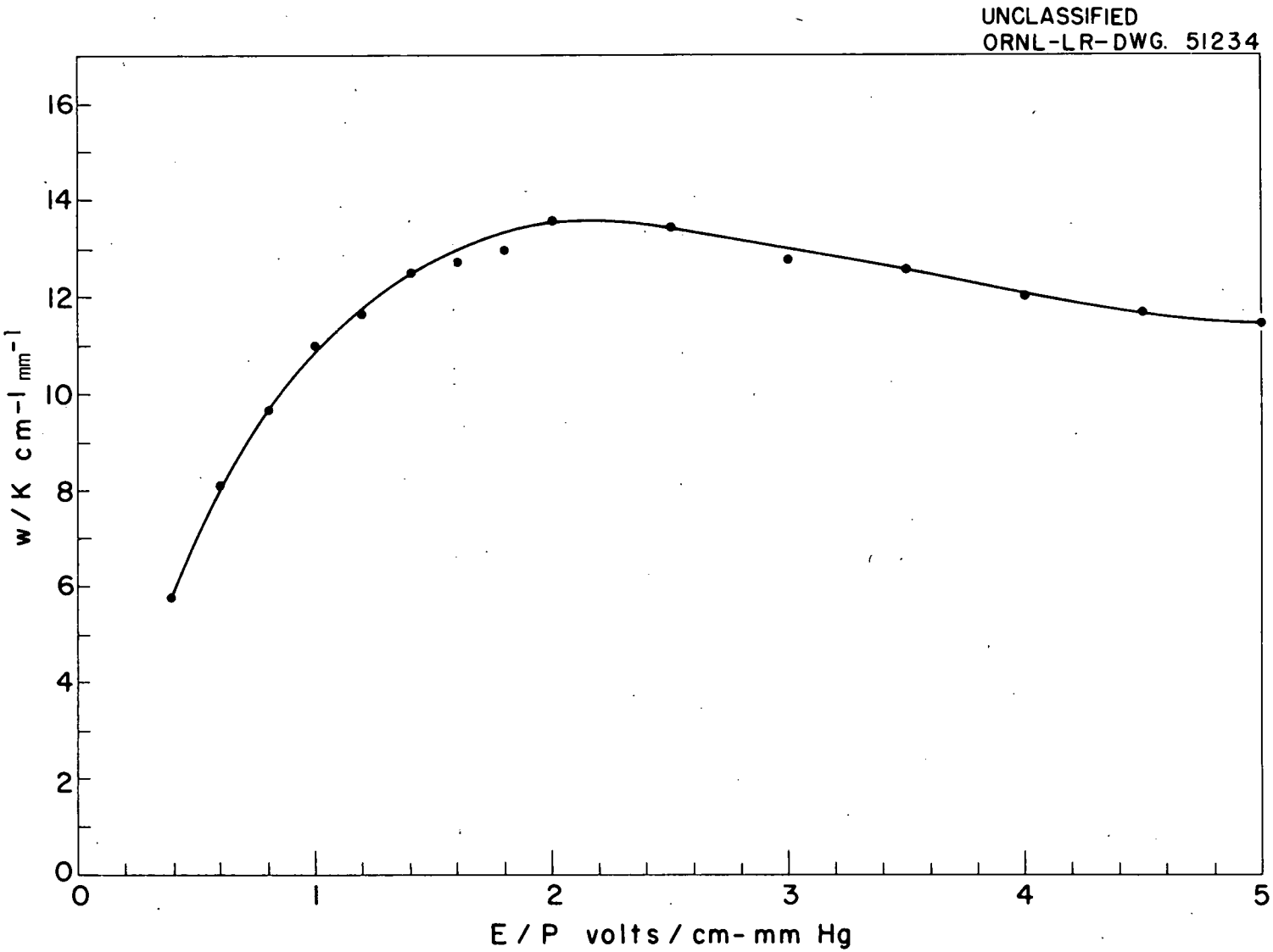

FIG. 34. w/K Vs. E/P FOR ETHYLENE.

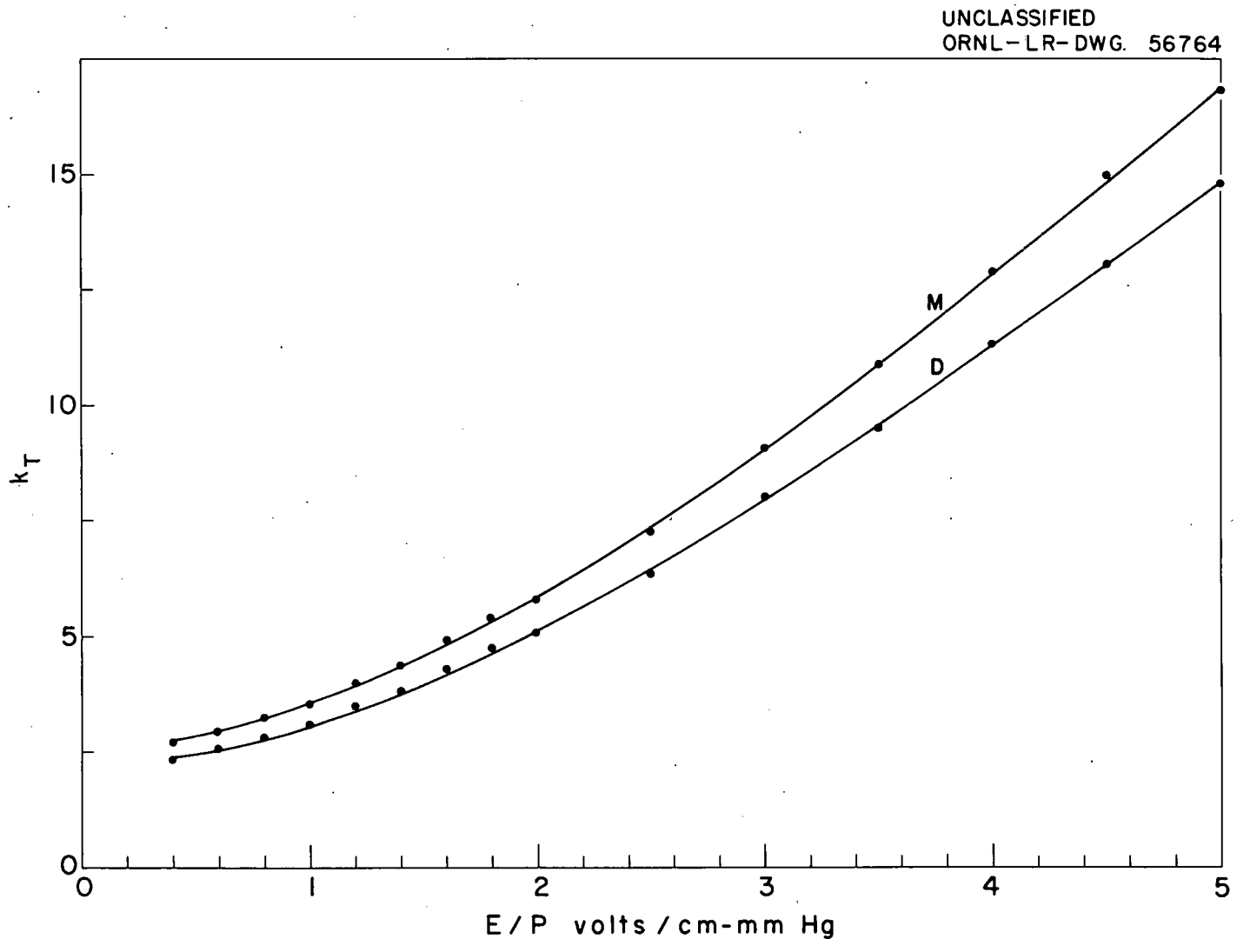

FIG. 35. TOWNSEND ENERGY FACTOR k_T Vs. E/P FOR ETHYLENE USING THE MAXWELLIAN AND DRUYVESTEYN DISTRIBUTIONS.

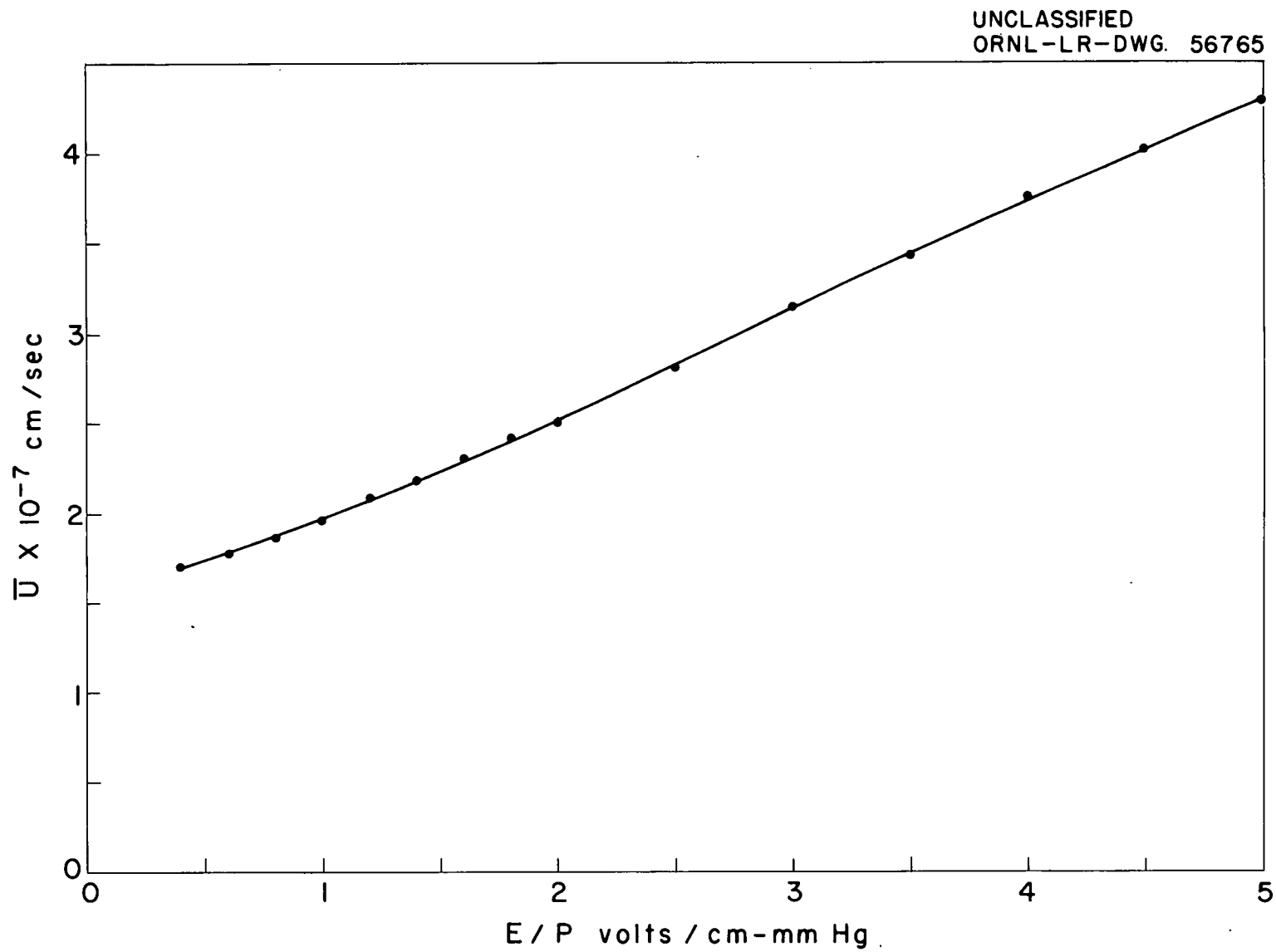

FIG. 36. $\bar{U}$ Vs. E/P FOR ETHYLENE USING THE DRUYVESTEYN DISTRIBUTION.

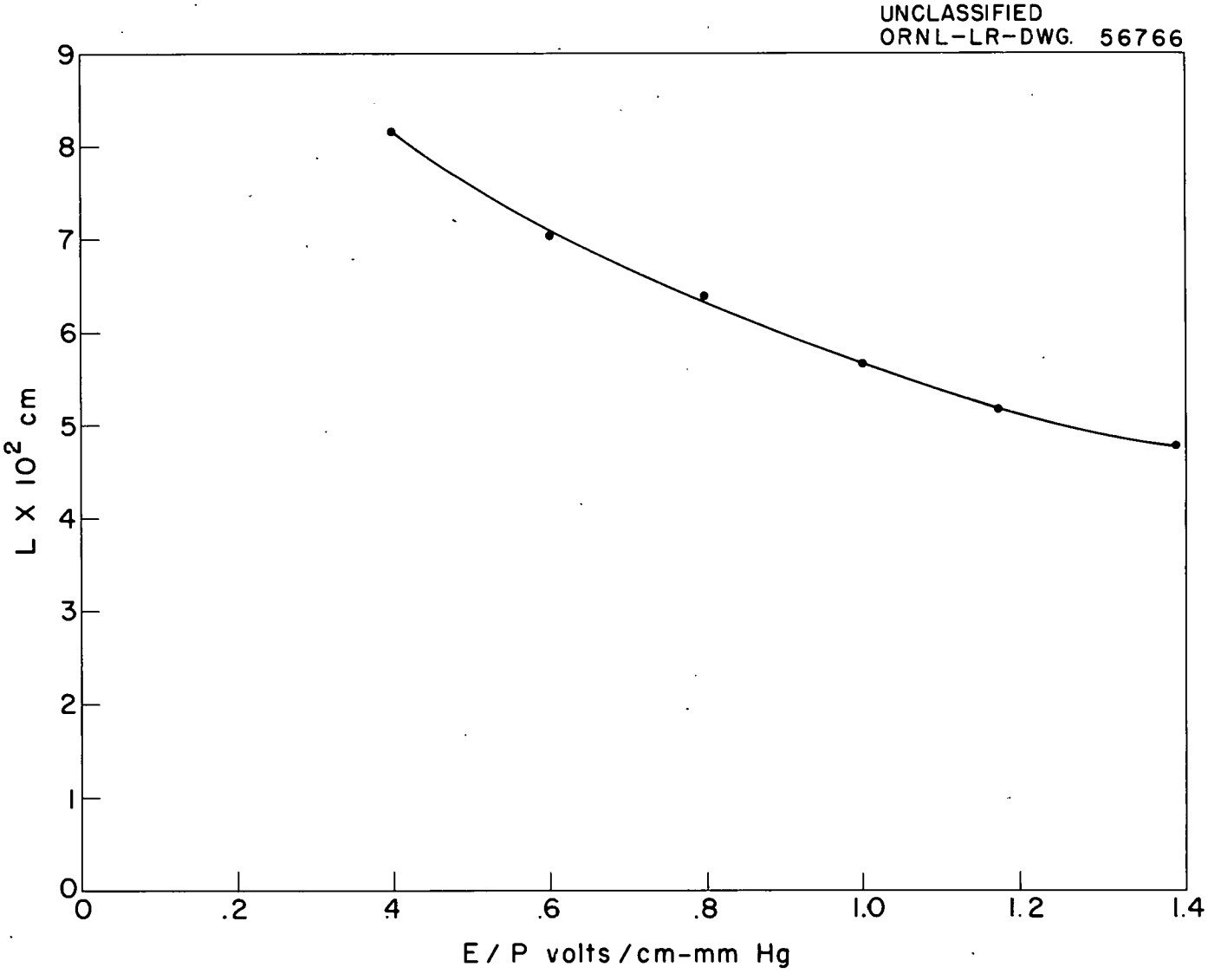

FIG. 37. L Vs. E/P FOR ETHYLENE USING THE DRUYVESTEYN DISTRIBUTION.

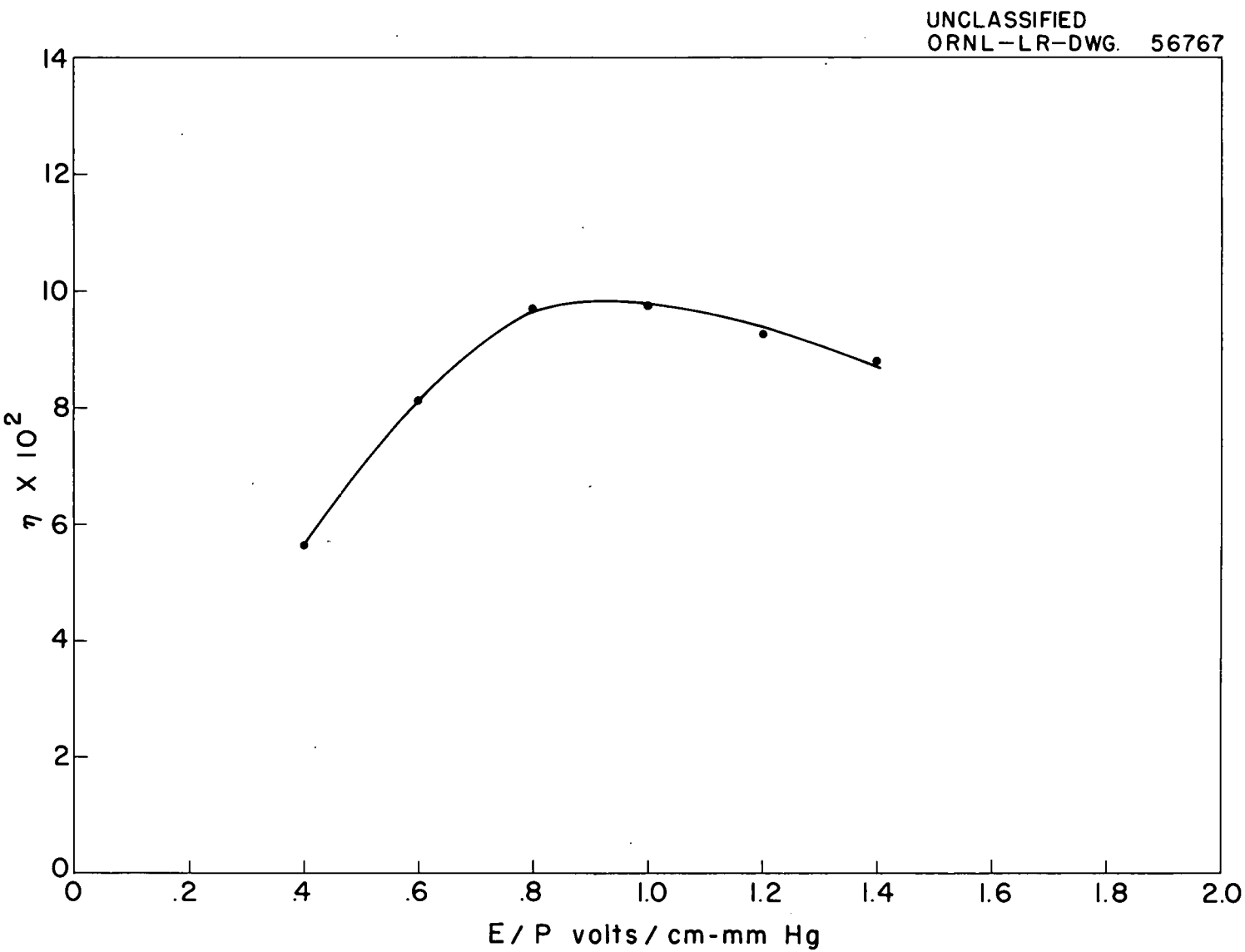

FIG. 38. η Vs. E/P FOR ETHYLENE USING THE DRUYVESTEYN DISTRIBUTION.

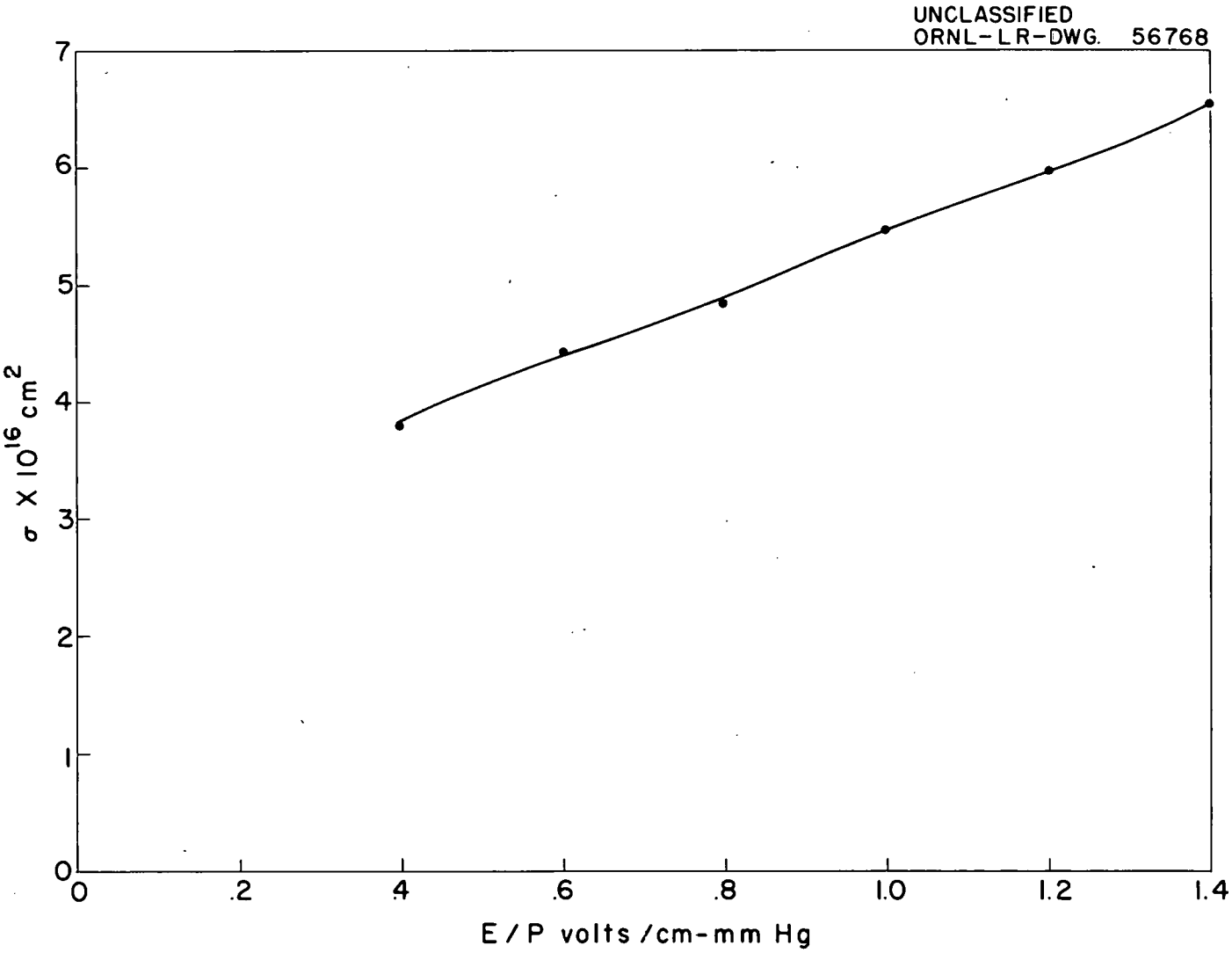

FIG. 39. COLLISION CROSS SECTION σ Vs. E/P FOR ETHYLENE USING THE DRUYVESTEYN DISTRIBUTION.

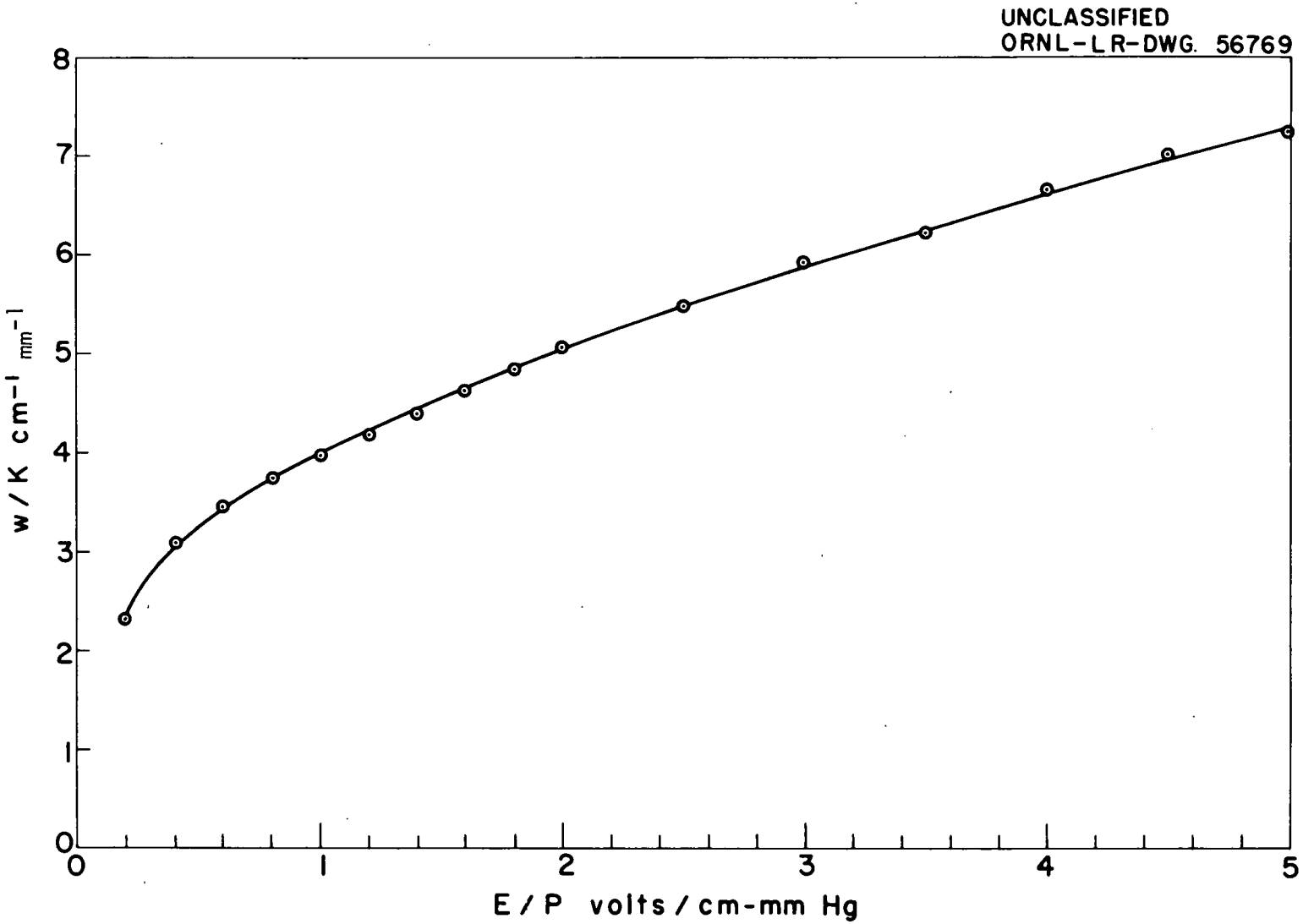

FIG. 40 w/K Vs. E/P FOR HYDROGEN.

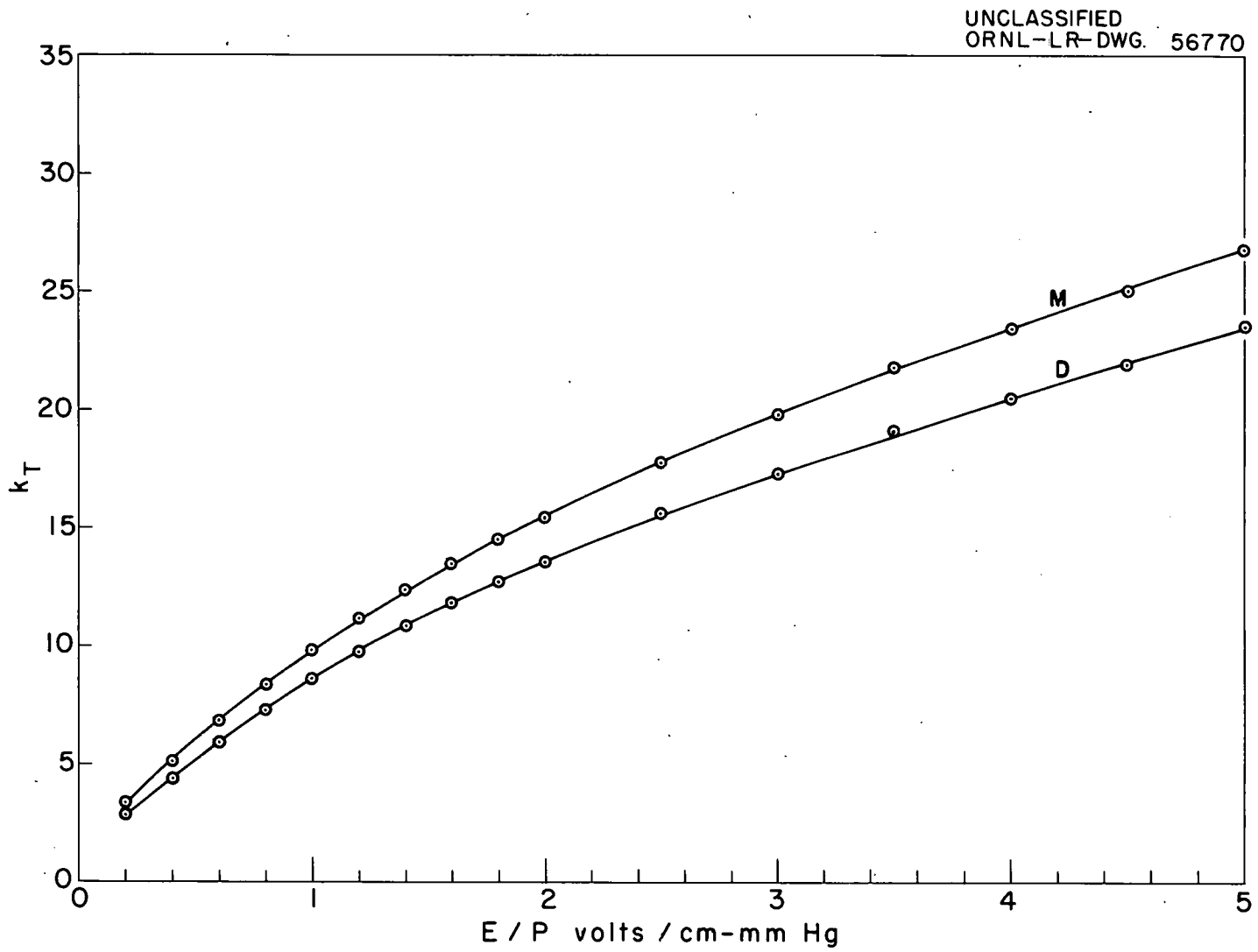

FIG. 41. TOWNSEND ENERGY FACTOR k_T Vs. E/P FOR HYDROGEN USING THE MAXWELLIAN AND DRUYVESTEYN DISTRIBUTIONS.

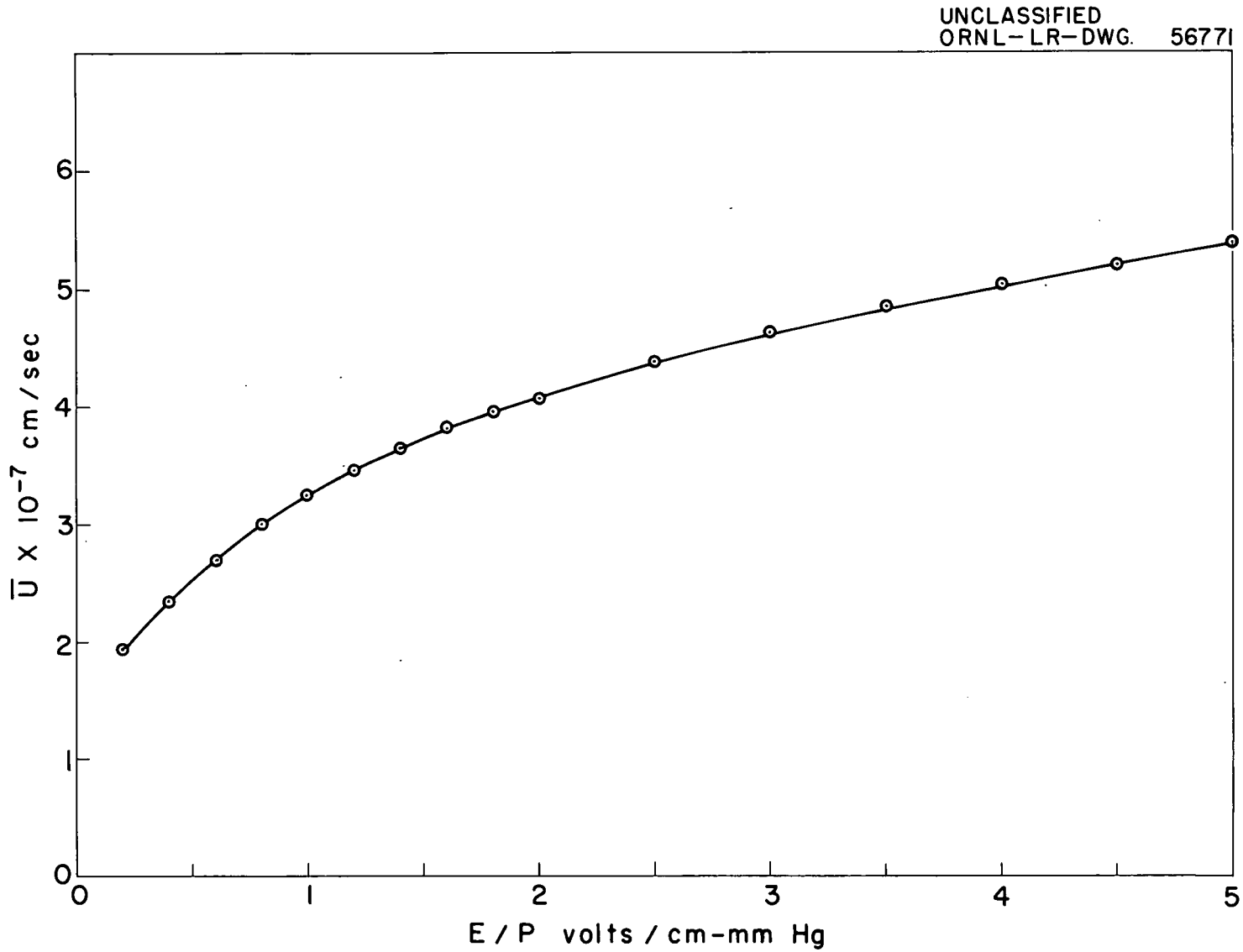

FIG. 42. $\bar{U}$ Vs. E/P FOR HYDROGEN USING THE DRUYVESTEYN DISTRIBUTION.

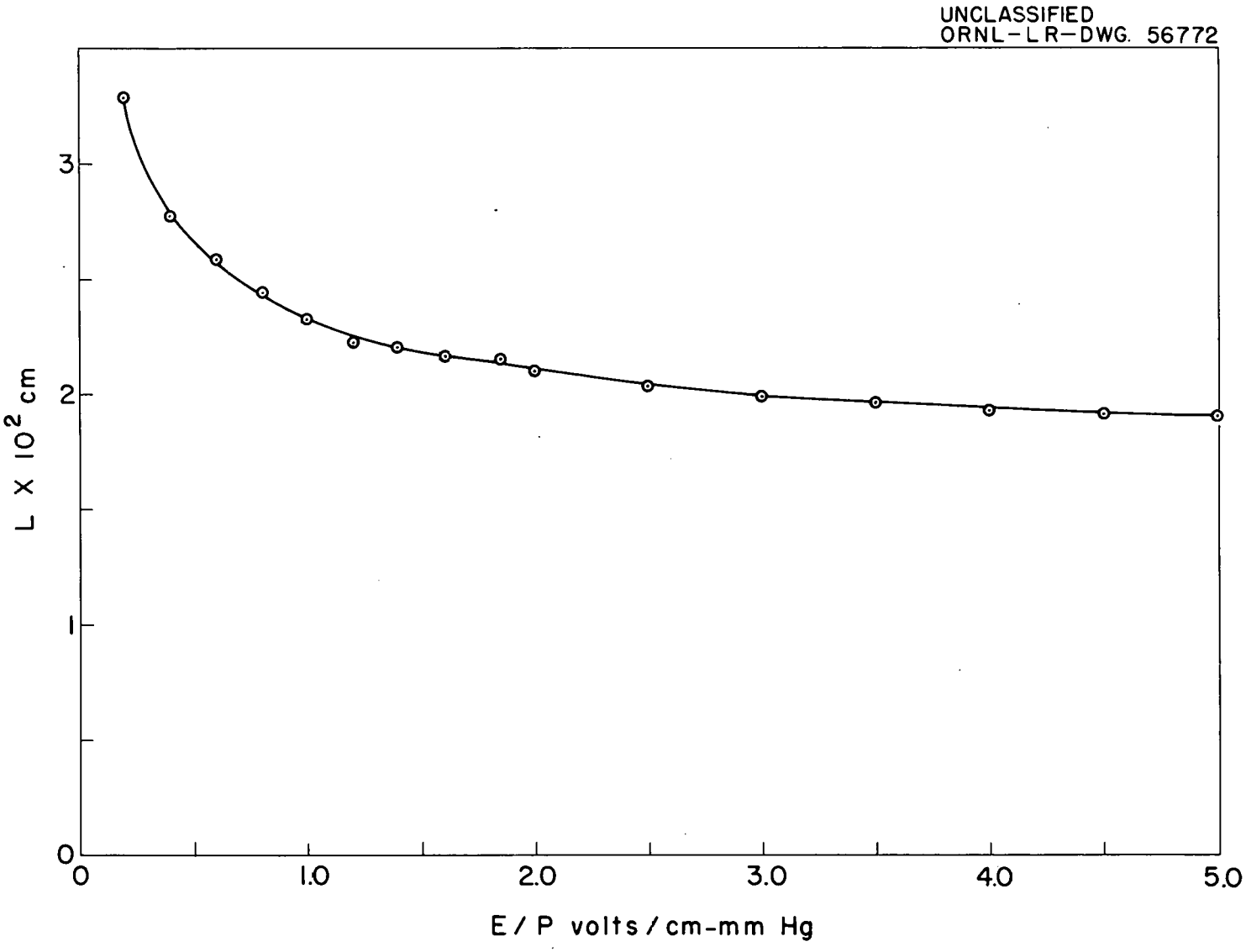

FIG. 43. L Vs. E/P FOR HYDROGEN USING THE DRUYVESTEYN DISTRIBUTION.

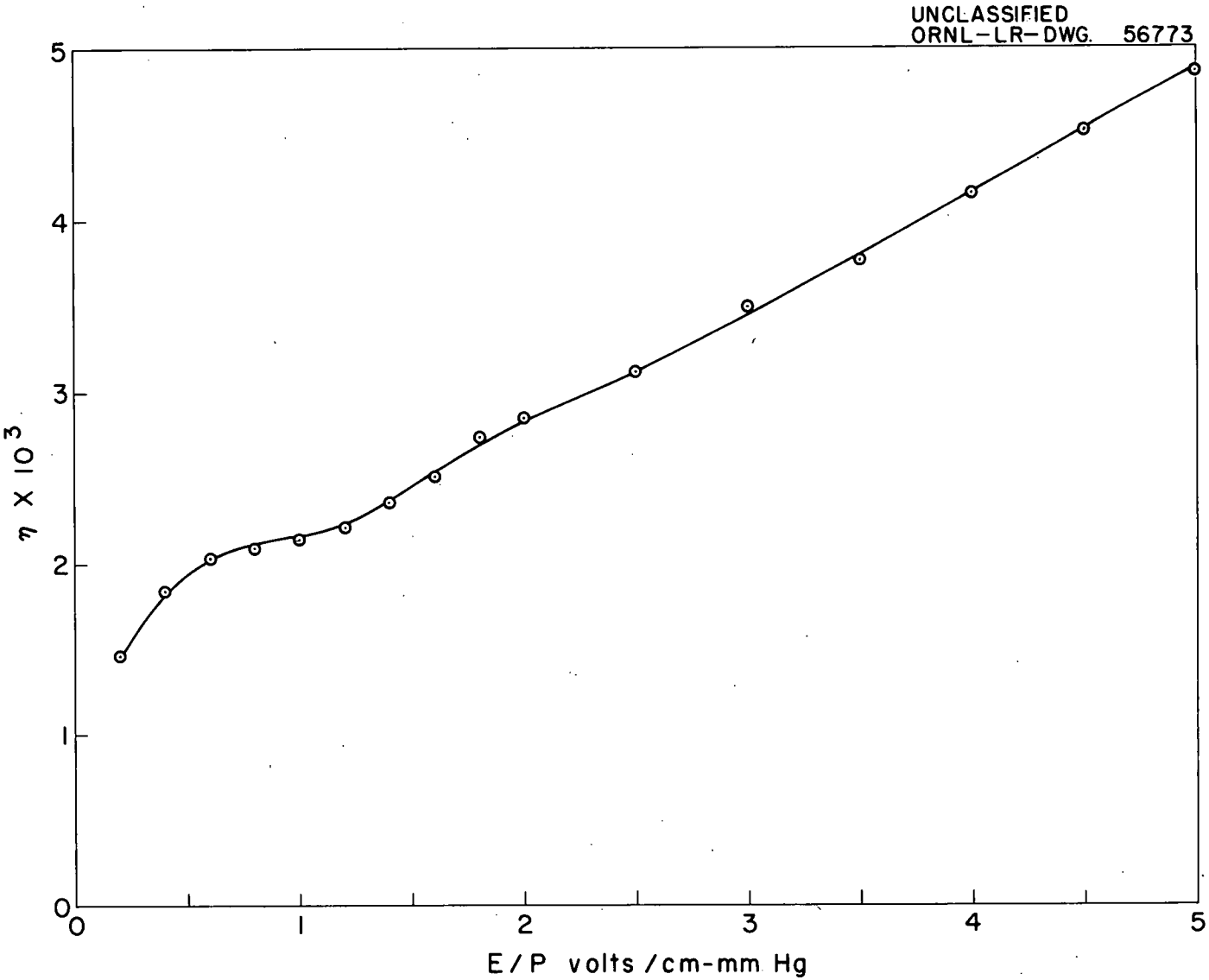

FIG. 44. η Vs. E/P FOR HYDROGEN USING THE DRUYVESTEYN DISTRIBUTION.

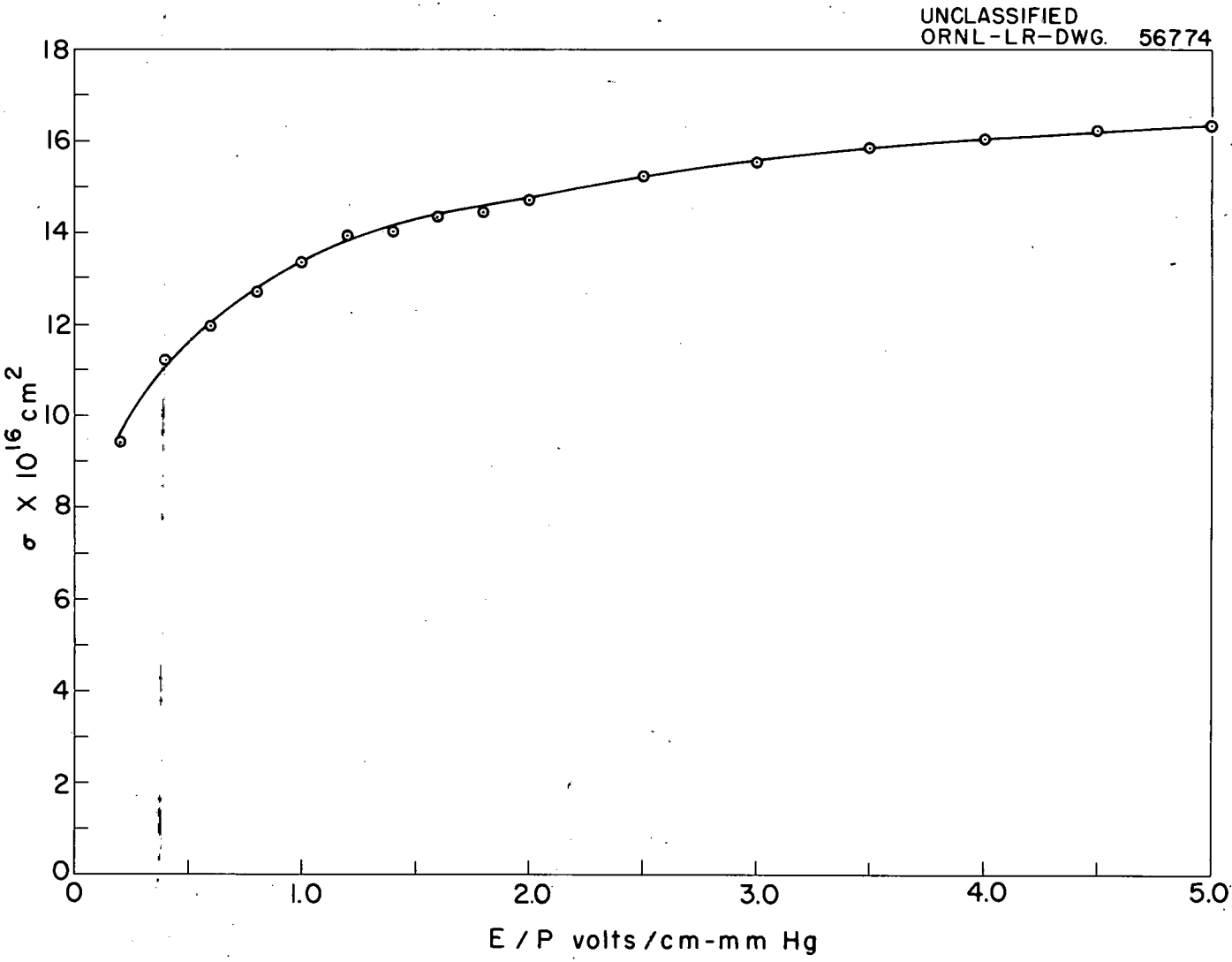

FIG. 45. COLLISION CROSS SECTION σ Vs. E/P FOR HYDROGEN USING THE DRUYVESTEYN DISTRIBUTION.

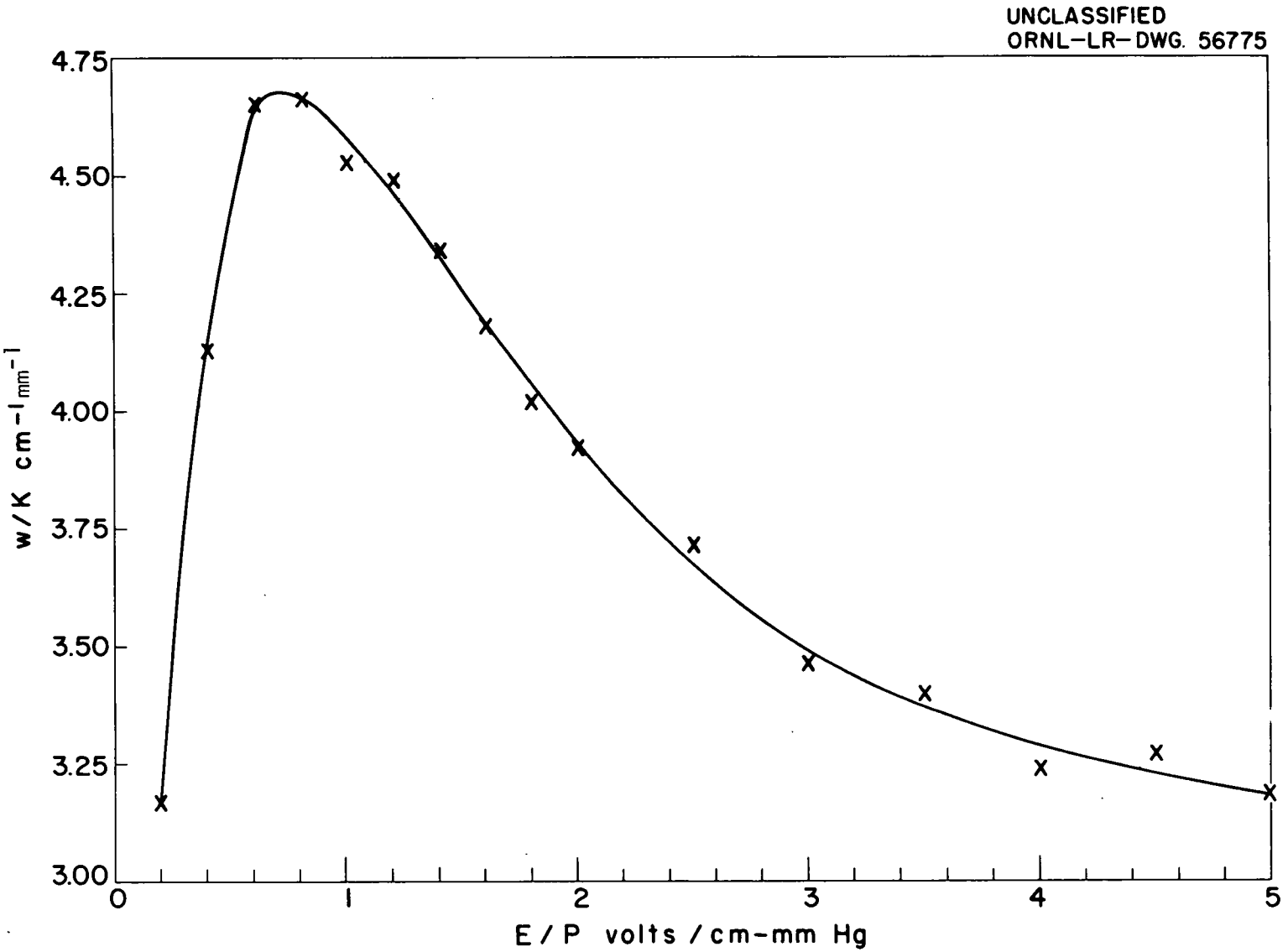

FIG. 46. w/K Vs. E/P FOR METHANE

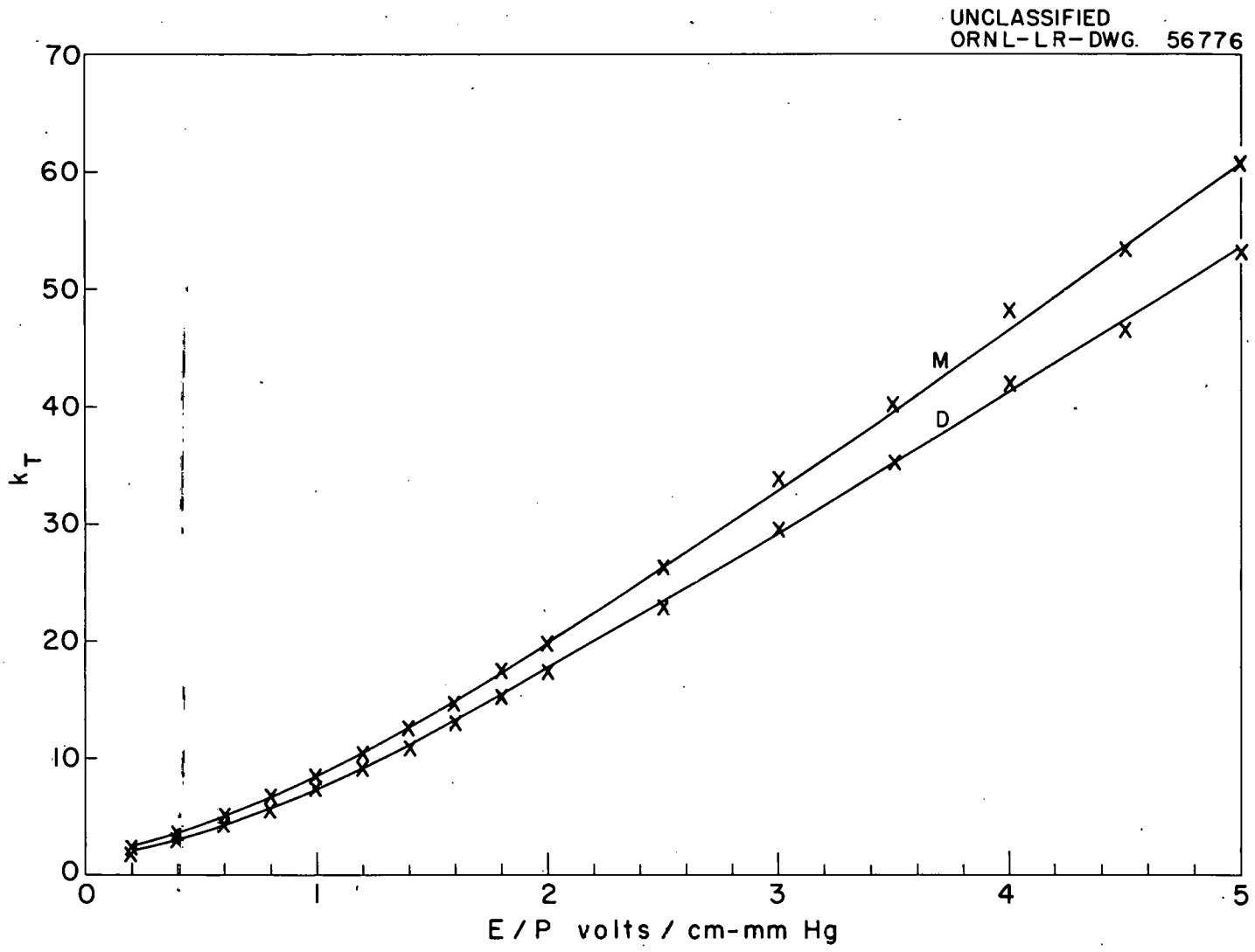

FIG. 47. TOWNSEND ENERGY FACTOR k_T Vs. E/P FOR METHANE USING THE MAXWELLIAN AND DRUYVESTEYN DISTRIBUTIONS.

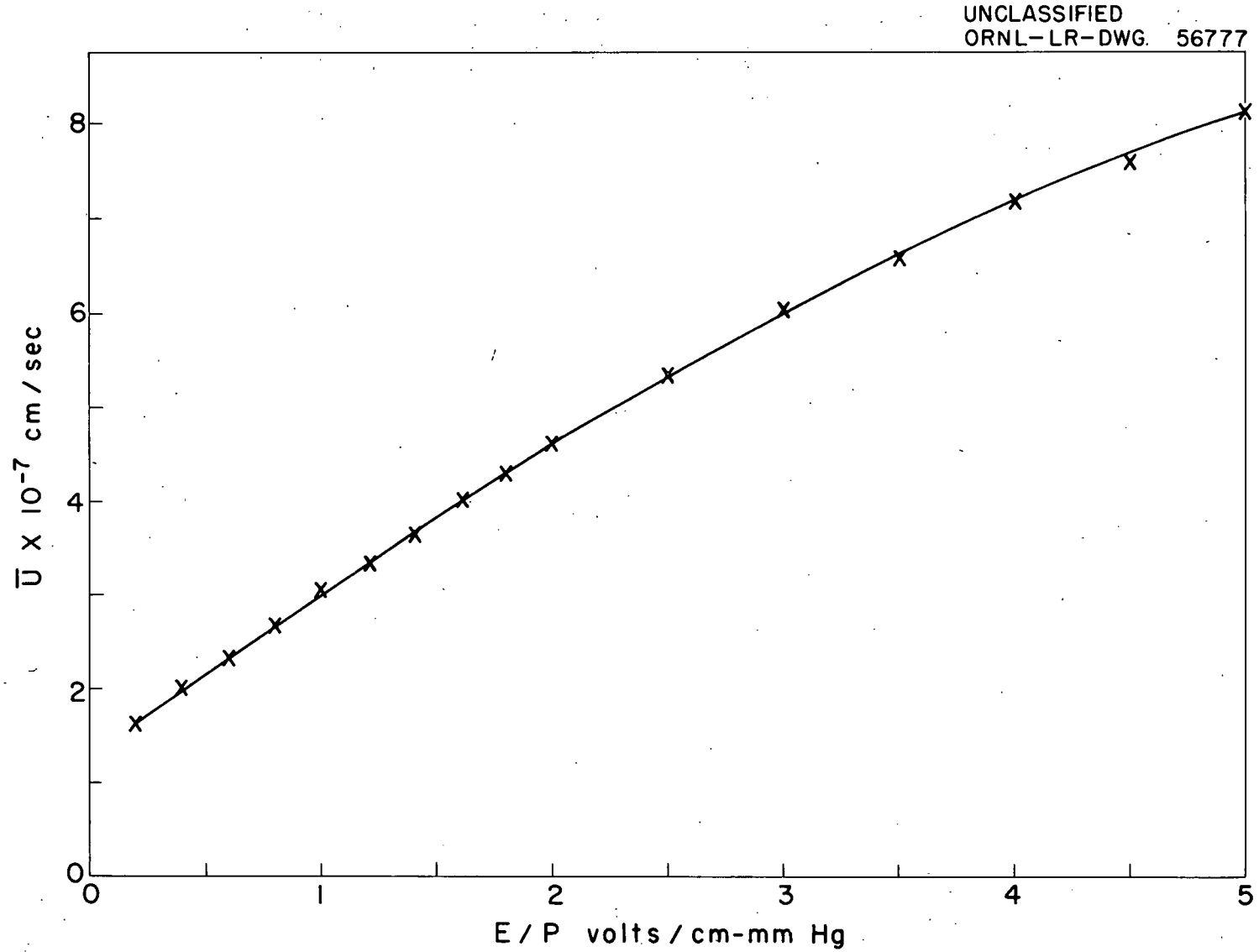

FIG. 48. $\bar{U}$ Vs. E/P FOR METHANE USING THE DRUYVESTEYN DISTRIBUTION.

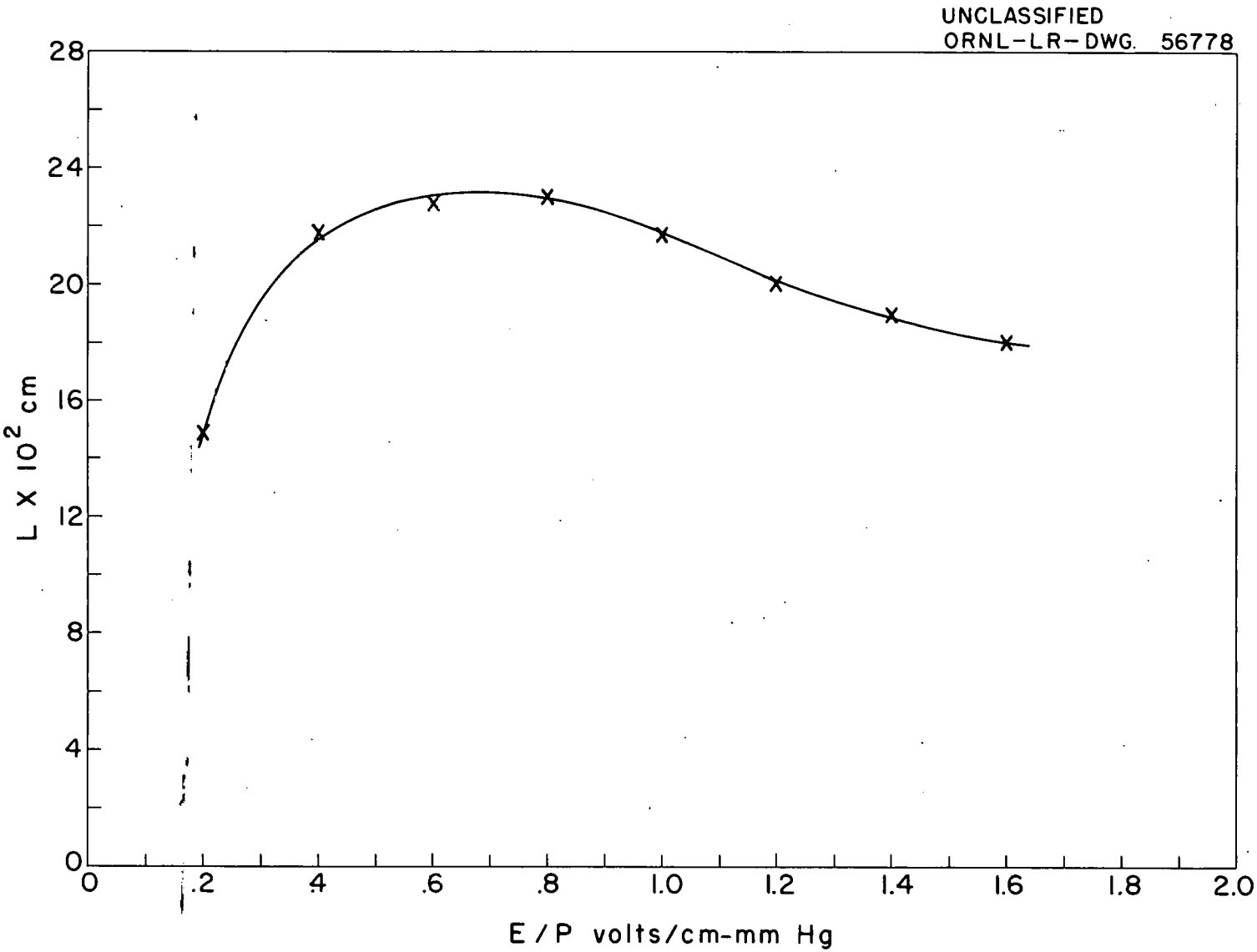

FIG. 49. L Vs. E/P FOR METHANE USING THE DRUYVESTEYN DISTRIBUTION.

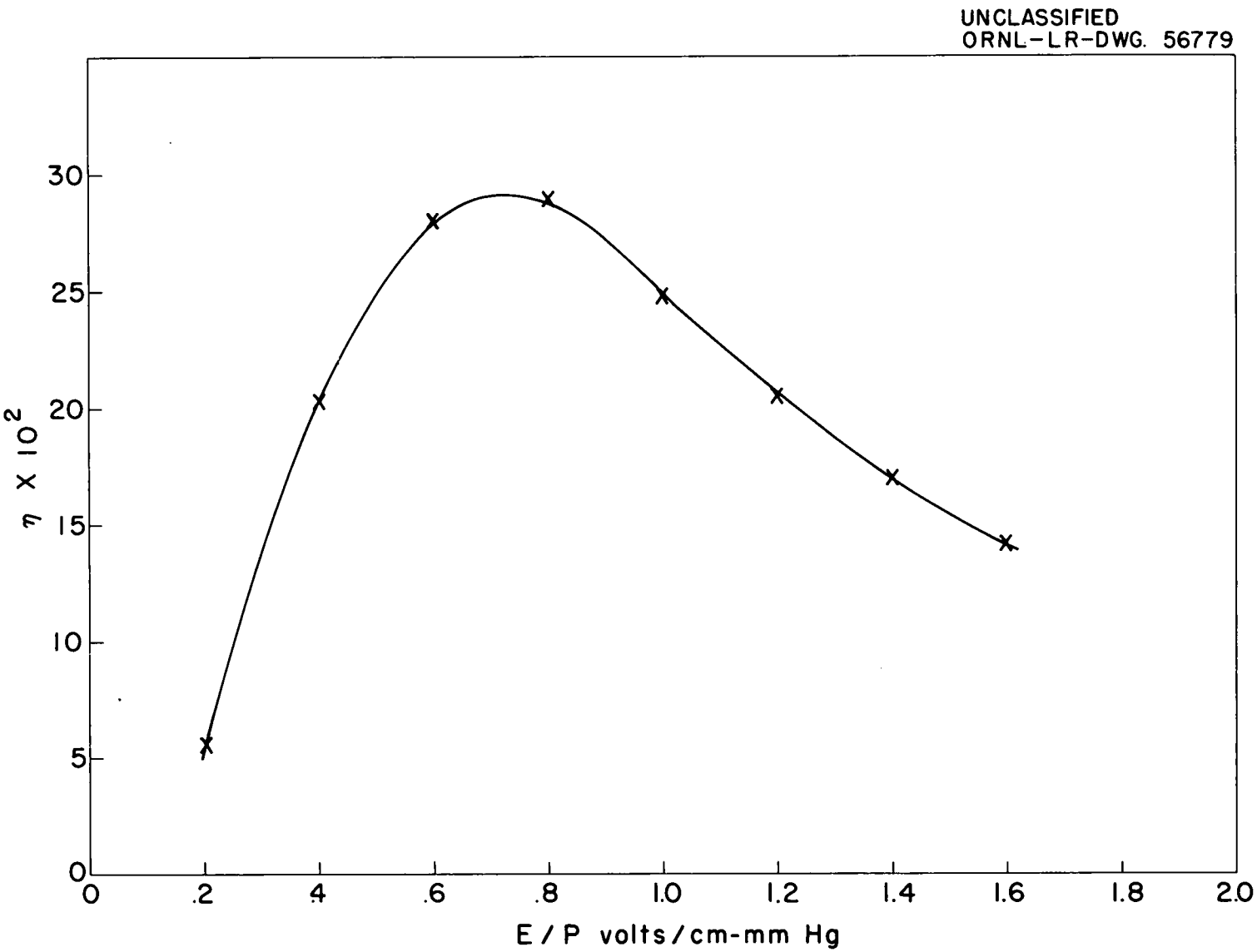

FIG. 50. η Vs. E/P FOR METHANE USING THE DRUYVESTEYN DISTRIBUTION.

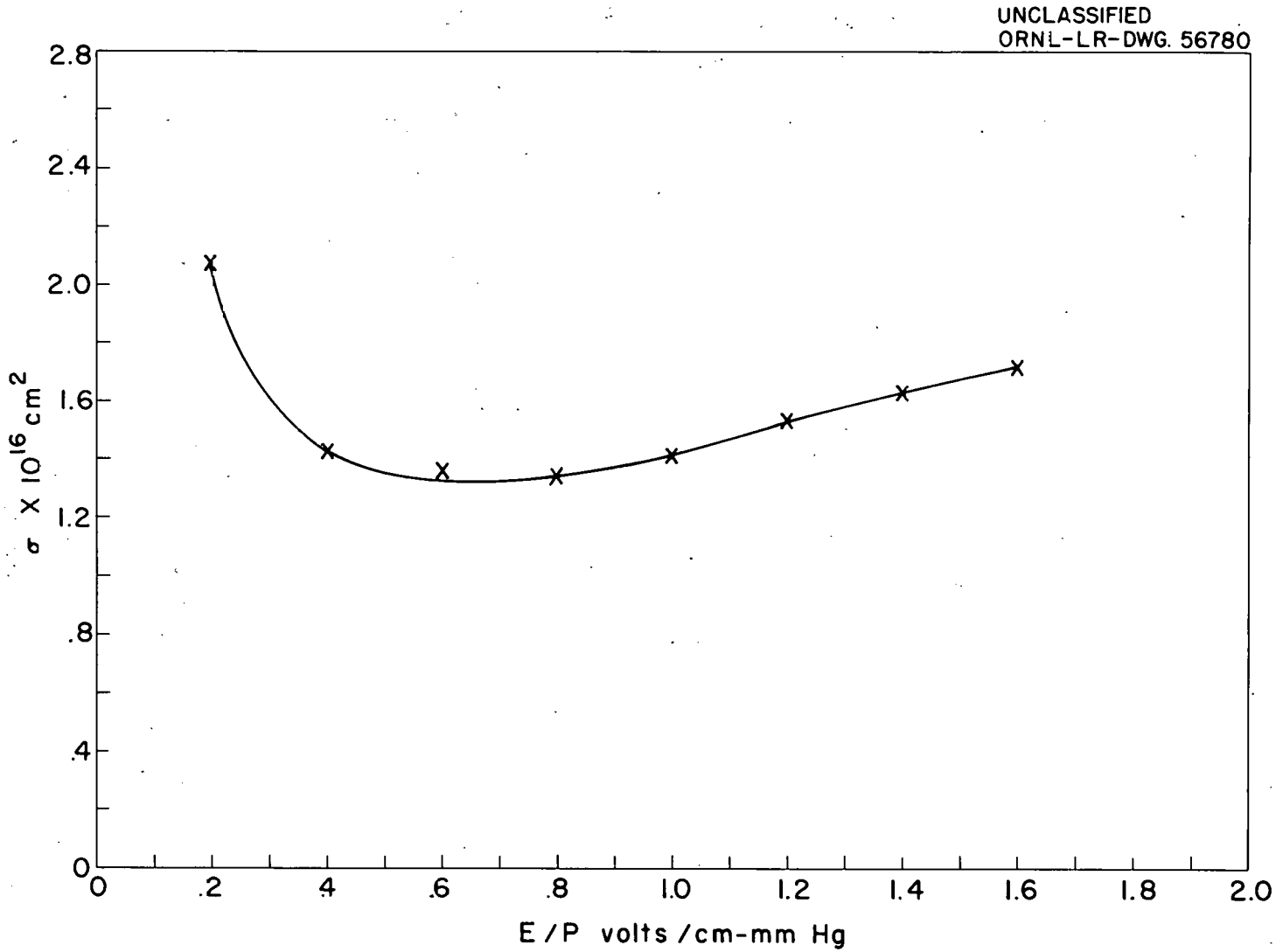

FIG. 51. COLLISION CROSS SECTION σ Vs. E/P FOR METHANE USING THE DRUYVESTEYN DISTRIBUTION.

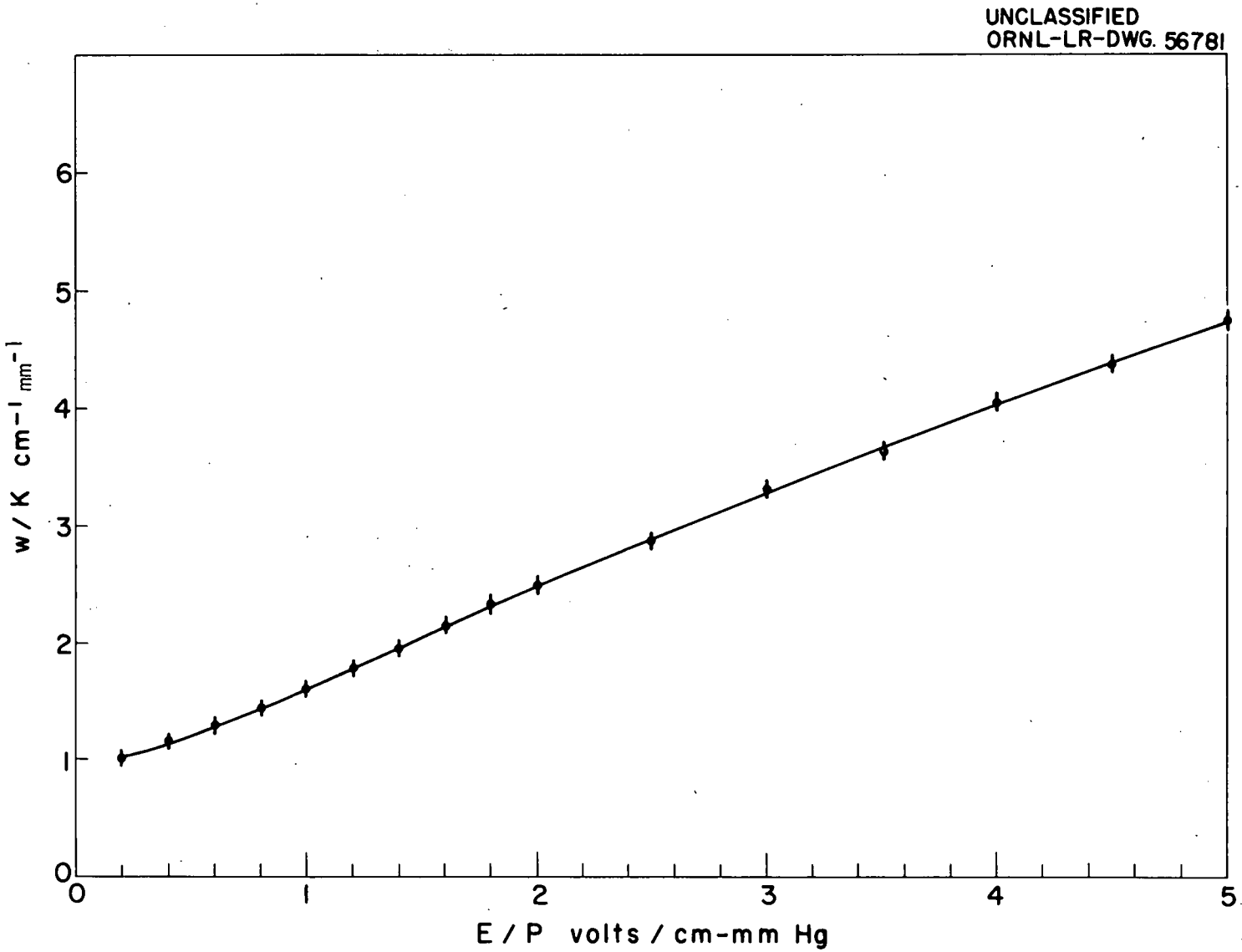

FIG. 52. w/K Vs. E/P FOR NITROGEN.

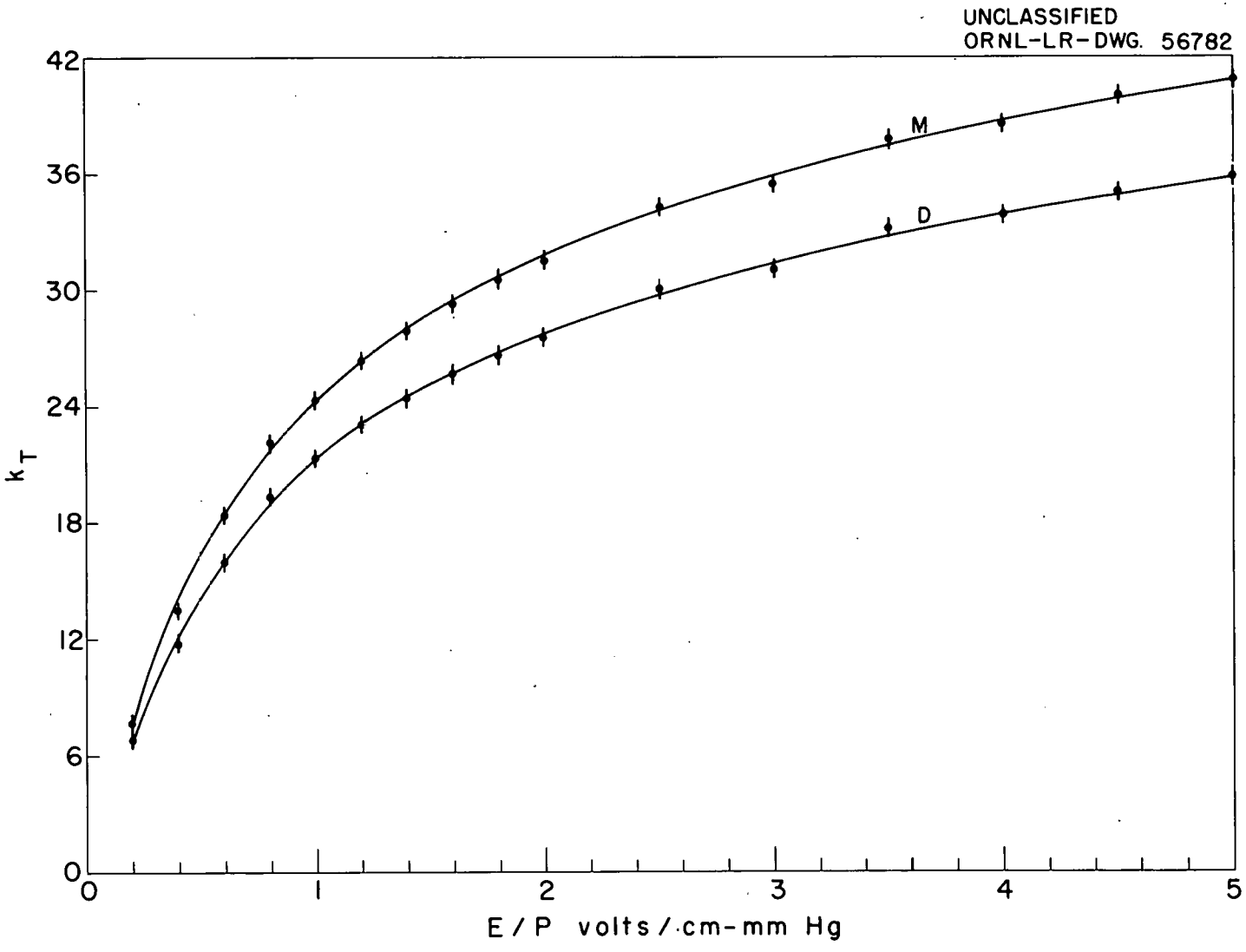

FIG. 53. TOWNSEND ENERGY FACTOR k_T Vs. E/P FOR NITROGEN USING THE MAXWELLIAN AND DRUYVESTEYN DISTRIBUTIONS.

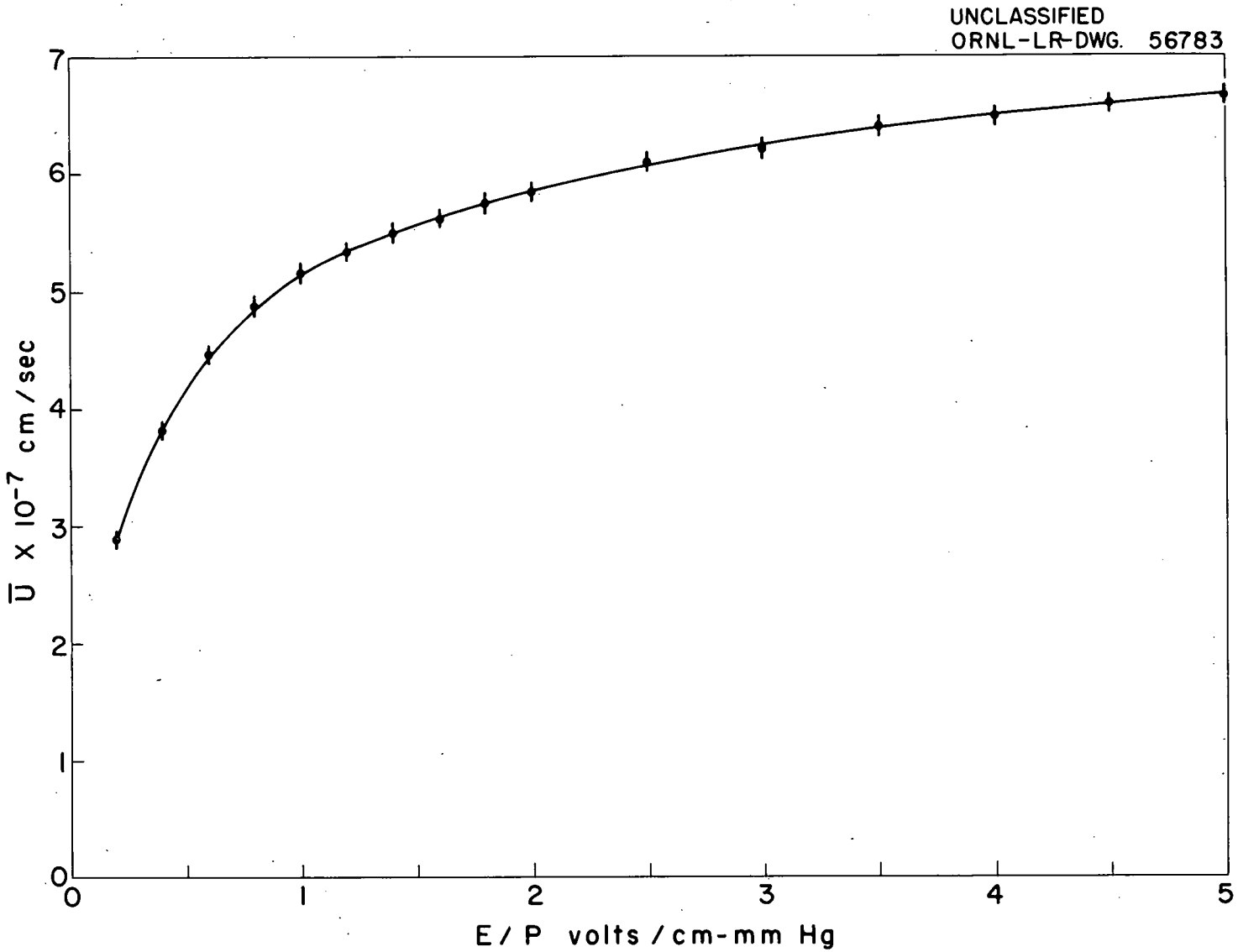

FIG. 54. $\bar{U}$ Vs. E/P FOR NITROGEN USING THE DRUYVESTEYN DISTRIBUTION.

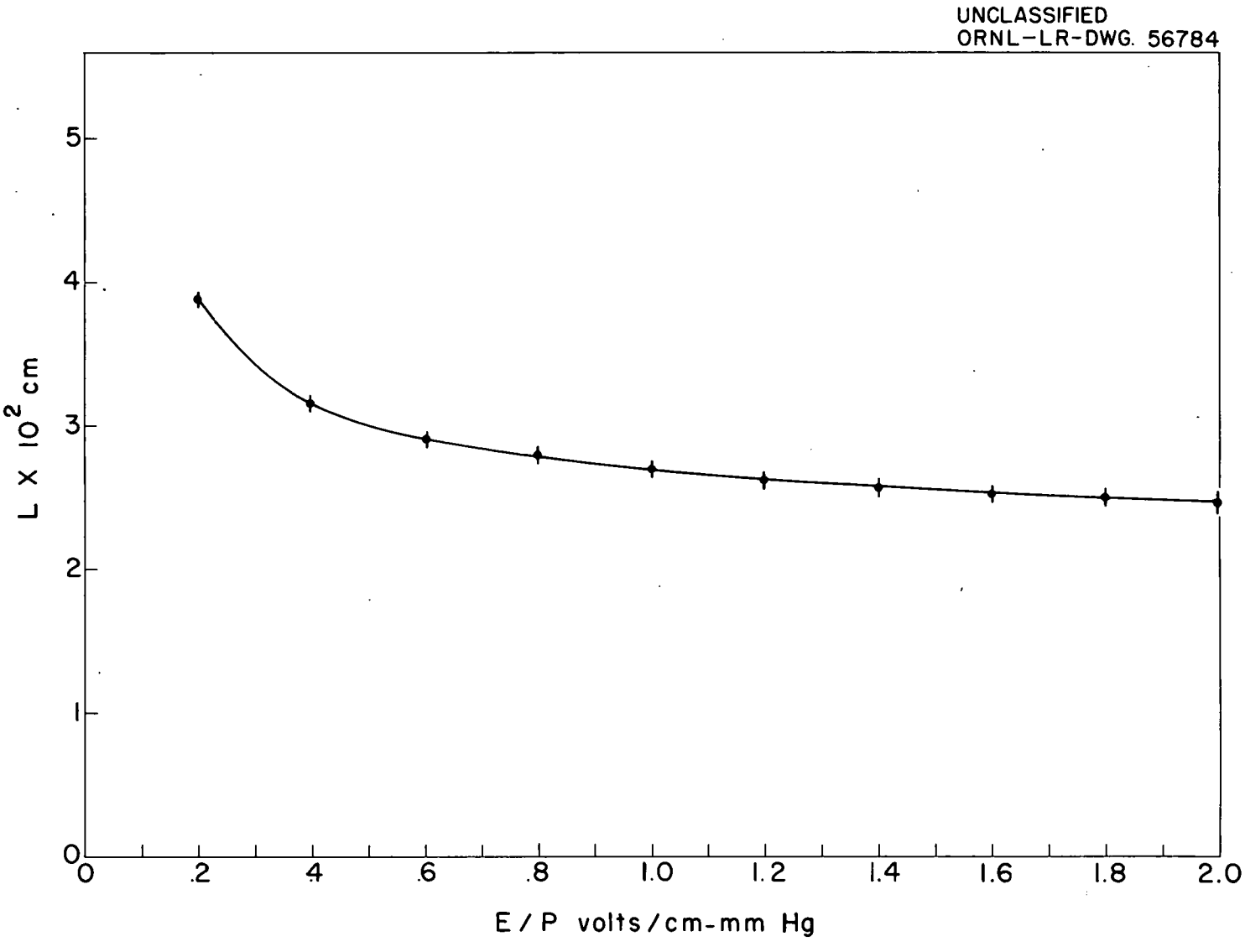

FIG. 55. L Vs. E/P FOR NITROGEN USING THE DRUYVESTEYN DISTRIBUTION.

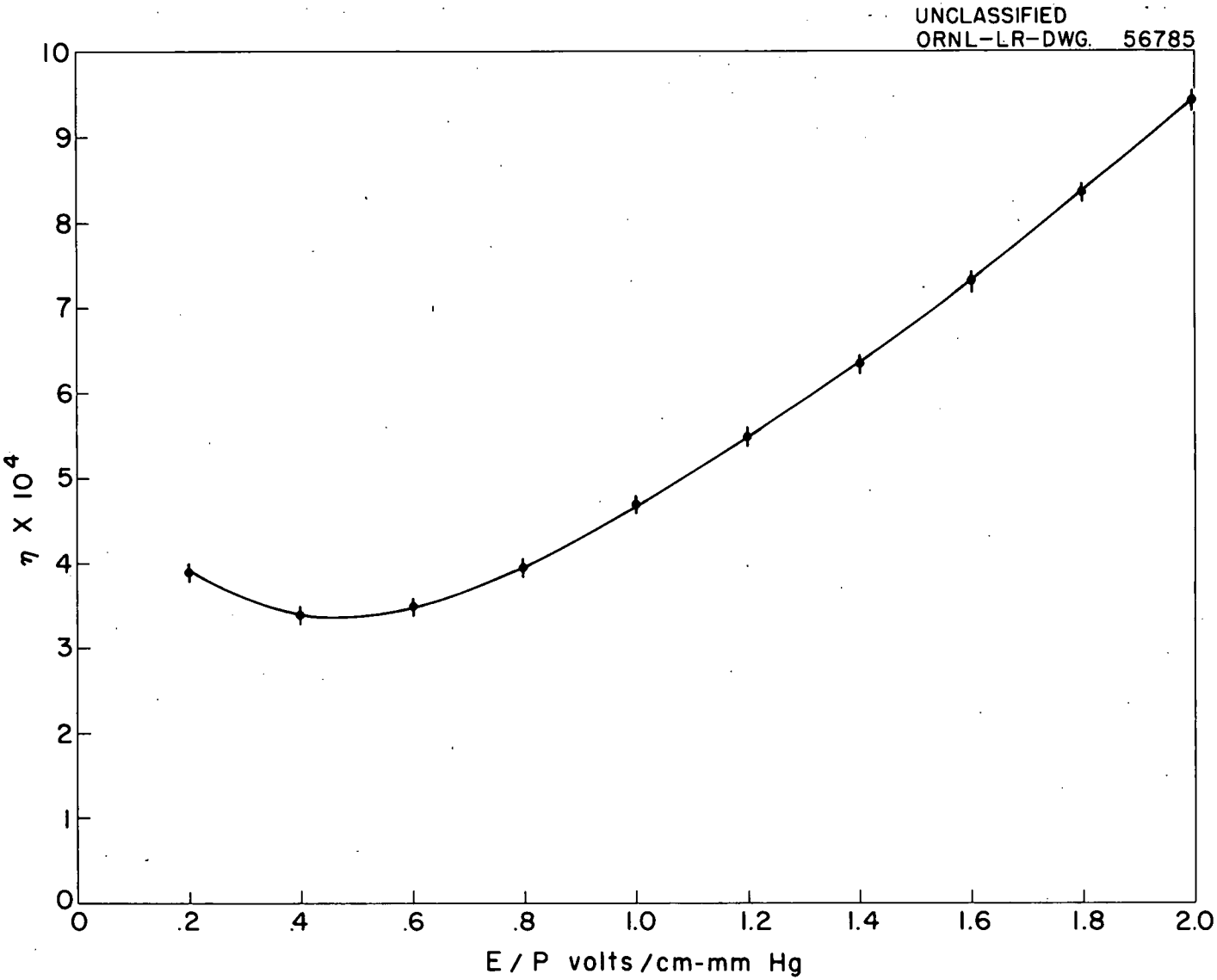

FIG. 56. η Vs. E/P FOR NITROGEN USING THE DRUYVESTEYN DISTRIBUTION.

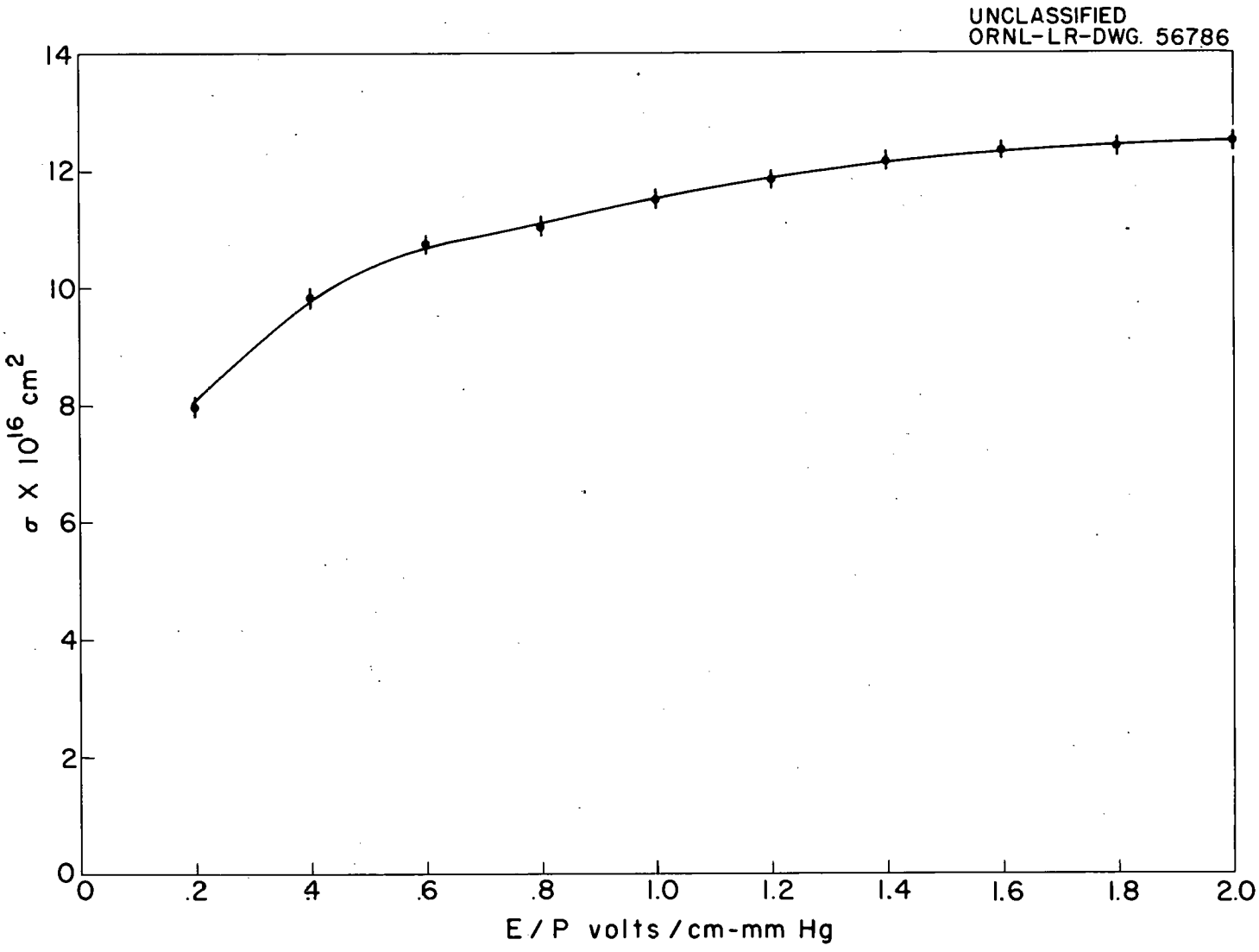

FIG. 57. COLLISION CROSS SECTION σ Vs. E/P FOR NITROGEN USING THE DRUYVESTEYN DISTRIBUTION.

for CO_2 are slightly larger than those obtained by Bailey and Rudd[4] and by Skinker,[5] and again different drift velocities have been used for L, η, and σ. For the lower E/P's the values of k_T are larger in C_2H_4 than those obtained by Bannon and Brose.[6] Argon data differ in many ways from earlier data by Townsend and Bailey[7] and will be discussed further below. CH_4 and C_3H_6 had not been investigated previously.

A new problem occurred with C_2H_4 and CO_2 which is not recorded in the literature. At lower E/P's the k_T values had a minimum in these two gases. In general, the position of this minimum and the amount of turnup at the lower end of the curve depended on pressure and perhaps b/h ratio. With C_2H_4, however, this behavior almost completely disappeared at higher pressures where higher ratios could be obtained at a given E/P. For this reason the problem appears to be instrumental. This peculiar behavior continued to occur in differing degrees with CO_2 even at higher pressures and a different b/h ratio. Rate-of-drift measurements in CO_2 at these low E/P's agreed exactly with the feedback amplifier measurements. Since consistent results could not be obtained at these low E/P's, k_T values were not tabulated at E/P of 0.2 in C_2H_4 and E/P's of 0.2, 0.4, and 0.6 in CO_2.

---

[4] V. A. Bailey and J. B. Rudd, Phil. Mag. 14, 1033 (1932).

[5] M. F. Skinker, Phil. Mag. 44, 994 (1922).

[6] J. Bannon and H. L. Brose, Phil. Mag. 6, 817 (1928).

[7] J. S. Townsend and V. A. Bailey, Phil. Mag. 44, 1033 (1922).

Argon data, although not as accurate as the data for the other gases, are presented because of their dependence on pressure and b/h ratio in this experiment. Tables VII and VIII and Figs. 18 through 21 present the data as a function of pressure at the two b/h ratios 0.3 and 0.5 used with this gas. Townsend and Bailey's data[8] showed no pressure dependence and gave a curve of k_1 vs E/P similar to the low pressure curves in Fig. 20 and with a maximum k_1 of 340 at E/P = 2. Deliberate contamination of argon with small percentages of impurity lowered the k_T values considerably but did not wash out the pressure dependence.

The ratios R obtained for argon were reproducible to about 3%, yielding a spread in k_T values of about 5% to 6%. Many readings were taken at a given E/P, though, and their average taken. The curves in Figs. 18 through 21 show that the pressure and b/h dependence could not possibly be due to such a comparatively small percentage spread in experimental readings. Impurity does not seem to explain the phenomena either because of the extremely high k_T values involved. These high k_T values also give energies which surpass excitation levels and at higher E/P's even the ionization potential of argon. That no considerable degree of ionization has been observed in argon and that no leveling off occurs when energies corresponding to excitation are reached would indicate that the values obtained are not realistic. The fault may be instrumental or it may be due to theoretical assumptions

---

[8] Townsend and Bailey, op. cit.

which do not hold for such a widely diffusing gas as argon and for a gas whose cross section varies so markedly with energy.

We note here that Townsend and Bailey in 1922, besides using impure gas, used a slit type source of electrons and a different receiving electrode arrangement. Results on other gases, however, seem to show that the two different types of apparatus yield equivalent results. We note also that their method of taking data at different pressures would not provide a sufficient test for pressure independence. Their method involved taking data with lower pressures at the high E/P's and increasing pressures as the E/P ratio was lowered. Figures 18 through 21 show that almost any curve desirable could be obtained in this manner if the pressure dependence shown there is valid.

It should be emphasized that Huxley's solution[9,10] relating the experimentally determined R to w/K is not completely satisfactory. This fact should be kept in mind because the entire success of the experimental study rests on the validity of this solution. It would seem that a straightforward boundary value solution using the same or appropriate boundary conditions with the assumption of a delta function source at the origin would be a better approximation to the problem. This type solution most certainly does not reduce to one term and should not be expected to do so. If, when recourse is made to

---

[9] L. G. H. Huxley and F. W. Bennett, Phil. Mag. 30, 396 (1940).

[10] L. G. H. Huxley and R. W. Crompton, Proc. Phys. Soc. B68, 381 (1955).

experiment, w/K values at a given E/P do vary with pressure, then explanations might be put forward; w/K might truly vary with pressure at a given E/P, which is not likely, or the basic diffusion equation, along with the boundary conditions, does not sufficiently approximate the problem. No matter how the problem is approached, it is a difficult one and perhaps too little is known to actually solve it for this type of geometry. Thus, the theoretical interpretation of experiment used in this paper is quite empirical and, at best, is only an approximation to the problem. This solution is used because it is the best one thus far set forth. A straightforward solution obtained by this author is somewhat different from Huxley's, having a different exponential and being a series which converges faster at lower values of w/K. A few points plotted seem to show a decrease in R with increase in w/K rather than an increase. It seems that an attempt at a more rigorous solution should be made before further analysis of experimental data is made.

BIBLIOGRAPHY

Bailey, V. A., and Rudd, J. B., "The Behaviour of Electrons in Nitrous Oxide," Phil. Mag., 14 (1932), 1033.

Bannon, J., and Brose, H. L., "The Motions of Electrons in Ethylene," Phil. Mag., 6 (1928), 817.

Bortner, T. E., Hurst, G. S., and Stone, W. G., "Drift Velocities of Electrons in Some Commonly Used Counting Gases," Rev. Sci. Instr., 28 (1957), 103.

Crompton, R. W., and Sutton, D. J., "Experimental Investigation of the Diffusion of Slow Electrons in Nitrogen and Hydrogen," Proc. Roy Soc. Lond.A196 (1949), 402.

Druyvesteyn, M. J., Physica, 10 (1930), 61.

Healey, R. H., and Reed, J. W., The Behaviour of Slow Electrons in Gases. Australia: Amalgamated Wireless Ltd., 1941.

Hurst, G. S., and Bortner, T. E., "Capture of Electrons in Molecular Oxygen," Oak Ridge National Laboratory Report ORNL-2670 (1959).

Huxley, L. G. H., and Bennett, F. W., "The Lateral Diffusion of a Stream of Ions in a Gas," Phil. Mag., 30 (1940), 396.

Huxley, L. G. H., and Crompton, R. W., "A Note on the Diffusion in a Gas of Electrons from a Small Source," Proc. Phys. Soc., B68 (1955), 381.

Huxley, L. G. H., and Zaazou, A. A., "Experimental and Theoretical Studies of the Behaviour of Slow Electrons in Air," Proc. Roy. Soc. Lond. A196 (1949), 402.

Loeb, L. B., Basic Processes of Gaseous Electrons. Berkeley and Los Angeles: University of California Press, 1955.

Morse, P. M., Allis, W. P., and Lamar, E. S., "Velocity Distribution for Elastically Colliding Electrons," Phys. Rev., 48 (1935), 412.

Nielsen, R. A., and Bradbury, N. E., "Absolute Values of Electron Mobility in Hydrogen," Phys. Rev., 49 (1936), 388.

Skinker, M. F., "The Motion of Electrons in Carbon Dioxide," Phil. Mag., 44 (1922), 994.

Townsend, J. S., in Electrons in Gases. New York: Hutchinson's Scientific and Technical Publications, 1948.

Townsend, J. S., and Bailey, V. A., "The Motion of Electrons in Argon and in Hydrogen," Phil. Mag., 44 (1922), 1033.

THIS PAGE

WAS INTENTIONALLY

LEFT BLANK

ORNL-3091
UC-34 - Physics
TID-4500 (16th ed.)

INTERNAL DISTRIBUTION

1. Biology Library
2. Reactor Division Library
3-4. Central Research Library
5. ORNL - Y-12 Technical Library, Document Reference Section
6-60. Laboratory Records Department
61. Laboratory Records, ORNL R.C.
62. J. A. Auxier
63. E. T. Arakawa
64. S. I. Auerbach
65. R. D. Birkhoff
66. C. E. Center
67. J. S. Cheka
68. F. L. Culler
69. F. J. Davis
70. H. B. Eldridge
71. J. H. Frye, Jr.
72. J. H. Gillette
73. C. S. Harrill
74. J. A. Harter
75. A. Hollaender
76. A. S. Householder
77. H. H. Hubbell, Jr.
78-102. G. S. Hurst
103. R. M. Johnson
104. R. G. Jordan (Y-12)
105. W. H. Jordan
106. M. T. Kelley
107. J. A. Lane
108. T. A. Lincoln
109. S. C. Lind
110. R. S. Livingston
111. C. E. Melton
112. K. Z. Morgan
113. J. P. Murray (K-25)
114. D. R. Nelson
115. M. L. Nelson
116. L. B. O'Kelley
117. D. Phillips
118. P. W. Reinhardt
119. R. H. Ritchie
120. P. S. Rudolph
121. F. W. Sanders
122. H. E. Seagren
123. M. J. Skinner
124. W. S. Snyder
125. E. G. Struxness
126. J. A. Swartout
127. T. Tamura
128. E. H. Taylor
129. J. H. Thorngate
130. E. B. Wagner
131. A. M. Weinberg
132. C. E. Winters
133. F. H. W. Noll (consultant)
134-143. L. W. Cochran (consultant)
144-153. D. W. Forester (consultant)
154. T. E. Bortner (consultant)
155. J. C. Frye (consultant)
156. W. H. Langham (consultant)
157. R. L. Platzman (consultant)
158. L. S. Taylor (consultant)
159. T. D. Strickler (consultant)

EXTERNAL DISTRIBUTION

160. Division of Research and Development, AEC, ORO
161. J. C. Bowe, Argonne National Laboratory
162. C. A. Markarian, Captain, USAF, MSC, Director
163. B. M. Wheatley, Central Electricity Generating Board, Berkeley Nuclear Laboratories, Berkeley, Glos., United Kingdom
164-716. Given distribution as shown in TID-4500 (16th ed.) under Physics category